FLUORESCENCE SIGNALING BEHAVIOR OF SOME *FLUOROPHORE-SPACER-RECEPTOR* SYSTEMS TOWARDS THE TRANSITION METAL IONS

A THESIS

SUBMITTED FOR THE DEGREE OF

DOCTOR OF PHILOSOPHY

by

Sankaran N. B.

School of Chemistry

University of Hyderabad

Hyderabad 500 046

INDIA

APRIL 2003

In fond memory of

my father

Dedicated to

my mother

The known is finite; the unknown is infinite. Intellectually we stand on an islet in the midst of an illimitable ocean of inexplicability. Our business in every generation is to reclaim a little more land.

-T.H. Huxley

Contents

STATEMENT

I hereby declare that the matter embodied in the thesis entitled ***"Fluorescence Signaling Behavior of Some Fluorophore-Spacer-Receptor Systems Towards the Transition Metal ions"*** is the result of investigations carried out by me in the School of Chemistry, University of Hyderabad, Hyderabad, India under the supervision of **Prof. Anunay Samanta**.

In keeping with the general practice of reporting scientific investigations, due acknowledgements have been made wherever the work described is based on the findings of other investigators. Any omission or error that might have crept in is regretted.

09.04.03

April 2003 **Sankaran N.B.**

SCHOOL OF CHEMISTRY
UNIVERSITY OF HYDERABAD
HYDERABAD-500 046, INDIA

Phone: +91-40-2301 1594 (office)
+91-40-2301 0715 (home)
Fax: +91-40-2301 2460
Email: assc@uohyd.ernet.in
anunay_s@yahoo.com

Anunay Samanta, F.A.Sc.
Professor

9 April, 2003

CERTIFICATE

Certified that the work embodied in the thesis entitled ***"Fluorescence Signaling Behavior of Some Fluorophore-Spacer-Receptor Systems Towards the Transition Metal ions"*** has been carried out by **Mr. Sankaran N. B.** under my supervision and that the same has not been submitted elsewhere for any degree.

Anunay Samanta
(Thesis Supervisor)

Dean
School of Chemistry
University of Hyderabad

DEAN
School of Chemistry
University of Hyd
Hyderabad-46.

Acknowledgement

I wish to express my sincere gratitude to Prof. Anunay Samanta, my research supervisor, for his cooperation and kind guidance. He has been quite helpful to me in both academic and personal fronts. I owe him very much in many ways in my life.

I would like to thank the Dean, School of Chemistry, for allowing me to avail the school facilities. I am extremely thankful individually to all the faculty members of the school for their help, cooperation and encouragement at various stages of my stay in the campus.

I thank all my seniors in the lab: Drs. Soujanya, Saroja, Ramachandram and Satyen, with whom I am associated at various stages of my stay in the lab. I cherish my association with all of them. I acknowledge my junior friends in the lab: Rana, Sandip, Prasun, Moloy & Aniruddha. I specially thank Prasun for his careful reading of the thesis.

I am thankful to Dr. Amitava Das of CSMCRI, Bhavnagar, for his collaborative efforts. I thank Dr. V. Jayathirtha Rao, IICT, Hyderabad, for allowing me to make use of his instrument facilities at various stages.

I thank all the non-teaching faculties of the school for their cooperation. They had all been quite helpful.

Financial assistance from CSIR, New Delhi is greatly acknowledged.

Special thanks to Tin Htwe, for helping me always with a pleasant smile whenever I approached him, and for providing me a computer when most needed.

The help by Pradeep & Anoop is also highly acknowledged. I would like to acknowledge Satyanarayan Pal for his help and company.

Friends are a wholesome lot and it is indeed a difficult task to mention them all here. I acknowledge whole-heartedly the contribution of each and every one of them. Even then, my association with Satyen, Sailaja and Hari are memorable. I particularly acknowledge Moorthy, Abbas, Kiran and Raghavaiah for their help right from my M.Sc. days. Also is highly acknowledged Rajettan & family for many reasons and friendship with Abey.

I salute my young friend, Srikanth, who, along with millions of soldiers keeps India's border guarded, trying to protect us all.

I offer tributes to my father, who was to me everything and who left me at an unexpected stage in my life. It was an incident that shattered many of my dreams for a longer time. I dedicate the thesis to my mother, whom I have never seen happy after my father's death and whose happiness is only my goal. I particularly acknowledge my sister, Ramani, and brothers, Narayanan, Suresan and Ramesan, but for whom all I would never have been able to reach here.

Sankaran

List of publications

1. *Structure of a Self-Assembled Chain of Water in a Crystal Host, S. Pal, **N. B. Sankaran** and A. Samanta. *Angew. Chem., Int. Ed.* (In Press).
2. Fluorescence Signaling of the Transition Metal Ions: Design Strategy Based on the Choice of the Fluorophore Component, **N. B. Sankaran,** S. Banthia and A. Samanta; *Proc. Indian Acad. Sci,(Chem. Sci.)* 2002, **114**, 539 - 545.
3. *Fluorescence Signaling of the Transition Metal Ions: A New Approach, **N. B. Sankaran,** S. Banthia, A. Das and A. Samanta; *New J. Chem.* 2002, **26,** 1529 - 1531.
4. *Interaction Between a Pyridyl and a Naphthyl/Pyrenyl Moiety in Covalently Linked Systems, **N. B. Sankaran,** A. Das and A. Samanta, *Chem. Phys. Lett.* 2002, **351**, 61 – 70.
5. Unusually High Fluorescence Enhancement of Structurally Simple Fluorophore-Spacer-Receptor Systems Induced by Transition Metal Salts, B. Ramachandram, G. Saroja, **N.B. Sankaran** and A. Samanta, *J. Phys. Chem. B* 2000, **104**, 11824 – 11832.
6. Fluorescence Signalling of Transition Metal Ions by Multi-Component Systems Comprising 4-Chloro-1,8-naphthalimide as Fluorophore, B. Ramachandram, **N.B. Sankaran**, R. Karmakar, S. Saha and A. Samanta, *Tetrahedron.* 2000, **56**, 7041 - 7044.

---

* Presented in the thesis

7. Fluorescence Response of Structurally Simple Fluorophore-Spacer-Receptor Systems Towards Transition Metal Ions and Protons, B. Ramachandram, **N.B. Sankaran** and A. Samanta, *Res. Chem. Interm.* 1999, **25**, 843 - 859.
8. Adsorption Dynamics of Phenol on Activated Charcoal Produced From Salvinia Molesta Mitchell by Single – Step Steam Pyrolysis, **N. B. Sankaran** and T. S. Anirudhan, *Indian. J. Eng. Mater. Sci.* 1999, **6**, 229 – 236.
9. Photophysical Study of Two Carbostyril Dyes: Investigation of the Possible Role of a Rotary Decay Mechanism, G. Saroja, **N. B. Sankaran** and A. Samanta, *Chem. Phys. Lett.* 1996, **249,** 392 – 398.

Abbreviations & IUPAC names of the compounds discussed in the thesis

NPY: 1-(1-naphthyl)-2-(4-pyridyl)ethane

PPY: 1-(1-pyrenyl)-2-(4-pyridyl)ethane

APMAC4: 5-Amino-2-[2-(1,4,7-trioxa-10-aza-cyclododec-10-yl)-ethyl]-isoindole-1,3-dione

APMAC5: 5-Amino-2-[2-(1,4,7,10-tetraoxa-13-aza-cyclopentadec-13-yl)-ethyl]-isoindole-1,3-dione

APMAC6: 5-Amino-2-[2-(1,4,7,10,13-pentaoxa-16-aza-cyclooctadec-16-yl)-ethyl]-isoindole-1,3-dione

APDAC: 5-Amino-2-[2-(1,4,10,13-tetraaoxa-7,16-diaza-cyclooctadec-7-yl)-ethyl]-isoindole-1,3-dione

APTAC: 5-Amino-2-[2-(1,4,7,10tetraaoxa-cyclododec-1-yl)-ethyl]-isoindole-1,3-dione

Chapter 1

Introduction

This chapter provides an introduction to signaling of chemical species using fluorescence technique. Fundamentals of molecular recognition, the principles involved in efficient binding of a substrate to a receptor, and development of molecular photonics and electronics have been discussed in brief. Importance of fluorescence as a means of signaling chemical species has been explained in detail. Even though special emphasis is given on the photoinduced electron transfer (PET) mechanism as an efficient mechanism for fluorescence signaling, various other mechanisms employed in the area are also touched upon.

1.1. Principles of molecular recognition

The binding between a receptor and a substrate takes place through weak intermolecular non-covalent interactions. Efficient binding of the substrate by the receptor can be achieved by employing a large number of binding sites. Molecular recognition refers to recognition of the substrate by the receptor leading to strong and specific complexation. Substrate binding to a receptor is controlled by steric and interactional complementarities, large contact areas and large number of interaction sites. Molecular recognition has become important in view of its bioorganic implications and significance in chemical selectivity.[1]

1.2. Molecular photonics and electronics

In the present day scenario, a molecule is more important for its significance than for its structure.[1] Macroscale machines developed in the past, employing the bulk properties of the molecules, later given way for faster and sophisticated microscale ones, which in turn has paved the way for nanoscale machines, machines of the size of individual molecules, in which functional interactions gain importance over the nature of connectivity.

A covalent molecule possessing characteristics of a supramolecular nature is considered a supramolecular device. A supramolecular device is, hence defined as a covalent system made up of molecular components with definite individual properties that are intrinsic to the molecular components. Molecular recognition events between the host and the guest are an intrinsic part of the operation of a supramolecular device, which is designed to bind and then signal the presence of a guest.

Among the various possible approaches to constructing a supramolecular device,[2-5] the use of a photochemically active component is considered to be a versatile one. The role of light in photosynthesis, its importance in inducing events such as charge separation and catalysis, its use in sensing applications and its ability to travel through a variety of media have contributed to the development of photochemically active supramolecular devices. In addition, useful processes such as energy migration, perturbations of optical transitions and polarisabilities, modification of ground and excited state redox potentials, photoregulation of binding properties and selective photochemical reactivity can

be achieved by incorporating photochemically active components into supramolecular systems.

Molecules that conceptually resemble electronic devices are called molecular electronic devices.[6-17] Making of nanoscale molecular devices such as molecular wires,[18-21] gates,[22,23] brakes,[24] ratchets,[25] rectifiers,[26-28] gears,[29] switches,[15,30] shuttles[31] etc. have become an important area of research. The basic requirement of all these is that on a molecular scale, exactly same characteristics are required as that for a bulk electronic device. Molecular logic devices that perform molecular arithmetic are gaining increasing importance and are being taken up as a challenge of today.[16,17,32-37]

Signaling of chemical species has become an active area of research. The area of supramolecular chemistry that is concerned with signaling devices is referred to as semiochemistry.[1,6] Sensing is a molecular recognition event involving binding of the substrate to the receptor. The binding is communicated to the outside world by means of a signaling unit, which generates a signal. This means that the receptor and the signaling unit must be in virtual contact and any change in the properties of the free and the bound receptors must be signaled. A spacer that connects the two helps in doing this. A useful sensor must be highly stable and guest selective, showing good affinity to the guest. In addition, efficient signal transduction, emission of radiation of detectable intensity, kinetically rapid sensitization, ease of delivery to the target system and easy availability make a sensor molecule handier and practically important.[1]

1.3. Fluorosensors and common analytes

Molecular sensors that employ fluorescence as the means of signal transduction are referred to as fluorosensors. As a technique, fluorescence is quite advantageous and superior to other techniques for various reasons such as sensitivity, resolution, multi-dimensionality and remote sensing capability.[38] To stop over for a moment, the sensitivity of fluorescence experiments down to single molecule detection limit has been reported.[39-41] Thus, fluorescence technique possesses microenvironmental sensing capability, with spatial resolution approaching molecular dimensions. Temporal resolution of a few picoseconds can be achieved using time-resolved fluorescence because of the short-lived excited state lifetime.[42-44] Further, real-time sensing is possible employing luminescence techniques.[45]

Fluorescence sensors have been developed for sensing quite a large number and varieties of analytes.[46] When the idea is to sense a chemical species, the sensor is a chemical sensor. However, according to the nature of the analyte being sensed, they are termed as chemosensors, biosensors, etc.[42] For the fluorescent part we can have intrinsic fluorescence probe wherein the mechanism of signal transduction involves interaction of the analyte with a ligand that is a part of the fluorophore π-system. We can also have a conjugate fluorescence probe in which the mechanism for signal transduction involves interaction of the analyte with a ligand electronically insulated from the fluorophore π-system.

The common analytes of interest in the signaling chemistry vary from cations to anions to neutral molecules.[47] Among the cations studied the interest was primarily on proton and the s-block metals of the periodic table owing to their

importance in biology.[48-57] Transition metal ions, though important in biology and environment, the sensing of these metal ions and heavy metal ions has been taken up actively only in recent years.[58-66]

The importance of sensing the analytes is mainly due to their significance in our day-to-day life. Sodium and potassium ions are established candidates in biology and many groups have actively taken up sensing of Na^+ and K^+.[67,68] Other alkali metals are also explored in semiochemistry and different types of sensors are reported towards their signaling.[69] Magnesium, calcium, strontium and barium have also attracted the sensor chemists. Monitoring the levels of Ca^{2+} is important in human body since it is responsible for muscle fatigue.[67,70,71] The importance of Zn^{2+} and Fe^{3+} in human metabolism is known from long back and sensing of these metal ions is being studied.[72-74] Importance is attributed to the signaling of transition metal ions in recent years.[66,75,76] The biological significance and toxicity of Cd^{2+}, Hg^{2+} and Pb^{2+} are growing concern among environmentalists and priority is being attached in developing sensors for these metal ions.[61,73,77,78] Among the neutral molecules, sensing of saccharides,[2,79-84] carbon monoxide,[85] alcohols[86] etc. are being studied vigorously besides other molecules.[87-89] The ubiquitous nature of the anions in numerous biological and chemical processes and their importance in medicine and environment are now being realized.[90] Alzheimer's disease has been linked to anion binding enzymes.[91] Anion sensing is now a hot field of research.[92-108]

In sensing of analytes using fluorescence, several mechanisms are being employed. These include monitoring the $n\pi^*$,[109-112] $\pi\pi^*$,[113] intramolecular

charge transfer (ICT),[114-119] metal to ligand charge transfer (MLCT),[120-125] twisted intramolecular charge transfer (TICT),[126-133] through-bond charge transfer[134,135] and triplet[136-138] excited states. Fluorescence sensing by monitoring the monomer-excimer emission bands is also an established technique for quite some time.[139-147] Electronic energy transfer (EET)[148-152] and fluorescence resonance energy transfer (FRET)[153] are also common mechanisms employed in fluorescence signaling of the analytes. Despite the availability of various mechanisms pointed out above, the most commonly employed one is the photoinduced electron transfer (PET) mechanism.[46,154] Newer approaches towards fluorescence signaling are being reported recently.[155-160]

1.4. PET mechanism

When we monitor the fluorescence for sensing of the guest molecules, we usually concentrate on three parameters: shift in the emission band, emission intensity and emission lifetime.[42] Generally when we add an external analyte to the sensor molecule, the sensor molecule produces changes in the fluorescence behavior. A shift in the emission band occurs if the charge transfer nature of the sensor molecule gets altered on binding of the analyte.[161,162] There occurs a change in the intensity of the emission band too on binding of the analyte.[163] The emission may either get quenched or enhanced depending on the nature of the interaction of the interacting components of the sensor molecule and also depending on the nature of the interaction of the analyte with the sensor molecule.[164] If there is an enhancement in the intensity of the emission on binding the analyte, this state represents an 'on' state of the fluorescence relative

to an initially weakly fluorescent 'off' state. A reverse of this case, in which the initial system is highly fluorescent (an 'on' state) and the bound system is weakly fluorescent (an 'off' state), is also possible. These types of sensors are called fluorescence 'off-on' or 'on-off' sensors.[46,164,165]

The commonly employed architecture for the design of sensor molecules based on PET mechanism is one with a *fluorophore-spacer-receptor* format. The fluorophore component of the three-component sensor molecule is the light absorbing or emitting species, the receptor is responsible for binding of the analyte and the spacer controls the communication between the receptor and the fluorophore. The transfer of an electron from the free receptor to photo-excited fluorophore leads to quenching of the fluorescence of the system. This corresponds to 'off' state of fluorescence as depicted in figure 1.1. Later, when the guest binds to the receptor, the electron transfer from the receptor to the excited fluorophore is blocked and this results in a revival of the fluorescence of the system. This situation is represented by figure 1.2. Thus, the signaling to the outside world is achieved by an enhancement or a quenching of the fluorescence. The receptors are chosen such that electron

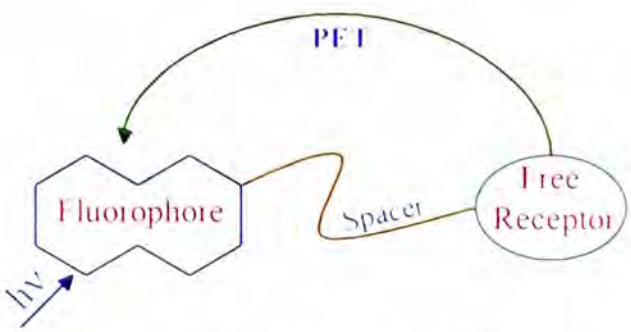

Fig. 1.1. Fluorescence 'off' state

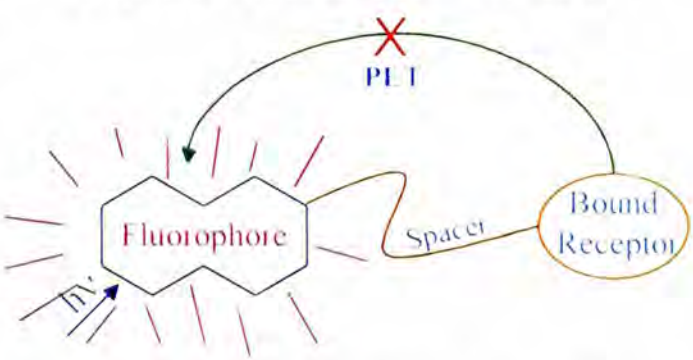

Fig. 1.2. Fluorescence 'on' state

transfer from the receptor to the fluorophore is allowed in the excited state. This suggests that the electrons associated with the receptor moiety are responsible for blocking the signal to the outside world. When these electrons are arrested by the analyte species, a fluorescence signal to the outside world is transmitted. This is what is termed as 'off-on' fluorescence signaling of the guest species.

The thermodynamic feasibility of the PET can be calculated from the knowledge of the redox potentials of the fluorophore and the receptor and the singlet energy of the fluorophore.[164,166] The receptors commonly empioyed in the design of PET fluorosensors contain amine functionalities that are generally efficient quenchers of the fluorescence and are also good ligands for various guests. The strength of the fluorescence PET signaling mechanism lies in the fact that the receptor systems can vary from very simple amines to very complex functionalities. A sensor can be made for various guest molecules by varying the receptor moieties satisfying the redox conditions. PET sensors have been developed for a wide variety of analytes ranging from cations to anions to neutral molecules.[46,53] It all started from N-methylbenzyl amine, one of the early fluorescent PET sensors to be synthesized.[167] A breakthrough was later achieved due to Tsien who developed a powerful molecule for real time and real space determination of the activity of Ca^{2+} within living cell by fluorescence.[70] From there on, we have come a long way in the development of PET sensors. Remarkable contributions to the development of fluorescent PET sensors have come from de Silva and coworkers.[46,48,163,164,168-172] Lehn,[7,8] Balzani,[9,10,173] Valeur,[52,150,161,162] Fabbrizzi,[59,60,95,165,174,175] Czarnik,[42,61,73,176] Shinkai,[82-

[84] Ueno,[145,177] Beer[92,93,178] and many others[4,54-57,62,96,97,100,106,144,179-186] have made significant contributions to this area.

While the most commonly employed receptors for PET sensors are simple amines, cyclic amines, where macrocyclic effect comes into the picture, are also quite popular and useful. The efficiency of a cyclic ligand to tightly bind the analyte compared to its open chain analogue is often referred to as the macrocyclic effect.[187] The discovery of crown ethers by Pederson has drastically changed the nature of the coordination chemistry of the metal ions.[188] Large amount of work has been done on the coordination chemistry of cations to crown ethers and a study of the macrocyclic effect.[1,189] A great deal of efforts are being made towards developing efficient molecular devices and sensors by changing the oxygen of the crowns to nitrogen and sulphur and by making cage like compounds, the cryptands.[6,10,35,174,190]

1.5. Some PET sensors for various analytes

Some typical PET sensors developed for various analytes have been highlighted here. A more detailed discussion on PET sensors and the examples can be found in some of the recent review articles.[46,52,53,62,95]

Compound **1** represents an early example of a PET sensor molecule.[167] Shizuka and coworkers[191] studied the pH dependent fluorescence of **1** and its derivatives and measured their ground and excited state pK_a values. They

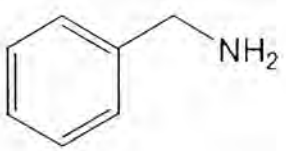

1

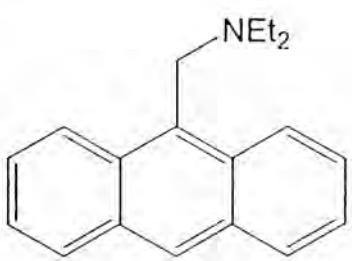

2

suggested that there is no CT interaction between the protonated amino group and the phenyl ring separated by methylene group in the excited state. Compound **2** is an early example of a fluorescent pH sensor developed by de Silva and coworkers.[164,168] The difference in the fluorescence quantum yields of the non-protonated and protonated forms of **2** was instrumental in the signaling behavior. It is one of the very early examples of a huge number of sensor molecules that have come from de Silva and coworkers.[16,17,53]

Compounds **3** and **4** are PET fluorosensors in which the receptor is a linear polyamine. **3** is reported to exhibit pH dependent fluorescence in acetonitrile/water solutions.[192] The fluorescence is particularly quenched above pH 4.0 when the amino groups are not protonated. The system was shown to

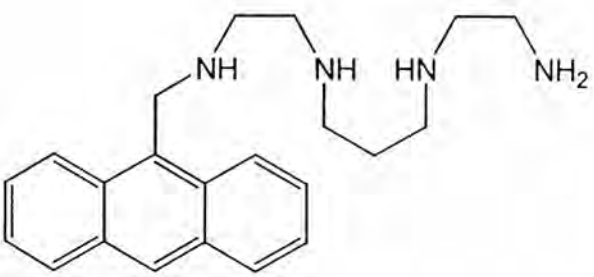

3

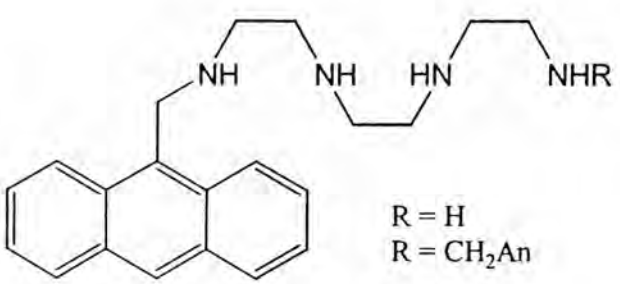

4

behave differently with Cu^{2+}, Ni^{2+} and Zn^{2+}. With Cu^{2+} and Ni^{2+}, the fluorescence gets quenched, whereas with Zn^{2+}, there is an enhancement in the fluorescence.[192] **4** is reported to be the first molecule useful for the ratiometric determination of Zn^{2+} in aqueous medium.[193] When two anthracene (An) moieties are used as the fluorophore components in **4**, (R = CH_2An), the free molecule shows excimer emission in the 450 - 600 nm region. Addition of Zn^{2+}

increases the excimer emission intensity. This behavior serves for a direct concentration measurement by following the monomer/excimer emission intensity ratio.

5 and **6** are examples of simple PET sensors that can bind transition metal ions.[185] A greater selectivity is reported for Cu^{2+} with these sensor systems in 2-propanol solution. These simple systems can detect Cu^{2+} at sub-ppm levels.[185] Ni^{2+} modulates the fluorescence intensity at much higher concentrations whereas other metal ions do not produce any change in the fluorescence behavior of the systems.

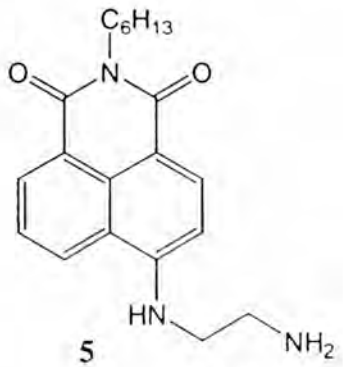

5

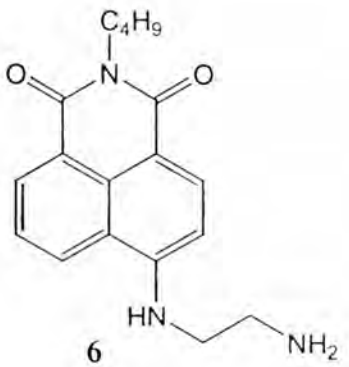

6

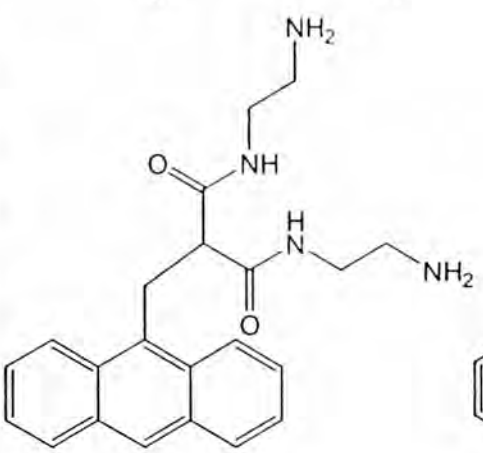

7

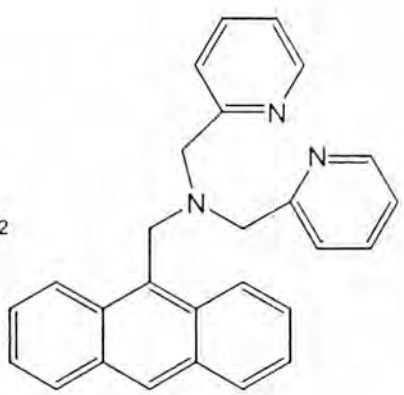

8

The higher ligand field stabilization energies of Ni^{2+} and Cu^{2+} have been employed by Fabbrizzi in designing selective sensor **7** for these metal ions by using a dioxo-tetramine ligand.[58,60,194] The complexation mechanism involves deprotonation of amide groups. This can take place only with metal ions that profit by large ligand field stabilization. The difference in ligand field stabilization energy between Cu^{2+} and Ni^{2+} allows their distinction too. **8** is an

'off-on-off' sensor for protons.[195] This system also exhibits 'off-on' fluorescence signaling behavior with Zn^{2+}.

In **9**, the luminescence of dansyl chromophore and the high affinity of the tetraaza crown, the cyclen moiety, is combined for binding of Zn^{2+}.[64,196] The system is found to bind Zn^{2+} with very high affinity at physiological pH. **10** is a cyclic analogue of **7** wherein the macrocyclic effect in binding the cations, Cu^{2+} and Ni^{2+} results disadvantageously in narrowing the pH window available for selective titration.[192]

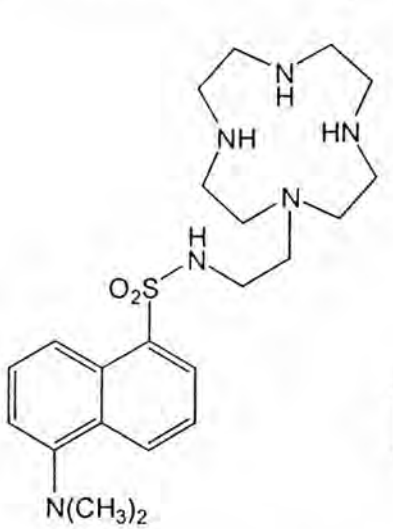

9

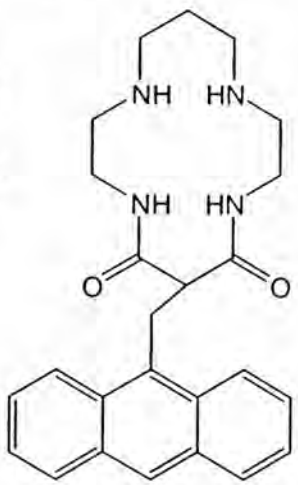

10

Sensor **11**, which is an extrapolation of **2**, is an excellent 'off-on' sensor for K^{+}.[48,53] Some derivatives of **12** are reported to bind Zn^{2+} and Cd^{2+} effectively in aqueous solution.[73]

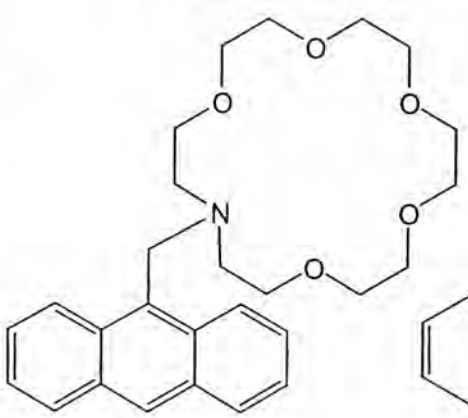

11

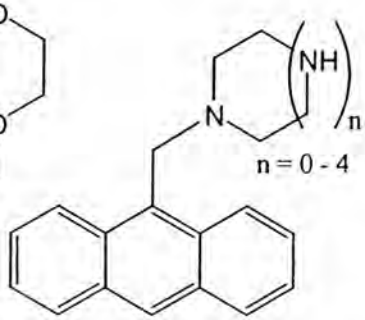

12

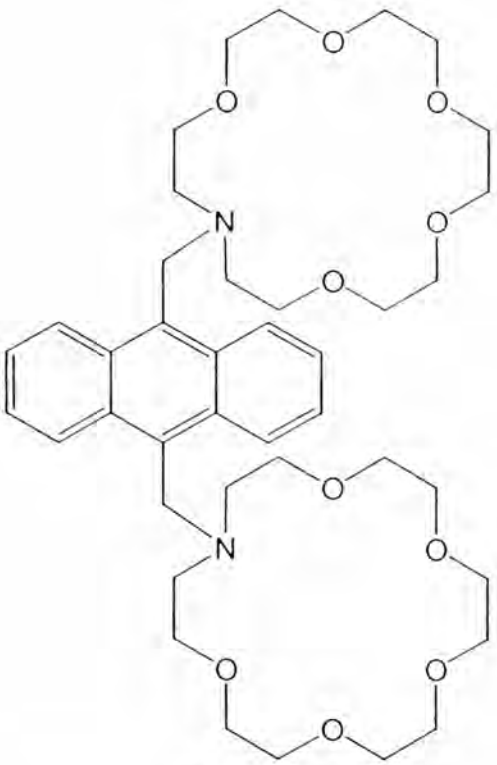

13

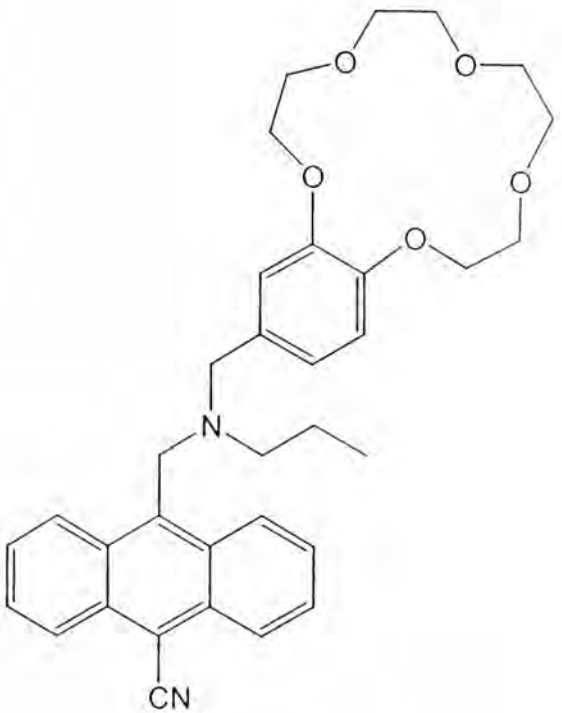

14

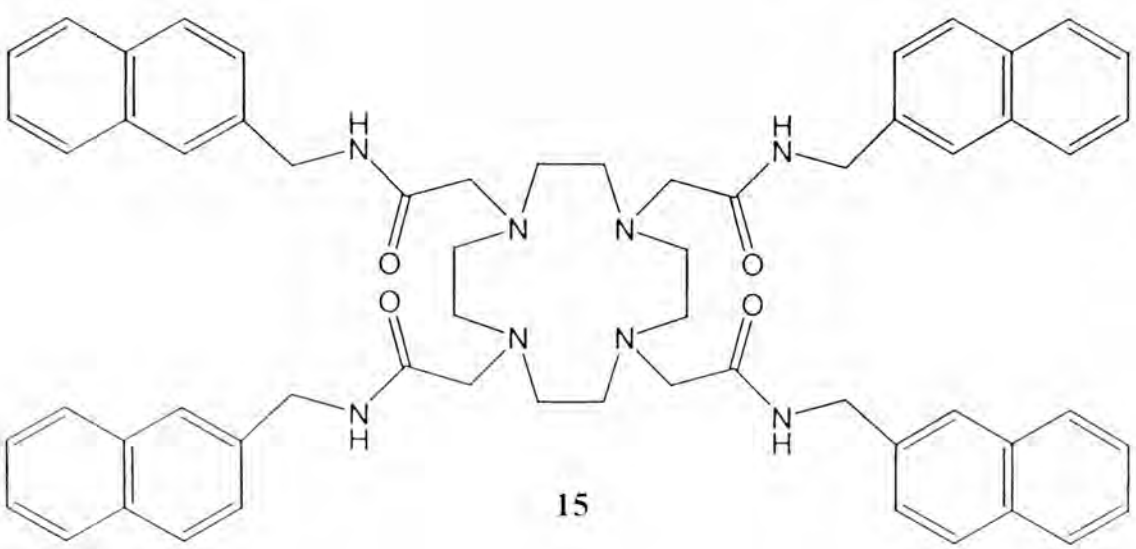

15

13 employs two PET active receptors and is a higher generation of **11**. A degree of length recognition is achieved with this system and excellent switching 'on' of fluorescence was found with α,ω-alkanediammonium ions.[169]

14 is capable of mimicking the switching phenomena in information technology based on molecular logic devices.[170] **14** acts as an AND logic gate when we consider H^+ and Na^+ as the two ionic inputs, fluorescence as the output and exciting light as the power supply.

Binding of Cd^{2+} and Pb^{2+} with **15** is monitored through the decrease in the excimer emission intensity.[179,197]

16 provides the first example of a metal-triggered metal-centered emission.[198] It contains a terpyridyl diester that can strongly bind Eu^{3+} and a crown to potentially bind K^+. PET from the aza crown moiety quenches the fluorescence of Eu^{3+} bound to the terpyridyl diester site. Binding of K^+ results in an enhancement in the fluorescence intensity of the system.

17 and **18** represent fluorescent PET sensors in which the monomer/excimer emission intensity ratio serves as the tool to study the sensing behavior towards metal ions.[144,199,200] **17** gives larger stability constants with K^+ and Ba^{2+}. In **18**, the monomer like emission enhances in intensity and the excimer emission vanishes on binding $H_3N^+(CH_2)_7N^+H_3 2Cl^-$.

19 and **20** employ cryptand based receptors.[201-203] The cavity in these receptors is suitable for K^+. **19** has been used quite successfully in monitoring the level of K^+ in blood and across biological membranes.

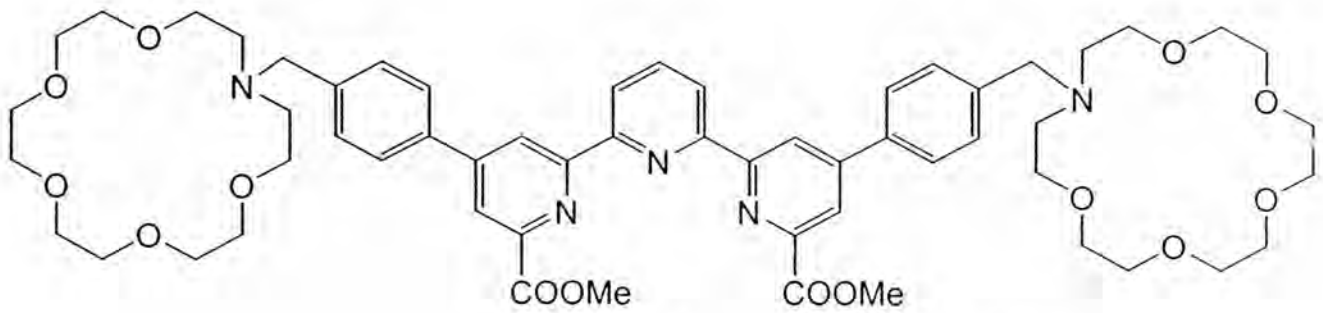

16

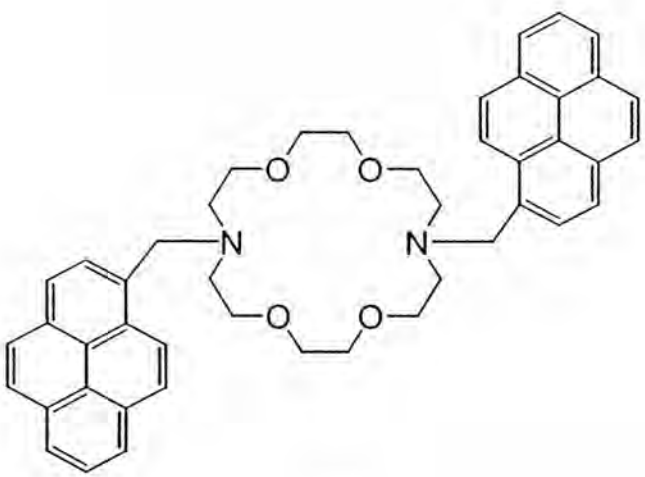

17

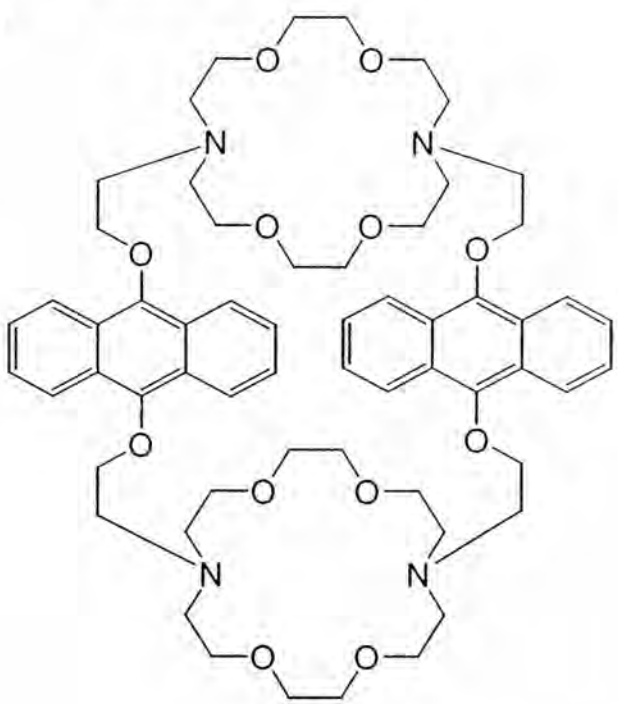

18

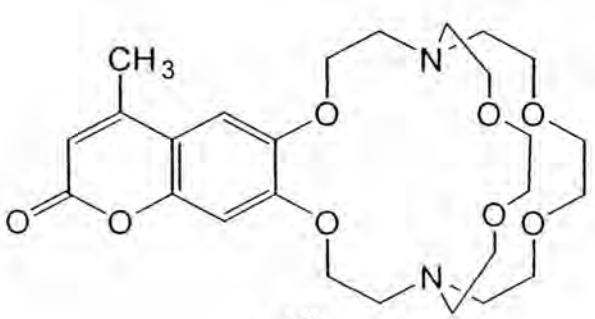

19

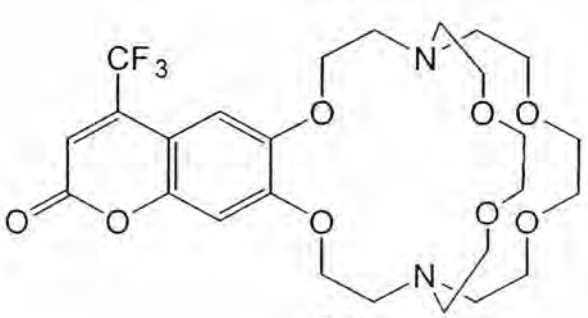

20

21 is developed to sense the γ-aminobutyric acid (GABA) zwitterions.[204] The carboxylate terminal of GABA is held by the guanidinium moiety in **21**. **22** is developed by Cooper and James and is shown to be an excellent sensor for glucosamine.[205]

23 contains a partially protonated receptor moiety and is a PET fluorosensor for phosphate ion.[206] **24**, when complexed with Zn^{2+}, serves as an efficient PET sensor for carboxylate ions.[95] The signaling of the anion is achieved by a quenching of the fluorescence of **24-Zn^{2+}** complex. The anion replaces the solvent molecule at the axial position of the trigonal bipyramidal complex and quenches the fluorescence of the system via an electron transfer process.

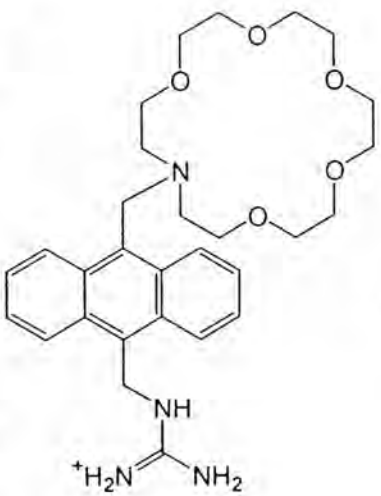

21

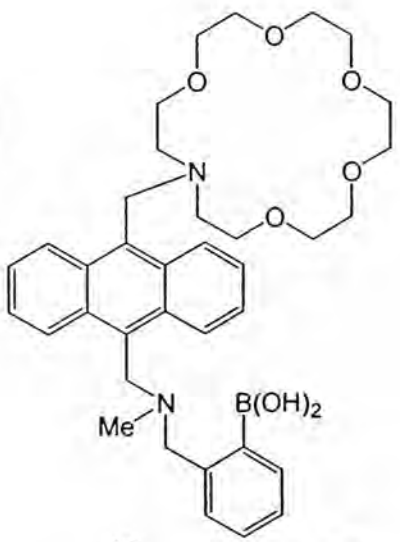

22

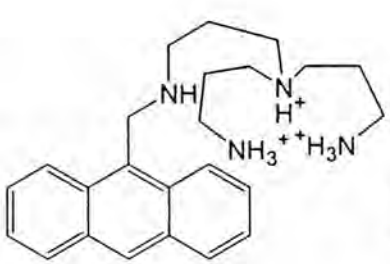

23

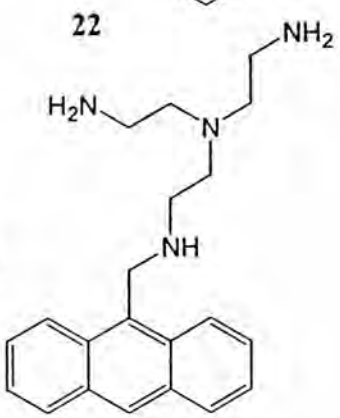

24

As evident from the above discussion, considerable work has been done on fluorescence signaling of the cations of s-block elements. What eluded the literature till recently were the sensor systems for some of the transition metal ions, though, as stated previously, these are metal ions of increasing importance in

biology and environment. This is believed to be due to the fact that the transition metal ions are notorious quenchers of fluorescence.[207,208] In order to develop efficient 'off-on' signaling systems for the transition metal ions, Ghosh et al. utilized a bitripodal cryptand receptor that not only binds the metal ions tightly but also insulates them from the fluorophore moiety thereby preventing the quenching interaction between the metal ions and the fluorophore.[182,209] This excellent design strategy led to the development of **25**,[182,209] reported to be one of the first fluorosensors for some of the transition metal ions that are notorious for their quenching abilities.

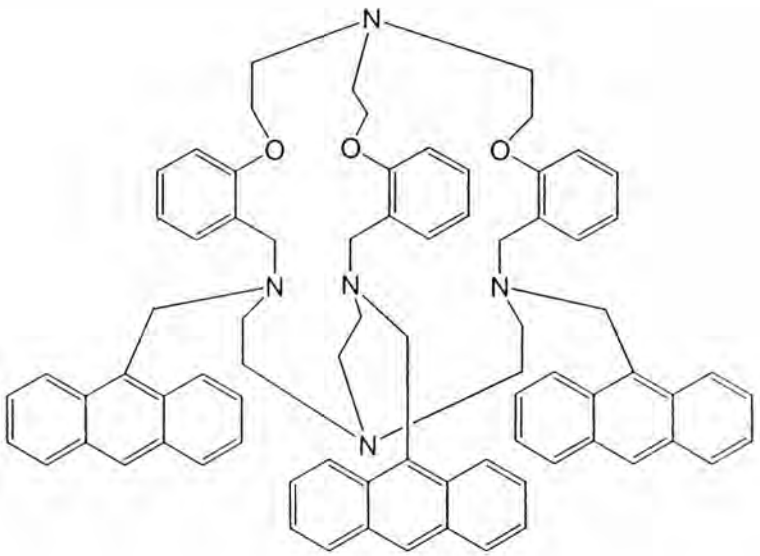

25

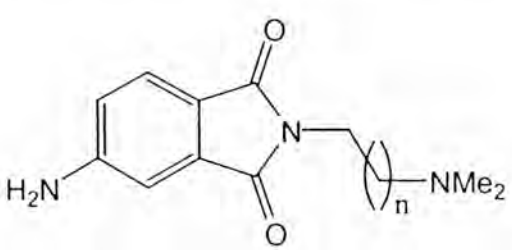

26

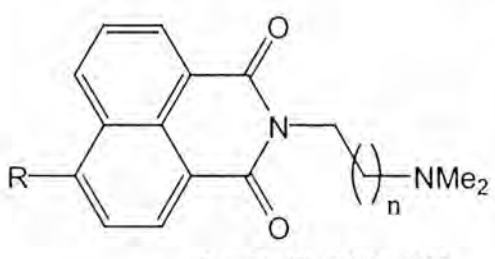

R = H, Cl, OMe, NH_2

27

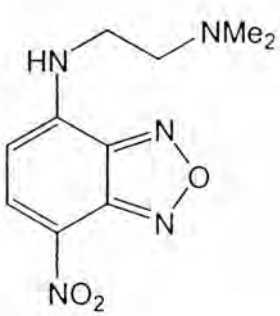

28

Samanta and coworkers, on the other hand, used a different strategy for the development of the 'off-on' sensor systems for the quenching metal ions.[210] Taking into consideration the fact that the interaction between the fluorophore and

the transition metal ions is predominantly redox in nature, they thought that this quenching interaction could be significantly reduced by employing an electronically deficient fluorophore in the *fluorophore-spacer-receptor* system. Studies along this direction gave birth to simple systems such as **26 – 28,** which show excellent fluorescence enhancement in the presence of quenching transition metal ions.[210-215]

1.6. Motivation of the thesis

It should be noted here that the PET sensors developed by Samanta and coworkers following the above approach, though exhibit excellent fluorescence signaling towards the transition metal ions, do not show any selectivity in binding the transition metal ions. Developing sensor molecule that is specific to a particular analyte is a challenging task and to accomplish this job one needs to select a receptor component for the *fluorophore-spacer-receptor* sensor system such that it selectively binds the specific guest leaving others, if any, in the medium. Another point of interest is to explore whether sensor molecules can be developed based on a signaling mechanism that has not been exploited so far. The present work is undertaken taking these two points into consideration.

Pyridine has been used earlier as a receptor component while developing the sensor systems owing to its ability to form complexes and because there occurs a large decrease of the reduction potential upon the formation of pyridinium ion by coordination with proton and other cations.[216-221] The photochemistry of transition metal compounds, particularly those of ruthenium with polypyridyl ligands, is as old as photochemistry itself.[222,223] Keeping the

coordination chemistry of pyridine towards the transition metal ions and its redox properties in mind, we decided to synthesize some *fluorophore-spacer-receptor* sensor systems with pyridine as the receptor moiety. Two structurally simple systems, **NPY** and **PPY** (Chart 1.1.) have been developed, and their photophysical and metal ion signaling behavior have been studied. We show that these systems represent an important class of compounds whose signaling mechanism is different from conventional PET sensing mechanism. Moreover, we show that these systems show wavelength window based 'on-off' and 'off-on' fluorescence signaling of the transition metal ions.

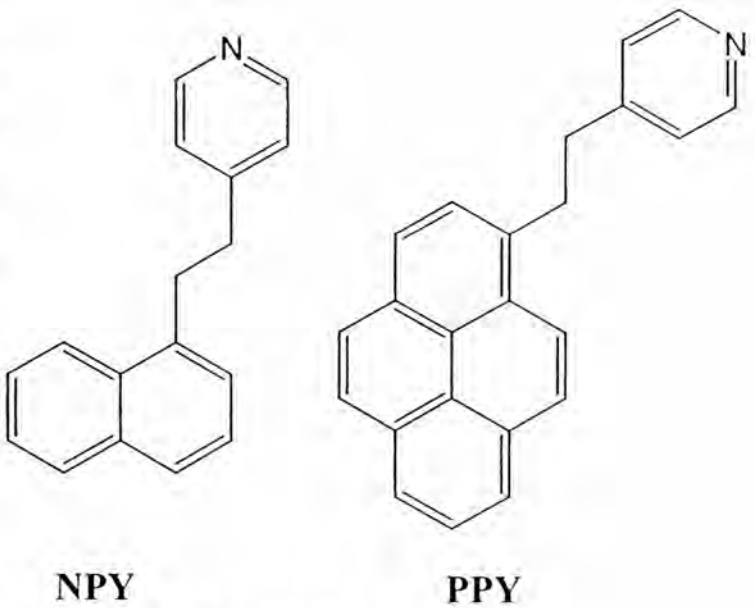

NPY **PPY**

Chart 1.1.

The crown compounds are expected to show better binding of the guest molecules compared to their linear analogues on account of the macrocyclic effect.[187] They also show excellent selectivity in binding the various guest molecules based on their cavity size.[1,188,224] The selective binding of Li^+, Na^+ and K^+ respectively with 12-crown-4, 15-crown-5 and 18-crown-6 are documented in the literature.[189] Oxygen crowns bind the s-block metals tightly. However, for the transition metal ions, the oxygen crowns are not good coordinating ligands. When the oxygen of the crown ether are replaced by

nitrogen, one can expect a stronger binding of the transition metal ions because of an enhanced binding ability of these metal ions with nitrogen.[224] With this background, we decided to develop some PET sensor molecules with various aza crowns as the receptor for efficient binding of the transition metal ions, particularly trace metal ions of importance in biology and in environment. We have developed a few sensor systems varying the receptor moieties with the idea of studying the effect of the ring size and the number and nature of binding sites. The fluorophore of our choice is 4-aminophthalimide (AP) as the photophysical behavior of this molecule is well understood[225-227] and previous studies have indicated that AP is an electron deficient molecule and hence ideally suited as the fluorophore component of the *fluorophore-spacer-receptor* sensor system.[210,213] Five systems, namely **APMAC4, APMAC5, APMAC6, APDAC** and **APTAC** (Chart 1.2.) differing in their receptor components have been synthesized and the

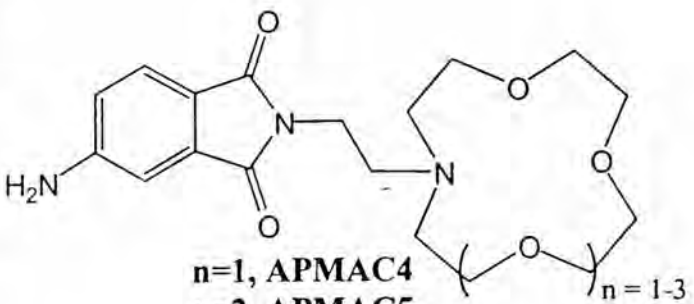

n=1, APMAC4
n=2, APMAC5
n=3, APMAC6

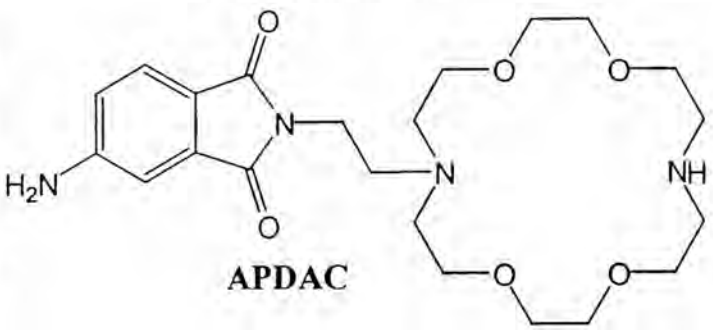

APDAC

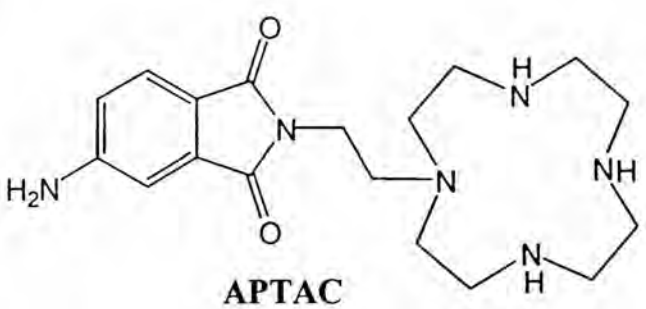

APTAC

Chart 1.2.

signaling behavior of these systems towards the transition metal ions has been investigated.

1.7. Layout of the thesis

The thesis consists of seven chapters. The first chapter provides an introduction to fluorescence signaling with focus on the systems based on photoinduced electron transfer (PET) mechanism. It also gives a brief idea on the principle of molecular recognition and looks into the development of molecular scale devices. The second chapter describes the various experimental procedures adopted in the thesis along with the detailed synthetic scheme and analytical data of the various multi-component sensor systems. Chapter 3 describes the photophysical behavior of the *fluorophore-spacer-receptor* systems, **NPY** and **PPY**. The cation signaling properties of **NPY** and **PPY** have been outlined in the fourth chapter. It is shown that 'off-on' fluorescence signaling mechanism of these systems is quite different from that in the conventional PET systems. Chapter 5 focuses on the photophysical and metal ion signaling behavior of the aza crown compounds. Specific sensing of certain metal ions that could be achieved by **APTAC** is discussed in detail. Chapter 6 presents the X-ray diffraction studies on the single crystal of cyclen, which has been used as one of the receptor components. The main finding of this investigation, characterization of a highly ordered water chain with a novel hydrogen bonding motif, is highlighted in this chapter. Chapter 7 concludes the work presented in the thesis touching upon the achievements and looking into the scope of further work that can be carried out based on the present finding.

1.8. References

(1) Steed, J. W.; Atwood, J. L. *Supramolecular Chemistry*; John Wiley & Sons: New York, 2000.

(2) Ward, C. J.; Patel, P.; James, T. D. *Org. Lett.* **2002**, *4*, 477.

(3) Zhong, Z.; Anslyn, E. V. *J. Am. Chem. Soc.* **2002**, *124*, 9014.

(4) Arimori, S.; Ushiroda, S.; Peter, L. M.; Jenkins, A. T. A.; James, T. D. *Chem. Commun.* **2002**, 2368.

(5) Bergonzi, R.; Fabbrizzi, L.; Lichelli, M.; Mangano, C. *Coord. Chem. Rev.* **1998**, *170*, 31.

(6) Lehn, J.-M. *Supramolecular Chemistry*; VCH, Weinheim, 1995.

(7) Lehn, J.-M. *Angew. Chem., Int. Ed.* **1988**, *27*, 89.

(8) Lehn, J.-M. *Angew. Chem., Int. Ed.* **1990**, *29*, 1304.

(9) Balzani, V.; Moggi, L.; Scandola, F. In *Supramolecular Photochemistry*; Balzani, V., Ed.; Reidel Publishing Company: Dordrecht, 1987.

(10) Balzani, V.; Gomez-Lopez, M.; Stoddart, J. F. *Acc. Chem. Res.* **1998**, *31*, 405.

(11) Aviram, A. *J. Am. Chem. Soc.* **1988**, *110*, 5687.

(12) Carter, F. L. *Physica* **1984**, *10D*, 175.

(13) Fox, M. A. *Acc. Chem. Res.* **1999**, *32*, 201.

(14) *Molecular Electronic Devices*; Carter, F. L.; Siatkowski, R. E.; Wohltjen, H., Eds.; Elsevier: Amsterdam, 1988.

(15) de Silva, A. P.; Fox, D. B.; Moody, T. S.; Weir, S. M. *Trends Biotechnol.* **2001**, *19*, 29.

(16) de Silva, A. P.; Fox, D. B.; Moody, T. S.; Weir, S. M. *Pure Appl. Chem.* **2001**, *73*, 503.

(17) de Silva, A. P.; McClenaghan, N. D. *Chem. Eur. J.* **2002**, *8*, 4935.

(18) Ball, P. *New Scientist* **1997**, *155*, 32.

(19) Bumm, L. A.; Arnold, J. J.; Cygan, M. T.; Dunbar, T. D.; Burgin, T. P.; Jones II, L.; Allara, D. L.; Tour, J. M.; Weiss, P. S. *Science* **1996**, *271*, 1705.

(20) Barigelletti, F.; Flamigni, L. *Chem. Soc. Rev.* **2000**, *29*, 1.

(21) Wagner, R. W.; Lindsey, J. S. *J. Am. Chem. Soc.* **1994**, *116*, 9759.

(22) Wagner, R. W.; Lindsey, J. S.; Seth, J.; Palaniappan, V.; Bocian, D. F. *J. Am. Chem. Soc.* **1996**, *118*, 3996.

(23) Credi, A.; Balzani, V.; Langford, S. J.; Stoddart, J. F. *J. Am. Chem. Soc.* **1997**, *119*, 2679.

(24) Kelly, T. R.; Bowyer, M. C.; Bhaskar, K. V.; Bebbington, D.; Garcia, A.; Lang, F.; Kim, M. H.; Jette, M. P. *J. Am. Chem. Soc.* **1994**, *116*, 3657.

(25) Kelly, T. R.; Tellitu, I.; Sestelo, J. P. *Angew. Chem., Int. Ed.* **1997**, *36*, 1866.

(26) Ahmed, F. R.; Burrows, P. E.; Donovan, K. J.; Wilson, E. G. *Synth. Met.* **1988**, *27B*, 593.

(27) Martin, A. S.; Sambles, J. R. *Adv. Mater.* **1993**, *5*, 580.

(28) Rong, D.; Mallouk, T. E. *Inorg. Chem.* **1993**, *32*, 1454.

(29) Clayden, J.; Pink, J. H. *Angew. Chem., Int. Ed.* **1998**, *37*, 1937.

(30) Raymo, F. M.; Giordani, S. *J. Am. Chem. Soc.* **2001**, *123*, 4651.

(31) Bissel, R. A.; Cordova, E.; Kaifer, A. E.; Stoddart, J. F. *Nature* **1994**, *369*, 133.

(32) Brown, G. J.; de Silva, A. P.; Pagliari, S. *Chem. Commun.* **2002**, 2461.

(33) de Silva, A. P.; McClenaghan, N. D. *J. Am. Chem. Soc.* **2000**, *122*, 3965.

(34) Gunnlaugsson, T.; Mac Donail, D. A.; Parker, D. *Chem. Commun.* **2000**, 93.

(35) Xu, H.; Xu, X.; Dabestani, R.; Brown, G. M.; Fan, L.; Patton, S.; Hai-Feng, J. *J. Chem. Soc. Perkin Trans. 2* **2002**, 636.

(36) Saghatelian, A.; Völker, N. H.; Guckian, K. M.; Lin, V. S.-Y.; Ghadiri, R. *J. Am. Chem. Soc.* **2003**, *125*, 346.

(37) Holten, D.; Bocian, D. F.; Lindsey, J. S. *Acc. Chem. Res.* **2002**, *35*, 57.

(38) Bryan, A. J.; de Silva, A. P.; de Silva, S. A.; Rupasinghe, R. A. D. D.; Sandanayake, K. R. A. S. *Biosensors* **1989**, *4*, 169.

(39) Thomas, J. K. *Chem. Rev.* **1980**, *80*, 283.

(40) Turro, N. J.; Gratzel, M.; Braun, A. M. *Angew. Chem., Int. Ed.* **1980**, *19*, 675.

(41) Zang, L.; Liu, R.; Holman, M. W.; Nguyen, K. T.; Adams, D. M. *J. Am. Chem. Soc.* **2002**, *124*, 10640.

(42) Czarnik, A. W. In *Fluorescent Chemosensors for Ion and Molecule Recognition*; Czarnik, A. W., Ed.; ACS Symposium Series: Washington DC, 1993; Vol. 538.

(43) Lakowicz, J. R. In *Topics in Fluorescence Spectroscopy*; Lakowicz, J. R., Ed.; Plenum Press: New York, 1994; Vol. 4.

(44) Szmacinski, H.; Lakowicz, J. R. In *Fluorescent Chemosensors for Ion and Molecule Recognition*; Czarnik, A. W., Ed.; ACS Symposium Series: Washington DC, 1993; Vol. 538.

(45) Alcala, J. R. In *Topics in Fluorescence Spectroscopy*; Lakowicz, J. R., Ed.; Plenum Press: New York, 1994; Vol. 4.

(46) de Silva, A. P.; Gunaratne, H. Q. N.; Gunnlaugsson, T.; Huxley, A. J. M.; McCoy, C. P.; Rademacher, J. T.; Rice, T. E. *Chem. Rev.* **1997**, *97*, 1515.

(47) Czarnik, A. W. In *Topics in Fluorescence Spectroscopy*; Lakowicz, J. R., Ed.; Plenum Press: New York, 1994; Vol. 4.

(48) de Silva, A. P.; de Silva, S. A. *Chem. Commun.* **1986**, 1709.

(49) de Silva, A. P.; Sandanayake, K. R. A. S. *Tetrahedron Lett.* **1991**, *32*, 421.

(50) de Silva, A. P.; Gunaratne, H. Q. N.; Maguire, G. E. M. *Chem. Commun.* **1994**, 1213.

(51) de Silva, A. P.; Gunaratne, H. Q. N.; Gunnlaugsson, T.; Nieuwenhuizen, M. *Chem. Commun.* **1996**, 1967.

(52) Valeur, B.; Leray, I. *Coord. Chem. Rev.* **2000**, *205*, 3.

(53) de Silva, A. P.; Fox, D. B.; Huxley, A. J. M.; Moody, T. S. *Coord. Chem. Rev.* **2000**, *205*, 41.

(54) Fages, F.; Desvergne, J.-P.; Bouas-Laurent, H.; Marsau, P.; Lehn, J.-M.; Kotzyba-Hilbert, F.; Albrecht-Gary, A.-M.; Al-Joubbeh, M. *J. Am. Chem. Soc.* **1989**, *111*, 8672.

(55) Prodi, L.; Ballardini, R.; Gandolfi, M. T.; Roversi, R. *J. Photochem. Photobiol. A: Chem.* **2000**, *136*, 49.

(56) Nishizawa, N.; Watanabe, M.; Uchida, T.; Terame, N. *J. Chem. Soc. Perkin Trans. 2* **1999**, 141.

(57) Gunnlaugsson, T.; Bichell, B.; Nolan, C. *Tetrahedron Lett.* **2002**, *43*, 4989.

(58) Fabbrizzi, L.; Lichelli, M.; Pallavicini, P.; Parodi, L.; Taglietti, A. In *Transition Metals in Supramolecular Chemistry*; Sauvage, J. P., Ed.; John Wiley & Sons: New York, 1999.

(59) Fabbrizzi, L.; Lichelli, M.; Pallavicini, P. *Acc. Chem. Res.* **1999**, *32*, 846.

(60) Fabbrizzi, L.; Licchelli, M.; Pallavicini, P.; Perroti, A.; Sacchi, D. *Angew. Chem., Int. Ed.* **1994**, *33*, 1975.

(61) Yoon, J.; Ohler, N. E.; Vance, D. H.; Aumiller, W. D.; Czarnik, A. W. *Tetrahedron Lett.* **1997**, *38*, 3845.

(62) Prodi, L.; Bolletta, F.; Montalti, M.; Zaccheroni, N. *Coord. Chem. Rev.* **2000**, *205*, 59.

(63) Sasaki, D. Y.; Padilla, B. E. *Chem. Commun.* **1998**, 1581.

(64) Kimura, E.; Koike, T. *Chem. Soc. Rev.* **1998**, *27*, 179.

(65) Kang, J.; Choi, M.; Kwong, J. Y.; Lee, E. Y.; Yoon, J. *J. Org. Chem.* **2002**, *67*, 4384.

(66) Rurack, K. *Spectrochim. Acta, Part A.* **2001**, *57*, 2161.

(67) Tsein, R. Y. In *Fluorescent Chemosensors for Ion and Molecule Recognition*; Czarnik, A. W., Ed.; ACS Symposium Series: Washington DC, 1993; Vol. 538.

(68) Masilamani, D.; Lucas, M. E. In *Fluorescent Chemosensors for Ion and Molecule Recognition*; Czarnik, A. W., Ed.; ACS Symposium Series: Washington DC, 1993; Vol. 538.

(69) Collado, D.; Perez-Inestrosa, E.; Suau, R.; Desvergne, J.-P.; Bouas-Laurent, H. *Org. Lett.* **2002**, *4*, 855.

(70) Grynkiewicz, G.; Poenie, M.; Tsien, R. Y. *J. Biol. Chem.* **1985**, *260*, 3440.

(71) Kuhn, M. A. In *Fluorescent Chemosensors for Ion and Molecule Recognition*; Czarnik, A. W., Ed.; ACS Symposium Series: Washington DC, 1993; Vol. 538.

(72) Huston, M. E.; Haider, K. W.; Czarnik, A. W. *J. Am. Chem. Soc.* **1988**, *110*, 4460.

(73) Akkaya, E. U.; Huston, M. E.; Czarnik, A. W. *J. Am. Chem. Soc.* **1990**, *112*, 3590.

(74) Maruyama, S.; Kikuchi, K.; Hirano, T.; Urano, Y.; Nagano, T. *J. Am. Chem. Soc.* **2002**, *124*, 10650.

(75) Jiang, L. J.; Wang, Z. L.; Jiang, X. Q.; Luo, Q. H. *Chin. Chem. Lett.* **2000**, *11*, 551.

(76) Ma, H.; Ma, Q.; Su, M.; Nie, L.; Han, H.; Xiong, S.; Xin, B.; Liu, G. *New J. Chem.* **2002**, *26*, 1456.

(77) Xia, W.-S.; Schmehl, R. H.; Li, C.-J.; Mague, J. T.; Luo, C.-P.; Guldi, D. M. *J. Phys. Chem. B* **2002**, *106*, 833.

(78) Costero, A. M.; Andreu, R.; Monrabel, E.; Martinez-Mamon, R.; Sancenon, F.; Sato, J. *J. Chem. Soc. Dalton Trans.* **2002**, 1769.

(79) Moreno-Bondi, M. C.; Wolfbeis, O. S.; Lerner, M. J. P.; Lerner, B. P. H.; Schaffar, B. P. H. *Anal. Chem.* **1990**, *62*, 2377.

(80) Yamamoto, T.; Seino, Y.; Fukumoto, H.; Koh, G.; Yano, H.; Inagaki, N.; Yamada, Y.; Inoue, K.; Manabe, T.; Imura, H. *Biochim. Biophys. Res. Commun.* **1990**, *170*, 223.

(81) Yasuda, H.; Kurokawa, T.; Fuji, Y.; Yamashita, A.; Ishibashi, S. *Biochim. Biophys. Acta.* **1990**, *1021*, 114.

(82) James, T. D.; Sandanayake, K. R. A. S.; Shinkai, S. *Nature* **1995**, *374*, 345.

(83) James, T. D.; Linnane, P.; Shinkai, S. *Chem. Commun.* **1996**, 281.

(84) James, T. D.; Shinmori, H.; Shinkai, S. *Chem. Commun.* **1997**, 71.

(85) Orellana, G.; Moreno-Bondi, M. C.; Segovia, E.; Marazuela, M. D. *Anal. Chem.* **1992**, *64*, 2210.

(86) Pinalli, R.; Nachtigall, F. F.; Ugozzoli, F.; Dalcanale, E. *Angew. Chem., Int. Ed.* **1999**, *38*, 2377.

(87) Lin, J.; Hu, Q.-S.; Xu, M.-H.; Pu, L. *J. Am. Chem. Soc.* **2002**, *124*, 2088.

(88) Wang, W.; Springsteen, G.; Gao, S.; Wang, B. *Chem. Commun.* **2000**, 1283.

(89) Fabbrizzi, L.; Francese, G.; Lichelli, M.; Perotti, A.; Taglietti, A. *Chem. Commun.* **1997**, 581.

(90) Frausto-deSilva, J. J. R.; Williams, R. J. P. *Struct. Bonding* **1976**, *29*, 67.

(91) Renkawek, K.; Bosman, G. J. C. G. M. *Neuroreport* **1995**, *6*, 929.

(92) Beer, P. D.; Cadman, J. *Coord. Chem. Rev.* **2000**, *205*, 131.

(93) Beer, P. D. *Acc. Chem. Res.* **1998**, *31*, 71.

(94) Fabbrizzi, L.; Faravelli, I.; Francese, G.; Lichelli, M.; Perotti, A.; Taglietti, A. *Chem. Commun.* **1998**, 971.

(95) Fabbrizzi, L.; Lichelli, M.; Rabaioli, G.; Taglietti, A. *Coord. Chem. Rev.* **2000**, *205*, 85.

(96) Nishizawa, S.; Kaneda, H.; Uchida, T.; Terame, N. *Chem. Commun.* **1998**, 2325.

(97) Nishizawa, S.; Kato, Y.; Terame, N. *J. Am. Chem. Soc.* **1999**, *121*, 9463.

(98) Mizukami, S.; Nagano, T.; Urano, Y.; Odani, A.; Kikuchi, K. *J. Am. Chem. Soc.* **2002**, *124*, 3920.

(99) Anzenbacher, P. J.; Tyson, D. S.; Jursíková, K.; Castellano, F. N. *J. Am. Chem. Soc.* **2002**, *124*, 6232.

(100) Gunnlaugsson, T.; Davis, A. P.; O'Brien, J. E.; Glynn, M. *Org. Lett.* **2002**, *4*, 2449.

(101) Liao, J.-H.; Chen, C.-T.; Fang, J.-M. *Org. Lett.* **2002**, *4*, 561.

(102) Fabbrizzi, L.; Licchelli, M.; Parodi, L.; Poggi, A.; Taglietti, A. *J. Fluoresc.* **1998**, *8*, 263.

(103) Beer, P. D.; Timoshenko, V.; Maestri, M.; Passaniti, P.; Balzani, V. *Chem. Commun.* **1999**, 1755.

(104) De Santis, G.; Fabbrizzi, L.; Lichelli, M.; Poggi, A.; Taglietti, A. *Angew. Chem., Int. Ed.* **1996**, *35*, 202.

(105) Lee, D. H.; Lee, H. Y.; Lee, K. W.; Hong, J.-I. *Chem. Commun.* **2001**, 1188.

(106) Parker, D.; Senanayake, K.; Williams, J. A. G. *Chem. Commun.* **1997**, 1777.

(107) Cooper, C. R.; Spencer, N.; James, T. D. *Chem. Commun.* **1998**, 1365.

(108) Kubo, Y.; Tsukahara, M.; Ishihara, S.; Tokita, S. *Chem. Commun.* **2000**, 653.

(109) Kalyanasundaram, K.; Thomas, J. K. *J. Phys. Chem.* **1977**, *81*, 2176.

(110) Lianos, P.; Lux, B.; Gerard, D. *J. Chim. Phys.* **1988**, *77*, 907.

(111) Ogawa, S.; Tsuchiya, S. *Chem. Lett.* **1996**, 709.

(112) Shirai, M.; Ishimaru, S.; Tsunooka, M. *J. Fluoresc.* **1993**, *3*, 51.

(113) Nagasaki, T.; Tajirl, Y.; Shinkai, S. *Rec. Trav. Chim. Pays Bas* **1993**, *112*, 407.

(114) Jones, G.; Jackson, W. R.; Kanoktanaporn, S.; Bergmark, W. R. *Photochem. Photobiol.* **1985**, *42*, 477.

(115) Martin, M. M.; Plaza, P.; Dai, H. N.; Meyer, Y. H.; Bourson, J.; Valeur, B. *Chem. Phys. Lett.* **1993**, *202*, 425.

(116) Martin, M. M.; Plaza, P.; Meyer, Y. H.; Badaoui, F.; Bourson, J.; Lefebvre, J. P.; Valeur, B. *J. Phys. Chem.* **1996**, *100*, 6879.

(117) Létard, J.-F.; Lapouyade, R.; Rettig, W. *Pure Appl. Chem.* **1993**, *65*, 1705.

(118) Dumon, P.; Jonasauskas, G.; Dupuy, F.; Pee, P.; Rullière, C.; Létard, J.-F.; Lapouyade, R. *J. Phys. Chem.* **1994**, *98*, 10391.

(119) Mathevet, R.; Jonasauskas, G.; Rullière, C.; Létard, J.-F.; Lapouyade, R. *J. Phys. Chem.* **1995**, *99*, 15709.

(120) MacQueen, D. B.; Schanze, K. S. *J. Am. Chem. Soc.* **1991**, *113*, 6108.

(121) Shen, Y.; Sullivan, B. P. *Inorg. Chem.* **1995**, *34*, 6235.

(122) Yoon, D. I.; BergBrennan, C. A.; Lu, H.; Hupp, J. J. *Inorg. Chem.* **1992**, *31*, 3192.

(123) Beer, P. D. *Chem. Commun.* **1996**, 689.

(124) Beer, P. D.; Dent, S. W.; Wear, T. J. *J. Chem. Soc. Dalton. Trans.* **1996**, 2341.

(125) Demas, J. N.; DeGraff, B. A. In *Topics in Fluorescence Spectroscopy*; Lakowicz, J. R., Ed.; Plenum Press: New York, 1994; Vol. 4.

(126) Kosower, E. M. *Acc. Chem. Res.* **1982**, *15*, 266.

(127) Cowley, D. J. *Nature* **1986**, *319*, 14.

(128) Shizuka, H.; Ogiwara, T.; Kimura, E. *J. Phys. Chem.* **1985**, *89*, 4302.

(129) Vogel, M.; Rettig, W.; Sens, R.; Drexhage, K. H. *Chem. Phys. Lett.* **1988**, *147*, 452.

(130) Jonker, S. A.; Ariese, F.; Verhoewen, J. W. *Rec. Trav. Chem. Pays Bas* **1989**, *108*, 109.

(131) Hamasaki, K.; Ikeda, H.; Nakamura, A.; Ueno, A.; Toda, F.; Suzuki, I.; Osa, T. *J. Am. Chem. Soc.* **1993**, *115*, 5035.

(132) Hamasaki, K.; Ueno, A.; Toda, F. *Chem. Commun.* **1993**, 331.

(133) Rettig, W.; Lapouyade, R. In *Topics in Fluorescence Spectroscopy*; Lakowicz, J. R., Ed.; Plenum Press: New York, 1994; Vol. 4.

(134) Hermant, R. M.; Bakker, N. A. C.; Scherer, T.; Krijnen, B.; Verhowen, J. W. *J. Am. Chem. Soc.* **1990**, *112*, 1214.

(135) Grenfield, S. R.; Svec, W. A.; Gosztola, D.; Wasielewski, M. R. *J. Am. Chem. Soc.* **1996**, *118*, 6767.

(136) Sousa, L. R.; Larson, J. M. *J. Am. Chem. Soc.* **1977**, *99*, 307.

(137) Larson, J. M.; Sousa, L. R. *J. Am. Chem. Soc.* **1978**, *100*, 1943.

(138) Shirai, M.; Tanaka, M. *Chem. Commun.* **1988**, 381.

(139) Emert, J.; Kodali, D.; Catena, R. *Chem. Commun.* **1981**, 758.

(140) Turro, N. J.; Okubo, T.; Weed, G. C. *Photochem. Photobiol.* **1982**, *35*, 325.

(141) Kakizawa, Y.; Akita, T.; Nakamura, H. *Chem. Lett.* **1993**, 1671.

(142) Bouas-Laurent, H.; Castellan, A.; Daney, M.; Desvergne, J.-P.; Guinand, G.; Marsau, P.; Riffaud, M. H. *J. Am. Chem. Soc.* **1986**, *108*, 315.

(143) Marquis, D.; Desvergne, J.-P.; Bouas-Laurent, H. *J. Org. Chem.* **1995**, *60*, 1784.

(144) Fages, F.; Desvergne, J.-P.; Kampke, K.; Bouas-Laurent, H.; Lehn, J.-M.; Meyer, M.; Albrecht-Gary, A.-M. *J. Am. Chem. Soc.* **1993**, *115*, 3658.

(145) Ueno, A.; Moriwaki, F.; Osa, T.; Hamada, F.; Murai, K. *Bull. Chem. Soc. Jpn.* **1986**, *59*, 465.

(146) Kubo, K.; Sakurai, T. *Chem. Lett.* **1996**, 959.

(147) Strauss, J.; Daub, J. *Org. Lett.* **2002**, *4*, 683.

(148) Chardon-Noblat, S.; Sauvage, J.-P.; Mathis, P. *Angew. Chem., Int. Ed.* **1989**, *28*, 593.

(149) Harriman, A.; Sauvage, J.-P. *Chem. Soc. Rev.* **1996**, *25*, 41.

(150) Valeur, B.; Bourson, J.; Pouget, J.; Kaschke, M.; Ernsting, N. P. *J. Phys. Chem.* **1992**, *96*, 6545.

(151) Godwin, H. A.; Berg, J. M. *J. Am. Chem. Soc.* **1996**, *118*, 6514.

(152) Sessler, J. R.; Wang, B.; Harriman, A. *J. Am. Chem. Soc.* **1995**, *117*, 704.

(153) Szmacinski, H.; Lakowicz, J. R. In *Topics in Fluorescence Spectroscopy*; Lakowicz, J. R., Ed.; Plenum Press: New York, 1994; Vol. 4.

(154) Bissel, R. A.; de Silva, A. P.; Gunaratne, H. Q. N.; Lynch, P. L. M.; Maguire, G. E. M.; McCoy, C. P.; Sandanayake, K. R. A. S. *Top. Curr. Chem.* **1993**, *168*, 223.

(155) McFarland, S. A.; Finney, N. S. *J. Am. Chem. Soc.* **2002**, *124*, 1178.

(156) Mello, J. V.; Finney, N. S. *Angew. Chem., Int. Ed.* **2001**, *40*, 1536.

(157) McFarland, S. A.; Finney, N. S. *J. Am. Chem. Soc.* **2001**, *123*, 1260.

(158) Klymchenko, A. S.; Demchenko, A. P. *J. Am. Chem. Soc.* **2002**, *124*, 12372.

(159) Rurack, K.; Resch-Genger, U. *Chem. Soc. Rev.* **2002**, *31*, 116.

(160) McFarland, S. A.; Finney, N. S. *Chem. Commun.* **2003**, 388.

(161) Valeur, B. In *Topics in Fluorescence Spectroscopy*; Lakowicz, J. R., Ed.; Plenum Press: New York, 1994; Vol. 4.

(162) Valeur, B.; Bourson, J.; Pouget, J. In *Fluorescent Chemosensors for Ion and Molecule Recognition*; Czarnik, A. W., Ed.; ACS Symposium Series: Washington DC, 1993; Vol. 538.

(163) Bissel, R. A.; de Silva, A. P.; Gunaratne, H. Q. N.; Lynch, P. L. M.; McCoy, C. P.; Maguire, G. E. M.; Sandanayake, K. R. A. S. In *Fluorescent Chemosensors for Ion and Molecule Recognition*; Czarnik, A. W., Ed.; ACS Symposium Series: Washington DC, 1993; Vol. 538.

(164) Bissel, R. A.; de Silva, A. P.; Gunaratne, H. Q. N.; Lynch, P. L. M.; Maguire, G. E. M.; Sandanayake, K. R. A. S. *Chem. Soc. Rev.* **1992**, *21*, 187.

(165) Fabbrizzi, L.; Poggi, A. *Chem. Soc. Rev.* **1995**, *24*, 197.

(166) Weller, A. *Pure Appl. Chem.* **1968**, *16*, 115.

(167) Wang, Y. C.; Morawetz, H. *J. Am. Chem. Soc.* **1976**, *98*, 3611.

(168) de Silva, A. P.; Rupasinghe, R. A. D. *Chem. Commun.* **1985**, 1669.

(169) de Silva, A. P.; Sandanayake, K. R. A. S. *Angew. Chem., Int. Ed.* **1990**, *29*, 1173.

(170) de Silva, A. P.; Gunaratne, H. Q. N.; McCoy, C. P. *Nature* **1993**, *364*, 42.

(171) Bissel, R. A.; de Silva, A. P.; Fernando, W. T. M. L.; Patuwathavithana, S. T.; Samarasinghe, T. K. S. D. *Tetrahedron Lett.* **1991**, 425.

(172) Bissel, R. A.; de Silva, A. P. *Chem. Commun.* **1991**, 1148.

(173) Balzani, V.; Juzis, A.; Venturi, A. M.; Campagna, S.; Serroni, S. *Chem. Rev.* **1996**, *96*, 759.

(174) Fabbrizzi, L.; Foti, F.; Lichelli, M.; Poggi, A. *Inorg. Chem.* **2002**, *41*, 4612.

(175) Engeser, M.; Fabbrizzi, L.; Lichelli, M.; Sacchi, D. *Chem. Commun.* **1999**, 1191.

(176) Czarnik, A. W. *Acc. Chem. Res.* **1994**, *27*, 302.

(177) Ueno, A. In *Fluorescent Chemosensors for Ion and Molecule Recognition*; Czarnik, A. W., Ed.; ACS Symposium Series: Washington DC, 1993; Vol. 538.

(178) Beer, G.; Rurack, K.; Daub, J. *Chem. Commun.* **2001**, 1138.

(179) Parker, D.; Williams, J. A. G. *J. Chem. Soc. Perkin Trans. 2* **1995**, 1305.

(180) Parker, D. *Coord. Chem. Rev.* **2000**, *205*, 109.

(181) *Chemosensors of Ion and Molecular Recognition*; Desvergene, J. P.; Czarnik, A. W., Eds.; Kluwer Academic: Dordrecht, 1997; Vol. C492.

(182) Ghosh, P.; Bharadwaj, P. K.; Mandal, S.; Ghosh, S. *J. Am. Chem. Soc.* **1996**, *118*, 1553.

(183) Arimori, S.; Bell, M. L.; Oh, C. S.; Frimat, K. A.; James, T. D. *Chem. Commun.* **2001**, 1836.

(184) Arimori, S.; Bell, M. L.; Oh, C. S.; James, T. D. *Org. Lett.* **2002**, *4*, 4249.

(185) Mitchell, K. A.; Brown, R. G.; Yuan, D.; Chang, S.-C.; Utecht, R. E.; Lewis, D. E. *J. Photochem. Photobiol. A: Chem.* **1998**, *115*, 157.

(186) Deviprasad, G. R.; D'Souza, F. *Chem. Commun.* **2000**, 1915.

(187) Schneider, H.-J.; Yatsimirsky, A. K. *Principles and Methods in Supramolecular Chemistry*; John Wiley & Sons: New York, 2000.

(188) Pedersen, C. J. *J. Am. Chem. Soc.* **1967**, *89*, 7017.

(189) Vögtle, F. *Supramolecular Chemistry*; John Wiley & Sons: Chichester, 1991.

(190) de Silva, S. A.; Amorelli, B.; Isidor, D. C.; Loo, K. C.; Crooker, K. E.; Pena, Y. E. *Chem. Commun.* **2002**, 1360.

(191) Shizuka, H.; Nakamura, M.; Morita, T. *J. Phys. Chem.* **1979**, *83*, 2019.

(192) Fabbrizzi, L.; Lichelli, M.; Pallavicini, P.; Perotti, A.; Taglietti, A.; Sacchi, D. *Chem. Eur. J.* **1996**, *2*, 75.

(193) Scalfani, J. A.; Maranto, M. T.; Sisk, T. M.; Van Arman, S. A. *Tetrahedron Lett.* **1996**, *37*, 2193.

(194) De Santis, G.; Di Casa, M.; Fabbrizzi, L.; Lichelli, M.; Mangano, C.; Pallavicini, P.; Perrotti, A.; Poggi, A.; Sacchi, D.; Taglietti, A. In *Transition Metals in Supramolecular Chemistry*; Fabbrizzi, L., Poggi, A., Eds.; Kluwer: Dordrecht, 1996.

(195) de Silva, S. A.; Zaveleta, A.; Baron, D. E.; Allam, O.; Isidor, E. V.; Kashimura, N.; Percarpio, J. M. *Tetrahedron Lett.* **1997**, *38*, 2237.

(196) Koike, T.; Watanabe, T.; Aoki, S.; Kimura, E.; Shiro, M. *J. Am. Chem. Soc.* **1996**, *118*, 12696.

(197) Beeby, A.; Parker, D.; Williams, J. A. G. *J. Chem. Soc. Perkin Trans. 2* **1996**, 1565.

(198) de Silva, A. P.; Gunaratne, H. Q. N.; Rice, T. E.; Stewart, S. *Chem. Commun.* **1997**, 1891.

(199) Kubo, K.; Kato, N.; Sakurai, T. *Bull. Chem. Soc. Jpn.* **1997**, *70*, 3041.

(200) Fages, F.; Desvergne, J.-P.; Bous-Laurent, H.; Lehn, J.-M.; Konopelski, J. P.; Marsau, P.; Barrans, Y. *Chem. Commun.* **1990**, 655.

(201) Golchini, K.; Mackovic-Basic, M.; Gharib, S. A.; Masilamani, D.; Lucas, M. E.; Kurtz, I. *J. Physiol.* **1990**, *258*, F438.

(202) Kastenholtz, F.; Grell, E.; Bats, J. W.; Quinkert, G.; Brand, K.; Lanig, H.; Schnieder, F. W. *J. Fluoresc.* **1994**, *4*, 243.

(203) Doldda, M.; Kastenholtz, F.; Lewitzki, E.; Grell, E. *J. Fluoresc.* **1996**, *6*, 159.

(204) de Silva, A. P.; Gunaratne, H. Q. N.; McVeigh, C.; Maguire, G. E. M. *Chem. Commun.* **1996**, 2191.

(205) Cooper, C. R.; James, T. D. *Chem. Commun.* **1997**, 1419.

(206) Huston, M. E.; Akkaya, E. U.; Czarnik, A. W. *J. Am. Chem. Soc.* **1989**, *111*, 8735.

(207) Kemlo, J. A.; Shepherd, T. M. *Chem. Phys. Lett.* **1977**, *47*, 158.

(208) Varnes, A. W.; Dodson, R. B.; Wehry, E. L. *J. Am. Chem. Soc.* **1972**, *94*, 946.

(209) Ghosh, P.; Bharadwaj, P. K.; Roy, J.; Ghosh, S. *J. Am. Chem. Soc.* **1997**, *119*, 11903.

(210) Ramachandram, B.; Samanta, A. *Chem. Commun.* **1997**, 1037.

(211) Ramachandram, B.; Samanta, A. *J. Phys. Chem. A* **1998**, *102*, 10579.

(212) Ramachandram, B.; Samanta, A. *Chem. Phys. Lett.* **1998**, *290*, 9.

(213) Ramachandram, B.; Sankaran, N. B.; Samanta, A. *Res. Chem. Interm.* **1999**, *25*, 843.

(214) Ramachandram, B.; Saroja, G.; Sankaran, N. B.; Samanta, A. *J. Phys. Chem. B* **2000**, *104*, 11824.

(215) Ramachandram, B.; Sankaran, N. B.; Karmakar, R.; Saha, S.; Samanta, A. *Tetrahedron* **2000**, *56*, 7041.

(216) de Silva, A. P.; Gunaratne, H. Q. N.; Lynch, P. L. M. *J. Chem. Soc. Perkin Trans. 2* **1995**, 685.

(217) Stryer, L. *Biochemistry*; 3rd ed.; Freeman: New York, 1988.

(218) Summers, L. A. *The Pyridinium Herbicides*; Academic Press: London, 1980.

(219) Kosower, E. M. *J. Am. Chem. Soc.* **1958**, *80*, 3253.

(220) Amabilino, D.; Stoddart, J. F. *New Scientist* **1994**, *141*, 25.

(221) Amabilino, D.; Stoddart, J. F. *Pure Appl. Chem.* **1993**, *65*, 2351.

(222) Kalyanasundaram, K. *Photochemistry of Polypyridine and Porphyrin Complexes*; Academic Press: San Diego, 1992.

(223) Juris, A.; Balzani, V.; Barigelletti, F.; Campagna, S.; Besler, P.; Von Zelewsky, A. *Coord. Chem. Rev.* **1988**, *84*, 85.

(224) Hiraoka, M. *Crown Compounds: Their Characteristics and Applications*; Elsevier: Amsterdam, 1982.

(225) Soujanya, T.; Krishna, T. S. R.; Samanta, A. *J. Photochem. Photobiol. A: Chem.* **1992**, *66*, 185.

(226) Soujanya, T.; Krishna, T. S. R.; Samanta, A. *J. Phys. Chem.* **1992**, *96*, 8544.

(227) Soujanya, T.; Fessenden, R. W.; Samanta, A. *J. Phys. Chem.* **1996**, *100*, 3507.

Chapter 2

Experimental details

This chapter provides the details of the experimental procedures followed at various stages of the investigation. This includes details of the method of purification of the various materials including the solvents procured from commercial sources, preparation of the sensor molecules and the analytical data used for their characterization. Also described in this chapter are a brief description of some of the instruments used in this study and some of the experimental methodologies.

2.1. Materials and purification

2.1.1. Materials

4-Aminophthalimide (hereafter AP) was obtained from TCI (Japan). This was recrystallised twice from an ethanol/water mixture prior to photophysical experiments. However, AP was used as received for synthesis. 1,2-Dibromoethane used for synthesis was obtained from Lancaster. Diethylene triamine, triethylene tetramine and tetraethylene pentamine used at various stages of synthesis were obtained from Aldrich. Diethylene glycol was obtained from BDH (India) and p-toluene sulfonyl chloride was obtained from Spectrochem (India). Naphthalene, 1-methylnaphthalene and pyrene used were obtained from Aldrich. Naphthalene was vacuum sublimed before use. 1-Methylnaphthalene and

pyrene were recrystallised prior to photophysical experiments. All the metal salts described in the investigation, except the mercuric salt, were hydrated perchlorate salts and were obtained either from Aldrich or Acros Organics. Mercuric chloride was obtained from Spectrochem (India). Unless stated otherwise, these salts were used as received. Silica gel and alumina used for column purifcation of compounds at various stages were purchased from Acme Scientifics (India). The various drying agents used such as calcium oxide, magnesium sulfate, sodium sulfate, potassium carbonate, self-indicating silica gel etc. and synthesis grade solvents were procured from local companies. Calcium hydride was obtained from Spectrochem (India). GR grade solvents were obtained from Merck (India) for spectroscopic purposes and were dry distilled before use. Deauterated chloroform used for NMR measurements was obtained either from Aldrich or from Merck (India).

2.1.2. Purification of solvents

The solvents used at various stages of the study were purified using the general procedures available in the literature.[1] We adopted the following procedures for the purification of various solvents.

Dioxane (Diox.) and Tetrahydrofuran (THF): The solvent was refluxed over metallic sodium for 3-4 h. and added benzophenone. The dark blue solution was refluxed for a further one hour and collected under dry conditions.

Acetonitrile (AN): Acetonitrile was pre-dried over self-indicating silica gel and distilled. This was then stirred over calcium hydride for 5-6 h. and then

distilled again. The distilled solvent was collected and stored under dry conditions.

Ethanol (EtOH): Ethanol was refluxed with stirring over anhydrous calcium oxide for 6 h. The solution was left at room temperature overnight. This was then distilled and further dried over magnesium and iodine and collected under dry atmosphere.

N,N-dimethylformamide (DMF): DMF was stirred with calcium hydride for 5-6 h. and distilled under vacuum at 80 ^{0}C. Precautions were taken to store the solvent under dry conditions.

Water: Water was initially distilled using potassium permanganate and potassium hydroxide. This was subsequently distilled twice before taken to study.

The extent of dryness of the solvents used for spectroscopic measurements was checked by monitoring the charge transfer absorption band of the betaine dye, commonly known as the $E_T(30)$ dye.[2,3] Based on the polarity scale formulated by Reichardt, the solvent polarity parameter $E_T(30)$ was calculated using the equation:

$$E_T(30) = 28591/\lambda_{max}\ (nm) \qquad (2.1)$$

Where, $E_T(30)$ is the molar transition energy of the dye measured in kcal mol^{-1} at room temperature (25 ^{0}C) and 1 atm. pressure and λ_{max} is the wavelength of the longest absorption band in nanometers. The measured $E_T(30)$ value was then compared with the literature value of the solvent to determine the water content in our solvent.[3] All the solvents used were optically transparent in the spectral region of interest.

2.2. Synthesis of the sensor molecules

2.2.1. Synthesis of NPY

The sensor system, **NPY** was prepared by following the procedure as described below. The synthetic outline is given in Scheme 2.1.

Step 1: To a solution of 4-picoline (0.93 g, 10 mmol) in ice cold THF (25 mL) under argon, a solution of $LiNPr^{i}_{2}$ (10 mmol, freshly prepared by mixing 6.64 mL of 1.6 M n-butyllithium in hexane and 1.33 mL of di-isopropylamine at room temperature under argon) was added dropwise in over 30 min. The deep purple solution was allowed to equilibrate at ~5 ^{0}C for 1 h, to which 1-naphthyl carbaldehyde (1.56 g, 10 mmol) dissolved in 15 mL THF was added dropwise keeping the reaction temperature at ~20 ^{0}C. Then the mixture was allowed to warm to room temperature and stirred overnight. After the reaction was quenched by ice, the reaction solution was evaporated to dryness in vacuo. An oily mass of the crude intermediate alcohol was obtained. About 50 mL of water was added to it and desired diol was extracted in dichloromethane (DCM) layer. It was evaporated to dryness under vacuo and the pale yellow solid obtained was used without purification for subsequent dehydration reaction. The oily mass was dissolved in minimum volume of dry pyridine (30 mL) and a solution of $POCl_3$ (1.9 g, 12 mmol; dissolved in 10 mL of pyridine) was added dropwise under argon at ~5 ^{0}C with stirring. After the addition, the reaction mixture was allowed to come to the room temperature and stirred for 3 h. Then the reaction was quenched with ice and volume was reduced under vacuo. pH of the solution was adjusted to 3 and undesired organic material was extracted in DCM. Solution pH was then adjusted to ~6.5 and desired product was extracted in DCM and dried in

vacuo. Crude solid was purified by column chromatography using silica column and 3% methanol in DCM as eluent. Second fraction was collected.

Step 2: The solid obtained from step 1 (850 mg) was reduced by 10% Pd/C catalyst at 40 ^{0}C under 300 psi H_2 pressure for 4 h. using 25 mL acetonitrile

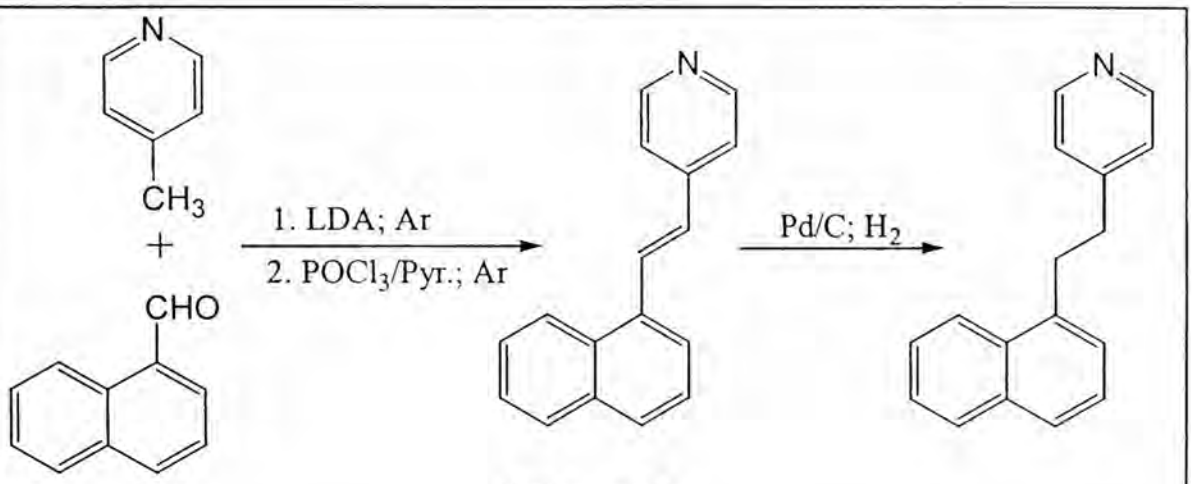

Scheme 2.1.

as solvent. Desired hydrogenated product was further purified by column chromatography using silica column and 2% methanol in chloroform as eluent. Major fraction was collected. Yield: 600 mg (69%). Details of the analytical data used for the characterization of the compound are given in Table 2.1.

2.2.2. Synthesis of PPY

Synthetic procedure for **PPY** is identical to that for **NPY** except that pyrene-1-aldehyde was used instead of 1-naphthyl carbaldehyde. The reduction was carried out at 50 ^{0}C under 410 psi H_2 pressure. Yield: 600 mg (75%). The details of characterization are provided in Table 2.1.

Table 2.1. Experimental characterization details for **NPY** and **PPY**.

NPY	Melting point	Oil
	IR (Neat, cm^{-1})	3051, 2933, 2869, 1597, 1558, 1508, 1413
	^1H NMR (δ)	8.44 (2H, d), 7.0-7.9 (7H, m), 6.99 (2H, d), 3.26 (2H, dd), 2.94 (2H, dd)
	E-I MS	m/z 233 (M^+ 100%)
PPY	Melting point	125 – 130 ^0C
	IR (KBr, cm^{-1})	2930, 1726, 1597, 1277, 846, 808, 754
	^1H NMR (δ)	8.475 (2H, d), 7.945-8.237 (7H, m), 7.71 (2H, d), 7.08 (2H, d), 3.6 (2H, dd), 3.11 (2H, dd)
	E-I MS	m/z 307 (M^+, 100%)

2.2.3. Synthesis of APMAC4

The monoaza crown derivatives of AP were prepared by following a multi-step procedure as stated below. The synthetic procedure is described for the monoaza 12-crown-4 derivative (**APMAC4**). The synthetic scheme followed is outlined in Scheme 2.2.

Step1: Diethylene glycol (10 g, 94 mmol) was stirred for 30 min. with an excess (80 mL, 530 mmol) of triethylamine at 0 ^0C. p-Toluene sulfonyl chloride (36 g, 188 mmol) was added to this solution and stirring continued for another 1 h. The reaction mixture was transferred into crushed ice and stirred well. The solid obtained was washed with 2% HCl (30 mL x 3), water (50 mL), 2% NaOH (30 mL x 3) and water (50 mL). The product was recrystallised from methanol. Yield: 30 g (77%).

Step 2: Diethanolamine (7 g, 68 mmol) and sodium metal (3.5 g, 150 mmol) were dissolved in t-butanol (500 mL) and diethyleneglycol di(toluene-p-sulfonate) (28 g, 68 mmol) in dioxane (300 mL) was added in drops to the solution at 40 ^{0}C over a period of 3 h. After the addition, the reaction was continued for 1 h, then the reaction mixture was filtered and the solvent was evaporated off. Water (50 mL) was added to the residue and the solution was extracted once with hexane to remove hexane soluble materials and then extracted several times with DCM. The DCM extracts were combined, the solvent was evaporated off and the residue was distilled to give an oily mass. Yield: 6 g (60%).[4]

Step 3: AP was reacted with 1,2-dibromoethane in the presence of NaH. AP (1 g, 6.2 mmol) was stirred for half an hour with NaH (1.5 g, 36 mmol) in dry DMF (10 mL). 1,2-Dibromoethane (3.1 mL, 36 mmol) was added drop wise to the above solution and the reaction mixture was stirred at room temperature for 24 h. The reaction was quenched using water and extracted with ethylacetate. The organic layer was dried using anhydrous sodium sulphate and concentrated. The compound was purified through a neutral alumina column using 40% ethylacetate in hexane as eluent. Yield: 1 g (60%).

Step 4: The bromo compound obtained in step 3 (0.5 g, 1.86 mmol) and the crown obtained in step 2 (1.35 g, 7.5 mmol) were stirred in acetonitrile at reflux temperature in the presence of potassium carbonate (1 g, 7 mmol) for 24 h. The crude solid obtained was purified using a neutral alumina column with 2% methanol in chloroform as the eluent. Yield: 0.4 g (62%).

The monoaza 15-crown-5 (**APMAC5**) and the monoaza 18-crown-6 (**APMAC6**) derivatives of AP were prepared following a similar procedure employing triethylene glycol and tetraethylene glycol respectively in step 1. The characterization details of the three derivatives are given in Table 2.2.

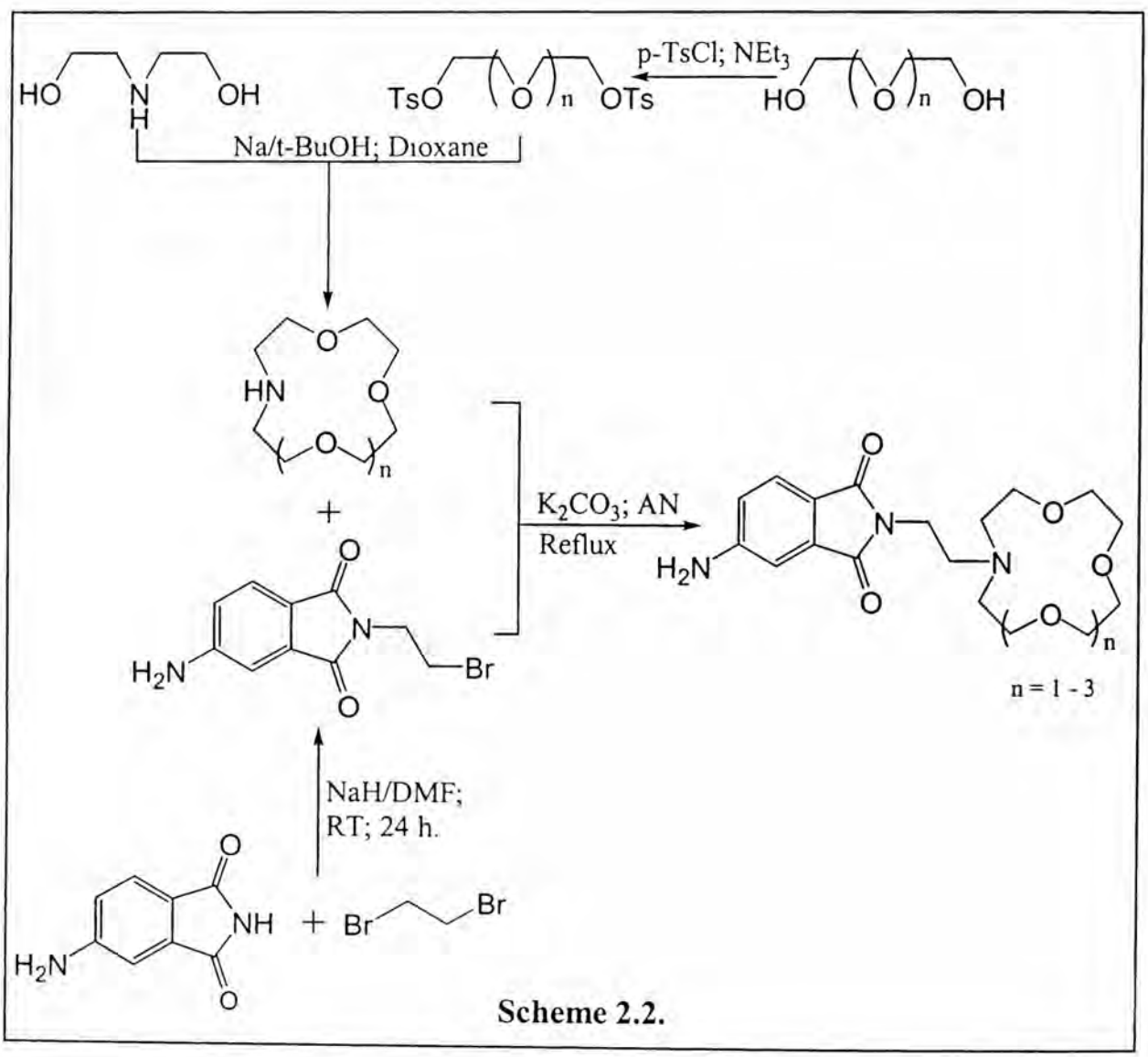

Scheme 2.2.

Table 2.2. Details of experimental characterization of **APMAC4**, **APMAC5** and **APMAC6**.

APMAC4	Melting point	Oil
	IR (Neat, cm^{-1})	3415, 2980, 2873, 1755, 1699, 1622, 1461, 1101, 956, 841
	^1H NMR (δ)	2.7 (m, 8H), 3.6 (m, 12H), 6.8 (d, 1H), 7.05 (s, 1H), 7.4 (d, 1H)
APMAC5	Melting point	Oil
	IR (Neat, cm^{-1})	3400, 3350, 3207, 2980, 2866, 1757, 1701, 1616, 1502, 1394, 1112, 939, 843, 748
	^1H NMR (δ)	2.7 (m, 8H), 3.6 (m, 16H), 6.8 (d, 1H), 7.05 (s, 1H), 7.4 (d, 1H)
APMAC6	Melting point	Oil
	IR(Neat, cm^{-1})	3417, 2980, 2873, 1701, 1616, 1461, 1355, 1110, 952, 839
	^1H NMR (δ)	2.7 (m, 8H), 3.6 (m, 20H), 6.8 (d, 1H), 7.05 (s, 1H), 7.4 (d, 1H)

2.2.4. Synthesis of APDAC

The procedure followed for the preparation of the diaza crown derivative of AP is given in Scheme 2.3. The detailed procedure is given below.

Step 1: Diethylenetriamine (10 g, 97 mmol) was stirred with aqueous sodium hydroxide (12 g, 290 mmol in 200 mL water) at 0 °C for 30 min. p-Toluenesulfonyl chloride (56 g, 290 mmol) dissolved in diethyl ether (200 mL) was added drop wise to the above solution at this temperature and stirred

vigorously. The reaction mixture was further stirred for 1 h. The solid obtained was filtered and recrystallised from methanol. Yield: 40 g (75%).

Step 2: Diethanolamine (10 g, 97 mmol) was stirred for 30 min. with an excess of triethylamine (60 - 70 mL) at ice temperature. TsCl ((p-toluene sulfonyl chloride) 56 g, 290 mmol) was added to the above solution and the reaction was continued for another hour. The reaction mixture was poured into crushed ice and stirred vigorously. The solid obtained was decanted, washed with 2% aq. HCl (30 mL x 3), water (50 mL) 2% aq. NaOH (30 mL x 3), water (50 mL) and finally with methanol. The solid was recrystallised from an excess of methanol. Yield: 40 g (75%).

Step 3: The solid obtained from step 1 (25 g, 44 mmol) was taken in absolute ethanol (60 mL) and heated to reflux. Na (2 g, 88 mmol) dissolved in absolute ethanol (60 mL) was added as fast as possible and left the reaction for cooling overnight. The sodium salt of the tosylated triamine crystallises.

Step 4: The above sodium salt (26 g, 43 mmol) was dissolved in dry DMF (350 mL) and heated to 100 ^{o}C. To this, the tosylate of diethanolamine obtained in step 2 (23 g, 41 mmol) in dry DMF (110 mL) was added drop wise. After heating for half an hour at this temperature, the heating bath was removed. Water (100 mL) was added to the reaction mixture and kept stirring for overnight. The tosylate of the cyclic amine was filtered, washed with methanol and recrystallised from excess of methanol. Yield: 25 g (85%).

Step 5: The tosylated cyclic crown (15 g, 26 mmol), 45% hydrogen bromide in glacial acetic acid (50 mL, 280 mmol) and phenol (15 g, 160 mmol) were combined and stirred at 40 ^{0}C until the crown ether was completely

dissolved (4 – 6 h). The solution was poured into dry ether (200 mL), the residual precipitate was dissolved in a minimal volume of water, basified with sodium hydroxide, and continuously extracted with chloroform for 12 h. The solvent was removed under reduced pressure. The Diazcrown was recrystallised from benzene – hexane mixture.[5]

Step 6: The bromo derivative of AP was prepared as described in step 3, section 2.2.3.

Step 7: The bromo compound (450 mg, 1.67 mmol) and the diazacrown (200 mg, 760 mmol) were mixed in acetonitrile (25 mL) and stirred well in the presence of potassium carbonate (1 g, 720 mmol) under refluxing conditions. The reaction was continued for 24 h. The reaction mixture was filtered, concentrated, washed with water and extracted using ethylacetate. The organic layer was dried using anhydrous sodium sulfate and reduced in volume. The resulting solid was purified using column chromatography using a neutral alumina column and the required fraction was eluted with a 2% methanol in chloroform as eluent. Yield: 0.5 g (66%). The details of characterization of the compound are given in Table 2.3.

Table 2.3. Details of experimental characterization of **APDAC**.

Melting point	138 – 145 ^{0}C
IR (KBr, cm^{-1})	3485, 2893, 2793, 1753, 1701, 1597, 1458, 1390, 1111, 987
^{1}H NMR (δ)	2.7 (m, 12H), 3.5 (m, 16H), 6.8 (d,1H), 7.05 (s, 1H), 7.4 (d, 1H)
Mass	m/z 451

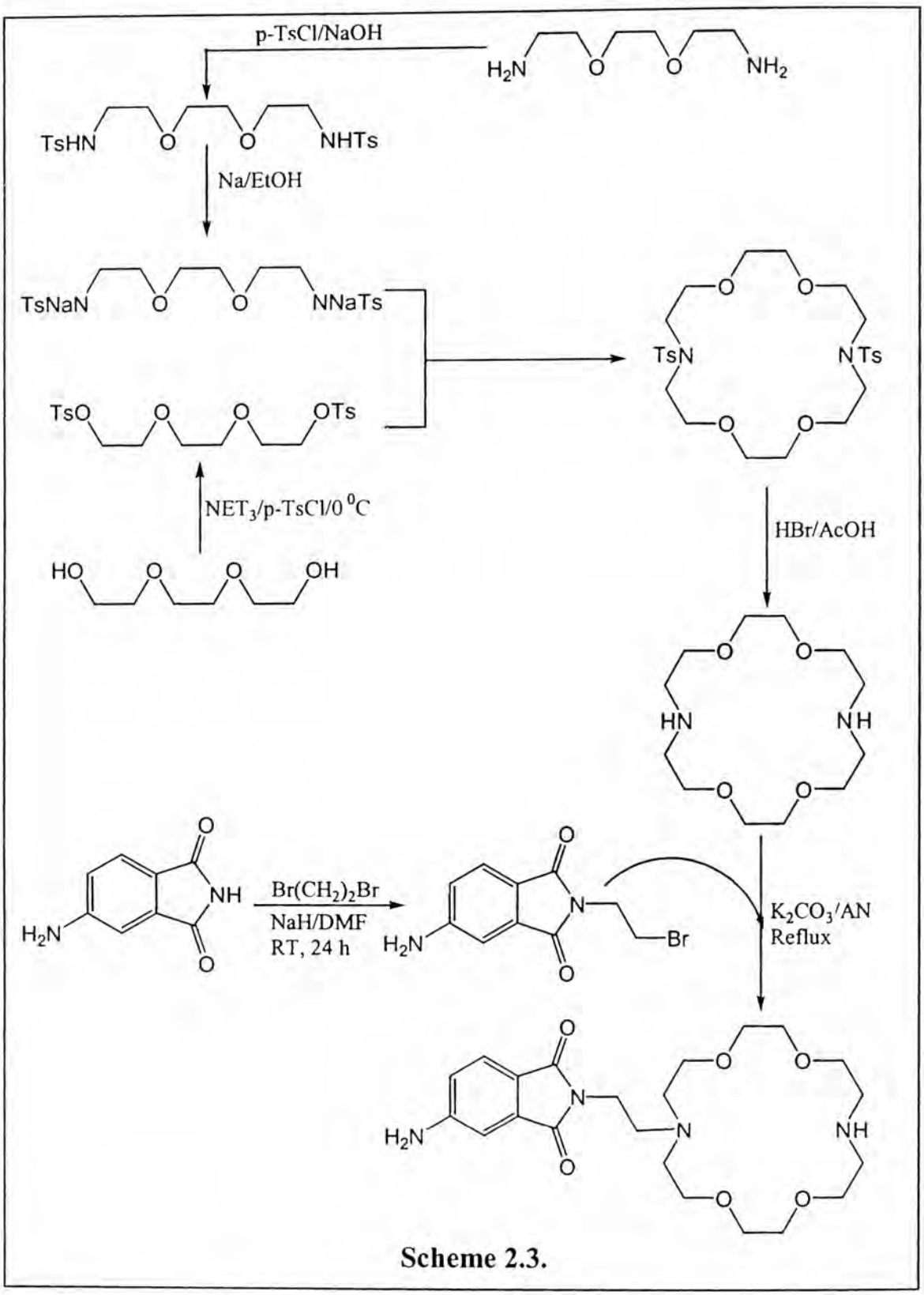
p-TsCl/NaOH
H2N O O NH2
TsHN O O NHTs
Na/EtOH
TsNaN O O NNaTs
TsO O O OTs
NET3/p-TsCl/0 °C
HO O O OH
TsN NTs
HBr/AcOH
HN NH
NH
H2N
Br(CH2)2Br
NaH/DMF
RT, 24 h
Br
K2CO3/AN
Reflux
N

Scheme 2.3.

2.2.5. Synthesis of APTAC

The procedure followed for the preparation of the tetraaza crown compound and the corresponding sensor molecule is outlined in Scheme 2.4. The details of the procedure followed are described below.

Step 1: Diethylenetriamine (10 g, 97 mmol) was stirred with aqueous sodium hydroxide (12 g, 290 mmol in 200 mL water) at 0 °C for 30 min. p-toluenesulfonyl chloride (56 g, 290 mmol) dissolved in diethyl ether (200 mL) was added drop wise to the above solution at this temperature and stirred vigorously. The reaction mixture was further stirred for 1 h. The solid obtained was filtered and recrystallised from methanol. Yield: 40 g (75%).

Step 2: Diethanolamine (10 g, 97 mmol) was stirred for 30 min. with an excess of triethylamine (60 - 70 mL) at ice temperature. TsCl (56 g, 290 mmol) was added to the above solution and the reaction was continued for one more hour. The reaction mixture was poured into crushed ice and stirred vigorously. The solid obtained was decanted, washed with 2% aq. HCl, 2% aq. NaOH, water and finally with methanol. It was recrystallised from an excess of methanol. Yield: 40 g (75%).

Step 3: The solid obtained from step 1 (25 g, 44 mmol) was taken in absolute ethanol (60 mL) and heated to reflux. Na (2 g, 88 mmol) dissolved in absolute ethanol (60 mL) was added as fast as possible and left the reaction for cooling overnight. The sodium salt of the tosylated triamine crystallises.

Step 4: The above sodium salt (26 g, 43 mmol) was dissolved in dry DMF (350 mL) and heated to 100 °C. To this, the tosylate of diethanolamine obtained in step 2 (23 g, 41 mmol) in dry DMF (110 mL) was added drop wise. After heating

for half an hour at this temperature, the heating bath was removed. Water (100 mL) was added to the reaction mixture and kept stirring for overnight. The tosylate of the cyclic amine was filtered, washed with methanol and recrystallised from excess of methanol. Yield: 25 g (85%).

Step 5: The cyclic tetramine tosylate (25 g, 32 mmol) was taken in conc. sulphuric acid (30 mL). The mixture was stirred at 60 °C until the solid was dissolved and then heated to 180 °C for ~10 min. The reaction mixture was cooled to room temperature first and then to ice temperature. Solvent ether (300 mL) was added slowly to the above mixture at 0 °C with vigorous stirring. The solid obtained was decanted and washed twice again with ether. This was then dried under vacuum and dissolved in hot water (15 mL). The hot solution was filtered and heated to 80 °C. Conc. HCl (15 mL) was added to the above solution drop wise and left for overnight. The crystallized solid was decanted, washed with cold conc. HCl (3 x 10 mL), absolute ethanol (3 x 25 mL) and diethyl ether (3 x 25 mL) and dried. The hydrochloride salt thus obtained was neutralized using aq. NaOH and extracted using chloroform. The crude cyclic tetramine was recrystallised from acetonitrile.[6,7] Yield: 5 g (90%).

Step 6: The bromo derivative of AP was obtained as stated in Section 2.2.3.

Step 7: The bromo compound (500 mg, 1.87 mmol) and the cyclic tetramine (1.6 g, 9.4 mmol) were taken in dry toluene (25 ml) and heated under reflux for 24 h. The reaction mixture was cooled first to room temperature and then to 0 °C. The hydrobromide salt of the crown and the unreacted cyclic amine were removed by filtration. The filtrate was stirred with potassium carbonate,

filtered and concentrated. The solid obtained was recrystallised twice from toluene. Yield: 500 mg (75%). The details of characterization are given in Table 2.4.

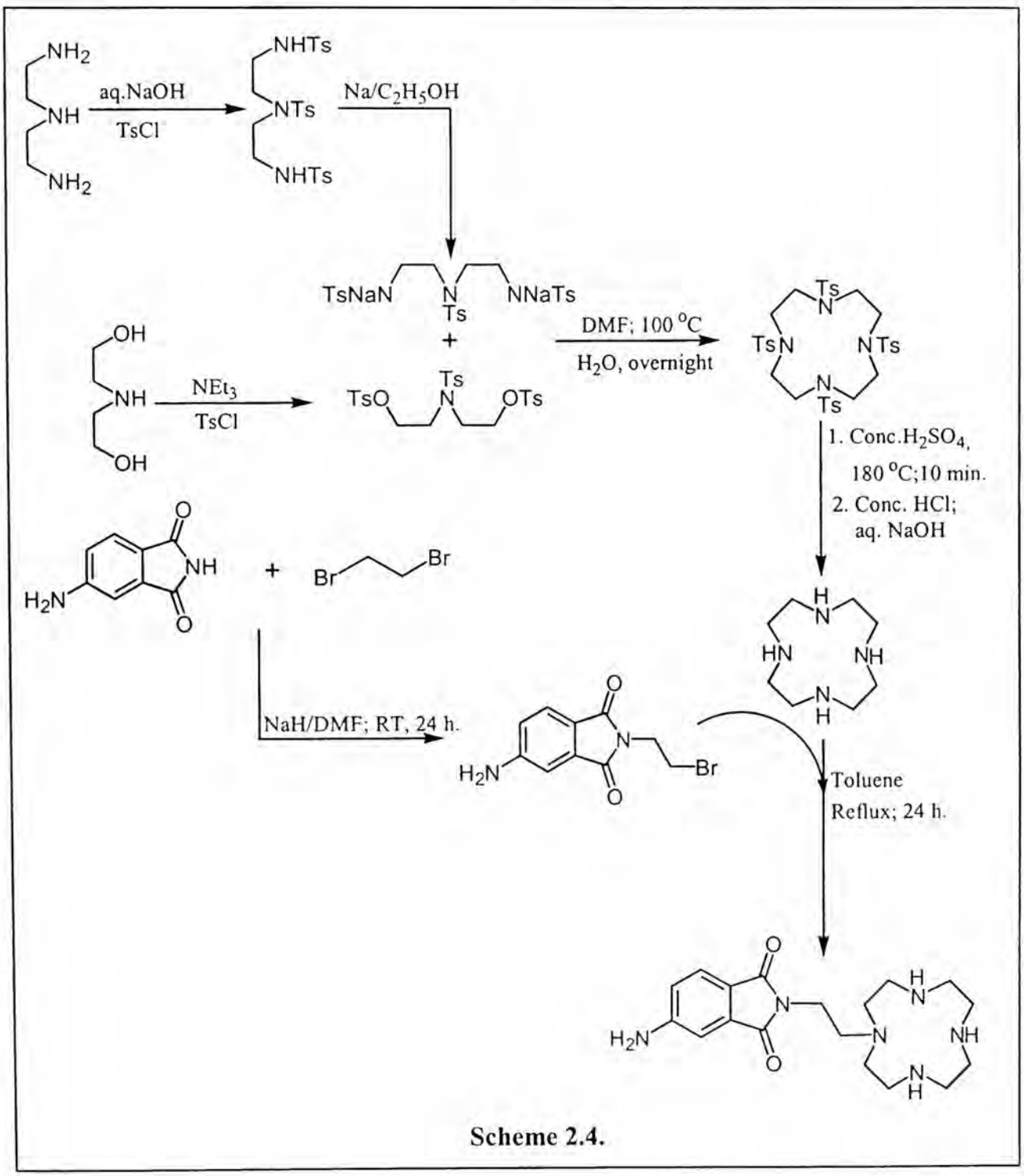

Scheme 2.4.

Table 2.4. Experimental characterization details of **APTAC**.

Melting point	95 – 97 ^{0}C
IR (KBr, cm^{-1})	3364, 2934, 2843, 1751, 1699, 1616, 1458, 1396, 733
^{1}H NMR (δ)	2.3 (s, 3H), 2.8 (m, 18H), 3.6 (t,2H), 4.8 (s, 2H), 6.7 (s, 1H), 7.3 (d, 1H), 7.6 (d, 1H)
Mass	m/z: 361, Base peak: 173

2.3. Solution preparation for spectral measurements

The solutions of the sensor systems were prepared such that the absorbance of the solution (1 cm pathlength cell) at the longest wavelength absorption maximum is between 0.1 and 0.2, except when a concentration dependent emission study was conducted. The actual concentrations of the sensor systems varied depending on the extinction coefficients of the systems. For **NPY** and **PPY**, the concentration corresponding to an absorbance value of 0.2 was ~1x10^{-6} M and for the crown systems it was ~1x10^{-4} M. A concentrated stock solution of the metal ion was prepared in any given solvent and this solution was added (using a microlitre syringe) to 3 mL solution of the sensor molecule taken in a quartz cuvette. Addition of the solution of the metal salt was limited to less than 150 μL.

2.4. Measurement of the fluorescence quantum yield

Fluorescence quantum yield of the various compounds was measured with reference to that of AP. We used a fluorescence quantum yield of 0.70 and 0.63 for AP in THF and AN.[8] In the case of **NPY** and **PPY**, the quantum yield was

determined with reference to that of the parent fluorophore, naphthalene or pyrene, as the case may be.[9,10] For quantum yield measurements, solutions of same absorbance of the sample and the standard at the same exciting wavelength were prepared. Quantum yield was calculated by measuring the integrated area under the emission curves and by using the following equation:[11]

$$\Phi_{sample} = \frac{I_{sample} \times OD_{standard}}{I_{standard} \times OD_{sample}} \times \Phi_{standard} \qquad (2.2)$$

2.5. Measurement of feasibility of electron transfer

The feasibility of the photoinduced electron transfer process in the systems was calculated using the equation:[12-15]

$$\Delta G^* = [E_{ox}\,(\text{receptor}) - E_{red}\,(\text{fluorophore}) - E_{0,0} \qquad (2.3)$$

Where ΔG^* is the free energy of the electron transfer process, E_{ox} (receptor) is the oxidation potential of the receptor, E_{red} (fluorophore) is the reduction potential of the fluorophore and $E_{0,0}$ is the singlet energy of the fluorophore. The oxidation potentials of pyrene, naphthalene and pyridine are 1.16, 1.54 and 2.09 V respectively and the reduction potentials are –2.10, –2.63 and –2.62 V respectively.[16] Singlet energy of naphthalene and pyrene are respectively 92 and 77 kcal/mol.[14]

2.6. Estimation of fluorescence enhancement

The magnitude of the maximum fluorescence enhancement was calculated by measuring the integrated area beneath the fluorescence curves and applying it to the equation:

$$FE = I_F \text{ (optimum)}/I_F \text{ (zero)} \quad (2.4)$$

Where, FE is the fluorescence enhancement, I_F (otimmum) is the maximum fluorescence intensity obtained on adding the metal ions and I_F (zero) is the fluorescence intensity at zero concentration of the metal ion.

2.7. Instrumentation

The IR spectra were recorded either on a Jasco FT-IR/5300 spectrometer or on a Shimadzu spectrometer. The NMR spectra were recorded using a Brucker ACF 200 MHZ instrument. High resolution mass spectra were recorded on a Micromass VG-70H instrument. The UV-vis absorption spectral measurements were made on a Shimadzu 3101 UV-vis spectrophotometer and on a Jasco model 7800 spectrophotometer. The flurescence spectra were recorded using a Spex FluoroMax-3 spectrofluorimeter. The fluorescence lifetimes were measured using a IBH-5000 single photon counting spectrofluorimeter.[17] A hydrogen flash lamp of pulse width 1.2 ns with a repetition rate of 40 kHz was employed as the excitation source. A small fraction of the excitation pulse was detected by a photomultiplier tube (IP28) and the photomultiplier signal was fed into a constant fraction discriminator (CFD) to discriminate the background noise and to generate a precise timing pulse. The output of CFD served as the START pulse of the time to amplitude converter (TAC). A fluorescence photon recorded by the emission photomultiplier (Hamamatsu 3235), as determined by the discriminator, generated a pulse, which served as the STOP signal for TAC. The TAC signal produced was proportional to the time taken from the excitation event to the first photon recorded. The signal from TAC was digitized by the analog to digital converter

(A/D converter) and sent to the appropriate channel, depending on the digitized value of the TAC voltage of a multi-channel analyzer (MCA). The whole process was repeated so that the MCA counts represented the number of photon events as a function of time. After many excitation pulses, the MCA memory contents represented a histogram of the emission decay i.e. time profile of the fluorescence intensity. For recording the lamp profile, a scatterer (dilute solution of Ludox in H_2O) was placed in the place of the sample.

Data Analysis: The program used for the estimation of fluorescence lifetimes from the fluorescence decay curves was based on reconvolution least squares method.[18] When the decay time is long compared to the decay time of the excitation pulse, the excitation may be described as a δ-function. However, when the lifetime is short, distortion of the experimental data occurs by the finite decay time of the lamp pulse and response time of the photomultiplier and associated electronics. Since the measured decay function is convolution of the true fluorescence decay, it is necessary to analyze the data by deconvolution in order to get the fluorescence lifetime. The mathematical statement of the problem is given by the following equation:

$$D(t) = \int_0^t P(t')G(t-t')dt' \qquad (2.5)$$

Where, D(t) is the fluorescence intensity at time t, P(t') is the intensity of the exciting light at time t' and G(t-t') is the response function of the experimental system. The experimental data D(t) and P(t') from the MCA were fed into a computer (IBM PC) to determine the lifetime. We used the IBH program to analyze the multi-exponential decays. An excitation pulse profile was recorded

and then deconvolution started with mixing of the excitation pulse and a projected decay to form a new reconvoluted set. The data was compared with the experimental set and the difference between the data points summed, generating χ^2 function for the fit. The deconvolution proceeded through a series of such iterations until an insignificant change of χ^2 occured between iterations. The quality of the fit was assessed by the inspection of reduced χ^2, a plot of weighted residuals and autocorrelation function of the residuals.

2.8. X-ray crystallography

The single crystals of cyclen were grown from toluene. A tiny single crystal (dimension 0.68 x 0.48 x 0.40 mm) was mounted on a capillary head by an appropriate fixing material and then mounted on the goniometer. The X-ray data were collected on an Enraf-Nonius Mach-3 single crystal diffractometer employing graphite monochromated Mo Kα radiation (λ = 0.71073 Å) by ω-scan method. Unit cell parameters were determined by least squares fit of 25 reflections having 2θ values in the range 18 - 21^0. Intensities of three check reflections were measured after every 1.5 h. during the data collection to monitor the stability of the crystals. The non-hydrogen atoms were refined anisotropically. The hydrogen atoms of the methylene groups were included in the structure factor calculation at idealized positions by using riding model, but not refined. The hydrogen atoms of the water molecules and the amino moieties were located from the difference Fourier map and refined isotropically. XTAL 3.4[19] version was employed for the data reduction. The solution and refinement for the crystal data

were done using SHELXS-97[20] and SHELXL-97[21] programs respectively. The details of the crystal structure are given in chapter 6 and in appendix 3.

2.9. Standard error limits

Standard error limits involved in the measurements are:

λ_{max} (abs/fluo)	± 3 nm
ϕ_f	± 10%
FE	± 10%
τ (>1ns)	± 5%
τ (<1ns)	± 15%

2.10. References

(1) Perrin, D. D.; Armerego, W. L. F.; Perrin, D. R. *Purification of Laboratory Chemicals*; Pergamon Press: New York, 1980.

(2) Dimorth, K.; Reichardt, C.; Siepmann, T.; Bohlmaun, F. *Liebigs Ann. Chem.* **1963**, *661*.

(3) Reichardt, C. *Solvents and Solvent Effects in Organic Chemistry*; VCH, Weinheim, 1988.

(4) Maeda, H.; Nakatsuji, Y.; Okahara, M. *Chem. Commun.* **1981**, 471.

(5) Bogatsky, A. V.; Lukyaninko, N. G.; Basok, S. S.; Ostrovskaya, L. K. *Synthesis* **1984**, 138.

(6) Richman, J. E.; Atkins, T. J. *J. Am. Chem. Soc.* **1974**, *96*, 2268.

(7) Atkins, T. J.; Richman, J. E.; Oettle, W. F. *Org. Synthesis.* **1978**, *58*, 86.

(8) Soujanya, T.; Fessenden, R. W.; Samanta, A. *J. Phys. Chem.* **1996**, *100*, 3507.

(9) Berlman, I. B. *Handbook of Fluorescence Spectra of Aromatic Molecules*; Academic Press: New York, 1971.

(10) *Practical Fluorescence*; 2nd ed.; Guilbault, G. G., Ed.; Marcel Dekker: New York, 1990.

(11) Austin, E.; Gouterman, M. *Bioinor. Chem.* **1978**, *9*, 281.

(12) Weller, A. *Pure Appl. Chem.* **1968**, *16*, 115.

(13) Rehm, D.; Weller, A. *Isr. J. Chem.* **1970**, *8*, 259.

(14) Kavarnos, G. J.; Turro, N. J. *Chem. Rev.* **1986**, *86*, 401.

(15) Kavarnos, G. J. *Top. Curr. Chem.* **1990**, *156*, 20.

(16) *Techniques of Chemistry*; Siegerman, H.; Weinberg, N. L., Eds.; John Wiley & Sons: New York, 1975; Vol. V, Part II.

(17) O'Connor, D. V.; Phillips, D. *Time-Correlated Single Photon Counting*; Academic Press: London, 1984.

(18) Bevington, P. R. *Data Reduction and Error Analysis for the Physical Sciences*; McGraw-Hill: New York, 1969.

(19) *Xtal 3.4. User's Manual*; Hall, S. R.; King, G. S. D.; Stewart, J. M., Eds.; University of Western Australia: Lamb, Perth, 1995.

(20) Sheldrick, G. M. *Acta Cryst.* **1990**, *A46*, 467.

(21) Sheldrick, G. M. *SHELXL-97, Program for the Refinement of Crystal Structures*; Universität of Göttingen: Göttingen, Germany, 1997.

Chapter 3

Photophysical behavior of 1-(1-naphthyl)-2-(4-pyridyl)ethane and 1-(1-pyrenyl)-2-(4-pyridyl)ethane

Photophysical properties of two simple *fluorophore-spacer-receptor* systems, 1-(1-naphthyl)-2-(4-pyridyl)ethane and 1-(1-pyrenyl)-2-(4-pyridyl)ethane, abbreviated as **NPY** and **PPY** respectively, are reported in this chapter. These structurally simple three-component systems have been designed and developed with a view to exploring the potential of these systems in sensing the metal ions, and the transition metal ions in particular. Taking into consideration the fact that pyridine is an excellent coordinating ligand for the metal ions, we thought that systems involving pyridine as the guest binding site could be ideal for metal ion sensing applications. It is shown in this chapter that the terminal moieties (naphthyl/pyrenyl and pyridyl) of the three-component systems (Chart 3.1.) interact through space leading to the formation of an intramolecular π-π

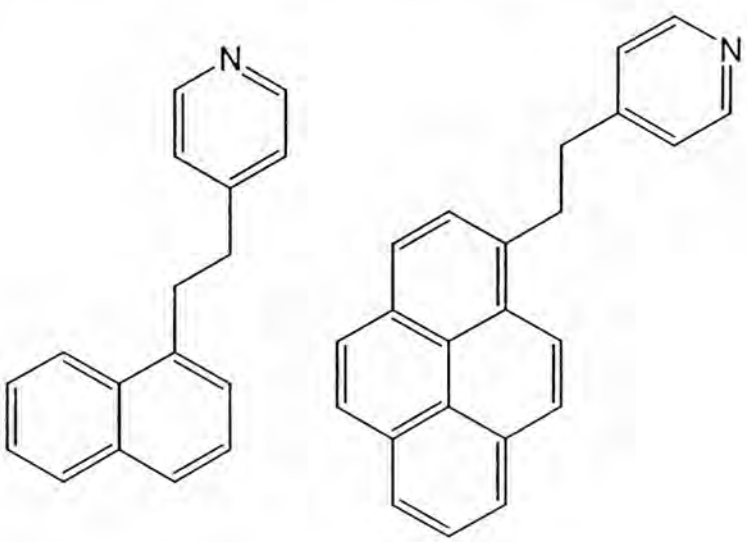

NPY **PPY**

Chart 3.1.

complex in the ground state. The lack of an intermolecular complexation between the interacting partners has been ascribed to a smaller change in entropy associated with the complexation process.

3.1. Spectral features

3.1.1. Absorption

The spectral behavior of the systems has been studied in tetrahydrofuran (THF) and acetonitrile (AN). In the case of **NPY**, the absorption spectrum consists of a featureless broad band in the long wavelength region of the spectrum and a structured absorption between 250 – 300 nm, which resembles the absorption of the parent chromophore, naphthalene. In the case of **PPY**, the spectrum is highly structured in both long and short wavelength region of the spectrum and the structured absorption is clearly due to the pyrenyl moiety of the system. The broad absorption band in the wavelength range 300 – 350 nm (with the peak at ~330 nm) of **NPY** is found to be rather insensitive to the solvent polarity and no significant spectral shift could be observed on change of the polarity of the media. Interestingly, no broad absorption band could be observed with **PPY** in polar or nonpolar solvents. The absorption spectra of **NPY** and **PPY** are presented in figure 3.1.

Absorption experiments were conducted with solutions of naphthalene in THF and AN by adding pyridine externally. The idea was to find out whether broad absorption band similar to what is observed in the case of **NPY** could be seen. Surprisingly, we did not find any noticeable change in the absorption spectra, particularly in the long wavelength region, of naphthalene on external

addition of pyridine. The spectra remained more or less unchanged and no broad band, similar to the long wavelength absorption band of **NPY**, could be observed.

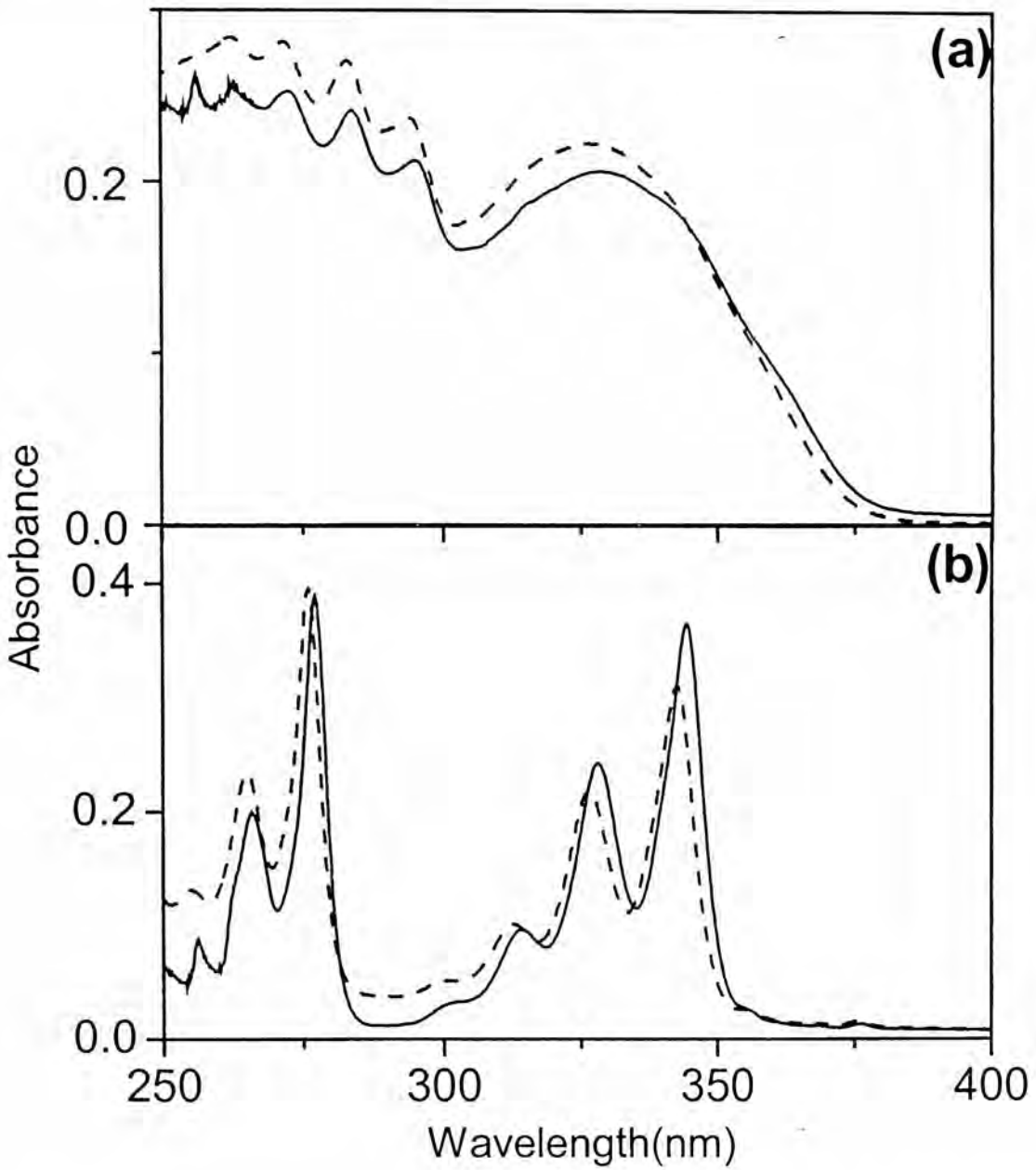

Fig. 3.1. Absorption spectra of **NPY** (a) and **PPY** (b) in THF (Solid) and AN (dashed).

3.1.2. Emission spectra

The fluorescence behavior of the systems has also been studied in non polar solvent, THF and polar AN. Both the systems exhibit excitation wavelength dependent emission spectra.

The excitation wavelength dependence of the emission behavior of **NPY** in THF and AN is illustrated in figure 3.2. When the excitation wavelength is 280 nm, the emission maximum is observed at 330 nm with a shoulder at around 400 nm. The emission band at 330 nm is structured and resembles that of naphthalene. As the excitation wavelength is shifted from 280 nm to 300 nm, the 330 nm emission becomes weak and the 400 nm band becomes stronger. When the compound is excited at 330 nm, only the long wavelength emission band could be observed. The emission at 400 nm shows some structure in THF but is devoid of any structure in AN.

In the case of **PPY** too, we see a similar behavior. Excitation of **PPY** at 315 nm leads to a structured emission with maximum at ~400 nm. But as the excitation wavelength is shifted from 315 to 415 nm, a fairly broad band appears with maximum at 450 nm. This band is most intense when the excitation wavelength is 375 nm. The new emission has very little structure in THF and is without any structure in AN. The emission features of **PPY** are shown in figure 3.2.

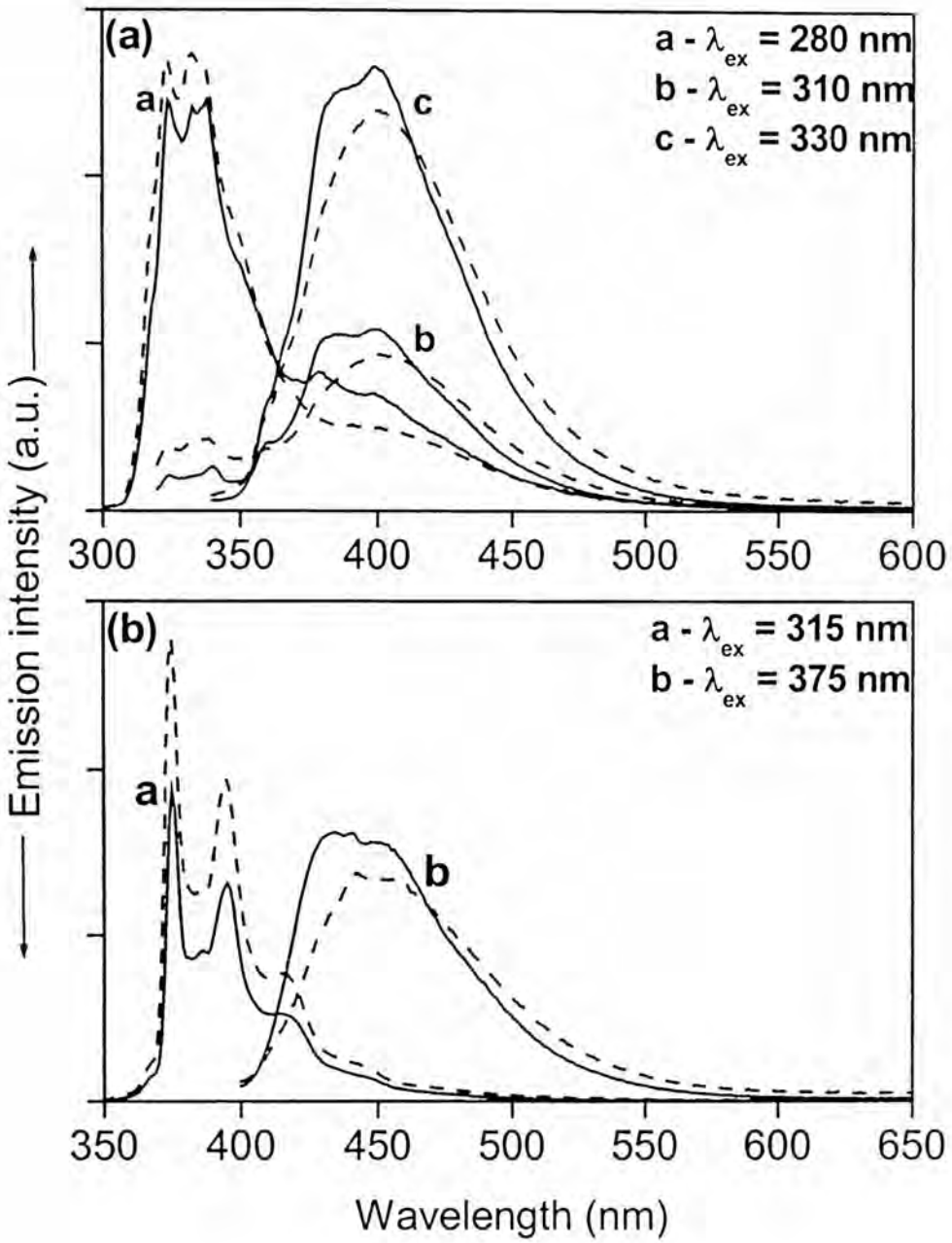

Fig. 3.2. Emission spectra of **NPY** (a) and **PPY** (b) in THF (solid) and AN (dashed) excited at various wavelengths.

3.1.3. Fluorescence excitation spectra

The fluorescence excitation spectra of the systems were recorded monitoring different emission wavelengths. The monitoring wavelengths were 340 and 400 nm for **NPY** and 400 and 450 nm for **PPY** in both THF and AN. When monitored at 340 nm, the excitation spectrum of **NPY** corresponds to the short wavelength region of the absorption spectrum and produces typical structured band of naphthalene. The excitation spectrum corresponding to the emission at 400 nm duplicates the broad band in absorption.

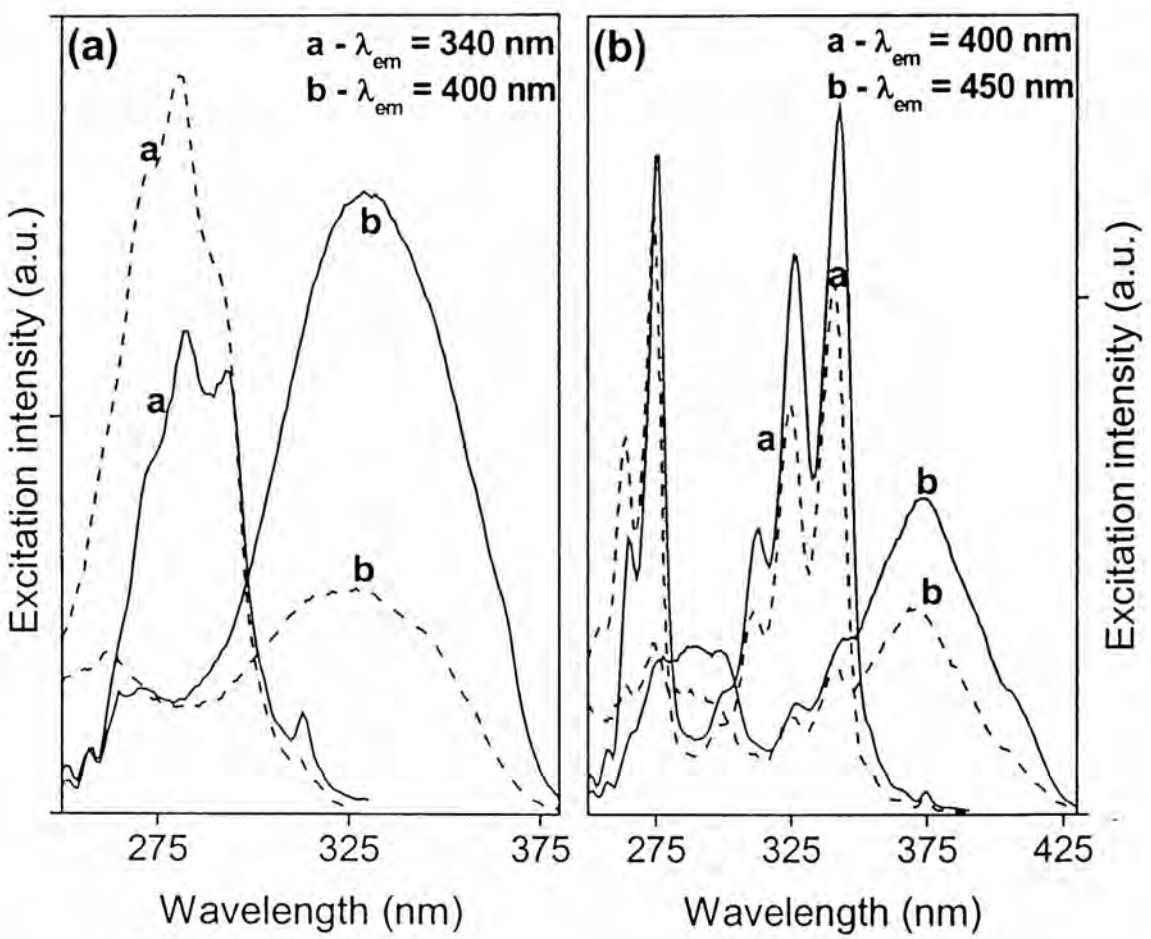

Fig. 3.3. Fluorescence excitation spectra of **NPY** (a) and **PPY** (b) in THF (solid) and AN (dashed) monitored at different emission wavelengths.

With **PPY**, the excitation spectrum, when monitored at 400 nm, corresponds to the structured absorption of the pyrene moiety. However, when monitored at 450 nm, the excitation spectrum shows a broad band with maximum at 375 nm. Interestingly, a broad band of this type was not observed in the absorption spectrum of this compound. The fluorescence excitation spectrum suggests that long wavelength emission of **PPY** originates from a species that absorbs at around 375 nm. Fluorescence excitation spectra of **NPY** and **PPY** in THF and AN are shown in figure 3.3.

3.1.4. Fluorescence lifetime

The fluorescence decay behavior of **NPY** and **PPY** has been studied monitoring the individual emission bands. The decay parameters are collected in Table 3.1. Representative decay plots for **NPY** in THF are provided in figure 3.4. When monitored at the short wavelength region, where the naphthyl or the pyrenyl moiety emits, the fluorescence decay consists of a long and a short-lived component. The relative weightage of the short to the long component is roughly 1:2 in the case of **NPY**. In the case of **PPY**, the short-lived component is the predominant one in THF, though the reverse is true in AN. While the long wavelength emission is also fitted to a biexponential decay behavior to obtain the best χ^2 and better residuals, the contribution of the second component is found to be too little compared with the dominant one. The predominant component has a lifetime of 0.2 ns in the case of **NPY** and 2.1 – 2.7 ns in the case of **PPY**.

Table 3.1. Fluorescence lifetime (ns) of **NPY** and **PPY** in THF and AN at various excitation and emission wavelengths (nm). The relative weightage of individual components (in %) are given in the bracket.

Compound	Wavelength parameters		THF			AN		
	λ_{ex}	λ_{em}	τ_1 (%)	τ_2 (%)	χ^2	τ_1 (%)	τ_2 (%)	χ^2
NPY	280	325	8.1 (28.6)	51.1 (71.4)	1.05	3.9 (36.4)	33.9 (63.6)	1.15
	320	420	0.2 (99.3)	2.3 (0.7)	1.18	0.2 (99.8)	11.8 (0.2)	1.28
PPY	315	375	3.1 (89.3)	192 (10.7)	1.26	6.5 (11.8)	122 (88.2)	1.00
	375	465	2.7 (98.4)	46 (1.6)	1.28	2.1 (99.8)	48 (0.2)	1.04

3.2. Possibility of complex formation in NPY and PPY

As stated above, a physical mixture of 1-methylnaphthalene/1-methylpyrene and 4-picoline does not give rise to the long-wavelength emission band as observed in the case of **NPY** and **PPY**. The interaction of various aliphatic and aromatic amines with hydrocarbons such as naphthalene, anthracene, pyrene, etc. has been studied earlier.[1-10] It is known that aliphatic and aromatic amines form intermolecular complexes with aromatic hydrocarbons and quench the fluorescence of the latter. Despite a plethora of reports available on the interaction of amines with aromatic hydrocarbons, very little information is available dealing with the interaction of pyridine with these hydrocarbons. This is

presumably due to the fact that pyridine does not form an exciplex readily with the aromatic hydrocarbons such as naphthalene or pyrene, whereas the aliphatic amines such as diethylamine, triethylamine, etc., and aromatic amines such as N,N-dimethylaniline do. We have independently verified that the addition of pyridine merely quenches the emission of the hydrocarbons with no new spectral features arising. This behavior can be rationalized when taken into consideration the fact that unlike the sp^3 hybridized nitrogen atoms of the aliphatic and aromatic amines, the lone pair of electrons of pyridine reside in an sp^2 hybridized orbital and hence not easily available for complex formation with the hydrocarbons.

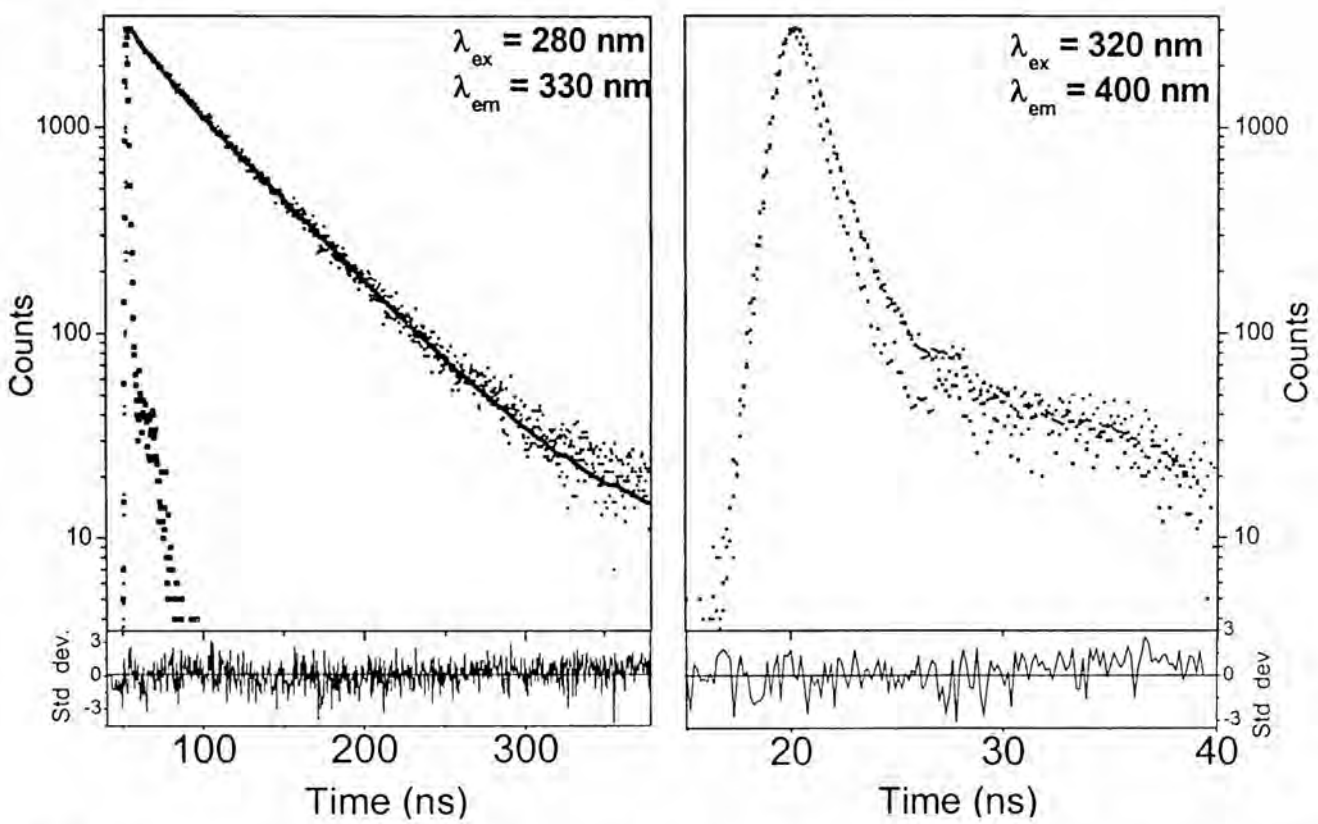

Fig. 3.4. Fluorescence decay curve of **NPY** in THF. The decay curve, the best-fit curve, the lamp profiles and the weighted residuals are shown.

Interestingly, though we have observed a new broad band in the absorption spectrum of **NPY**, no such broad absorption band could be observed in the case of **PPY**. This adds to some amount of perplexity in understanding the behavior of two very similar systems under similar experimental conditions. However, as is seen from figure 3.3., when the excitation spectrum of **PPY** is monitored at 450 nm (the longest wavelength emission band), we see a broad and fairly strong band with maximum at 375 nm. The fact that this band is not detectable in the absorption experiments is either because of the fact that the extent of complex formation is very low or the extinction coefficient of the absorption due to the complex formed is too low. But, since the complex formed is highly fluorescent it is easily detectable in the excitation spectrum.

Since our systems show spectral characteristics suggestive of some interaction between the terminal moieties, we must expect that the spacer that connects the two terminal moieties plays a role and is important in determining the spectral features discussed above. In literature, few systems are reported wherein a pyridyl moiety is attached to naphthalene and anthracene.[11,12] Systems of the cyclophane type, reported by Haenel et al., consist of naphthalene attached to pyridine in a bridged fashion.[13] This leads to restricted arrangement of pyridine over naphthalene and the two components are forced to interact. The absorption spectrum of [2,2]-naphthalinopyridinophane, in which the pyridyl moiety is connected at the 2,6-positions to the naphthayl moiety at the 1,4-positions, does have a long wavelength absorption resembling the absorption spectrum of **NPY**.[13]

The spectral characteristics reported for the cyclophane systems are attributed to the formation of an exciplex formed as a result of the π-π overlap of

the chromophores.[13] The crystal structure reported by Haenel et al. points to an almost planar arrangement of the chromophore moieties in which the interacting constituents make a small angle between them. This angle is reported to be 14.3^0. Hence, the spectral features reported for the cyclophane systems are due to a constrained geometry enforced on the molecules in which the interacting moieties were forced to overlap by virtually tying them at two ends.

Our systems consist of naphthyl/pyrenyl and pyridyl chromophores that are allowed to freely rotate around the single bond. The restriction imposed by Haenel et al. in the cyclophane systems is absent here. The fact that our systems still show spectral features suggestive of a complex formation thus leads to the conclusion that one does not need to really impose geometrical restriction by tying the terminal moieties in order to interact and form a complex in such systems. Our results show that the terminal naphthyl/pyrenyl and pyridyl moieties can interact and give rise to new absorption and emission characteristics by bringing them to constrained geometry by just connecting them covalently.

3.3. Ground-state complex or exciplex?

Formation of exciplexes between aromatic hydrocarbons and amines is reported in the literature.[3,14] The possibility that the new emission we observe in our systems could be due to the formation of an exciplex is easily discounted on certain grounds. The ground state formation of the complex is clearly evident from the broad absorption band in the case of **NPY**. Even though a ground state interaction between the pyridyl and pyrenyl moieties is not evident from the absorption features of **PPY**, the fluorescence excitation spectrum corresponding

to the new emission of **PPY** confirms that the fluorescence indeed occurs from the excitation of a weak complex in the ground state. This complex is quite fluorescent and hence gives strong emission at 450 nm when excited at 375 nm. The complex formed in the case of **PPY** is unable to show any specific absorption characteristics, perhaps due to a very low extinction coefficient.

3.4. Intermolecular vs intramolecular complex

Assigning that a ground state complex is formed as a result of the interaction of the terminal moieties in **NPY** and **PPY**, the question still prevails is whether the complex formed is intermolecular or intramolecular. In order to study this, we performed experiments by varying the concentration of the systems in the cuvette. The concentrations of the systems were varied from 1×10^{-7} to 1×10^{-2} M in the case of both **NPY** and **PPY**. These studies led to the observation that a proportionate enhancement in the fluorescence intensity of each of the bands takes place as we increase the concentration from a very low to a very high value. The fact that each of the emission bands go up in intensity as the concentration is increased is suggestive of an intramolecular nature of the complex. Further, the nature of the emission at higher concentration resembles the same at very low concentration. This observation substantiates the formation of an intramolecular complex. Had it been an intermolecular complex, we must expect a change in the emission characteristics with varying concentration. The possibility of formation of intermolecular excimers in similar systems in the case of hydrocarbons is well known.[14,15] If the interaction is intermolecular, we should have observed that the intensity of one band, the monomer band, going down in intensity and the other,

the excimer one, increasing with increasing concentration. Since this is not observed, we believe that the interaction that exists within our systems is an intramolecular one and not intermolecular.

3.5. Nature of the complex: CT or π-π?

In order to understand the nature of the complex formed in our systems, the absorption and emission spectra of the compounds were recorded in dioxane, THF, AN, ethanol (EtOH) and water. We hardly observed any shift in the absorption or emission maxima as we move from the low polar dioxane to high polar water. Only minor shifts (3 – 4 nm) could be observed in the wavelength maxima of absorption and emission. This suggests that the complex formed is not a charge transfer one. The spectral features are suggestive of a π-π character for the complex. CT complexes generally show greater influence of the solvent polarity and larger shift in the emission maxima.[16] π-π complexes are generally encountered in the formation of dimers and excimers of aromatic hydrocarbons.[17]

Formation of sandwich complexes in the case of dimers, excimers and exciplexes is reported in the literature.[6,18,19] We looked into the possibility of a sandwich complex in our systems wherein the pyridyl moiety and the naphthyl/pyrenyl moieties come one on top of the other and form a parallel arrangement. Both molecular modeling and the literature suggest that at least three carbons are necessary for π-π arrangement of the interacting terminal moieties and for a maximum overlap.[17] In both **NPY** and **PPY**, a perfectly parallel arrangement is not possible and there exists a small angle between the interacting moieties. But the distance between the two nearly parallel moieties is

small enough to have a π-π overlap and give rise to features characteristic of the intramolecular π-π complex formed between the terminal moieties.

3.6. Why intramolecular complex and not intermolecular?

Studies on intramolecular and intermolecular excimer or exciplex have shown that the entropy change associated with its formation depends strongly on whether the complexing partners are linked or not.[20] While the entropy change associated with the formation of an intermolecular complex is typically –80 $JK^{-1}mol^{-1}$, the same in the case of an intramolecular complex vary between –20 - 30 $JK^{-1}mol^{-1}$.[20] This large difference in the magnitude of the entropy change can account for a greater stability of an intramolecular complex compared to an intermolecular one, as the free energy change associated with the formation of a complex, which determines the stability of a complex is equal to $\Delta H - T\Delta S$. A simple calculation suggests that at room temperature (25 ^0C) it may not be possible to detect intermolecular complexes when the ΔH values are smaller than –24 kJ mol^{-1}. Hence, an unfavourable entropy change is responsible for the lack of the formation of an intermolecular complex between 4-methylpyridine and 1-methylnaphthalene or pyrene.

The redox potentials of the molecular components are compiled in Table 3.2 with a view to understanding whether a charge/electron transfer is thermodynamically allowed between the pyridyl and naphthyl/pyrenyl moieties. The oxidation potentials of pyrene, naphthalene and pyridine are 1.16, 1.54 and 2.09 V respectively and the reduction potentials are –2.10, –2.63 and –2.62 V respectively.[21] Since the electron accepting tendencies of pyridine and

naphthalene are very similar and naphthalene (or pyrene) is easier to oxidize compared to pyridine, the naphthyl (or pyrenyl) moiety should act as a donor in a hypothetical photoinduced electron or charge transfer process. A rough estimate of the free energy changes (ΔG) associated with the photoinduced intramolecular electron transfer process has been made using the Rehm-Weller equation:

$$\Delta G \text{ (kcal mol}^{-1}) = 23.06[E_{ox}(D) - E_{red}(A)] - E_{00} \quad (3.1)$$

Where E_{ox} (D), E_{red} (A), and E_{00} are the oxidation potential of the donor, the reduction potential of the acceptor and the excitation energy of the fluorophore respectively.[22-24] The calculated ΔG values, shown in Table 3.2 are –8.5 and –2.3 kcal mol^{-1} respectively for **NPY** and **PPY**. These values show that the photoinduced intramolecular electron transfer (PET) is possible from the excited naphthalene (or pyrene) to pyridine. This perhaps explains why an addition of pyridine to a solution of pyrene or naphthalene leads to the quenching of the fluorescence of the latter.

Table 3.2. Redox potentials of the interacting constituents, [21] singlet state energy of the fluorophores[24] and the free energy changes of electron transfer in **NPY** and **PPY**.

Component	E_{ox} (V)	E_{red} (V)	E_s (kcal/mol)	ΔG (kcal/mol)
Pyridine	2.09	–2.62	-	-
Naphthalene	1.54	–2.63	92.0	–8.52
Pyrene	1.16	–2.10	77.0	–2.29

Even though the results unambiguously point to a ground state interaction between the two terminal chromophores leading to the formation of a complex

that emits at a longer wavelength, a closer look at the time-resolved data of the systems (Table 3.1) does also indicate an excited state interaction between the terminal moieties. Had there been only a ground state interaction, the fluorescence lifetimes of the systems (when monitored the short wavelength emission) would have been very similar to that of 1-methylnaphthalene or 1-methylpyrene. The fluorescence lifetimes (in ns) of the systems when monitored at short wavelength are 51.1 (71.4%) and 33.9 (63.6%) for **NPY** and 192 (10.7%) and 122 (88.2%) for **PPY** in THF and AN respectively. The lifetime values reported in the literature for 1-methylnaphthalene and 1-methylpyrene are respectively 67 ns and 176 ns.[25,26] The measured lifetimes for **NPY** and **PPY** are, hence, significantly lower than the literature values for the parent fluorophore components, indicating an excited state interaction also between the two terminal moieties. The rate constants for this quenching interaction (presumably PET), estimated using these values as τ_0 and the measured lifetime of the short-lived component as τ and using $k_q = 1/\tau - 1/\tau_0$ are between $1.1 - 2.4 \times 10^8$ M^{-1} s^{-1} in **NPY** and $1.5 - 3.2 \times 10^8$ M^{-1} s^{-1} in **PPY**. The short-lived and the long-lived components are presumably due to the existence of two predominant conformers (a compact form and an open one) of the molecules. The absence of any growth (a negative pre-exponential factor) in the fluorescence decay profiles of the complex suggest that no fluorescent complex is formed as a result of the excited state interaction between the terminal moieties.

3.7. Conclusions

It has been concluded from the photophysical behavior of **NPY** and **PPY** that the nature of the interaction of a pyridyl moiety with a naphthyl or pyrenyl moiety strongly depends on how/whether the two moieties are connected. While an intermolecular interaction between the two does not lead to the formation of any observable complex, when linked through a dimethylene group, the π-π interaction of the two terminal moieties gives rise to the formation of hetero-dimer-type stable fluorescent complex. This difference in the behavior of the linked and unlinked systems has been ascribed to the difference in the entropy change associated with the formation of the two types of complexes.

3.8. References

(1) Lakowicz, J. R. *Principles of Fluorescence Spectroscopy*; Plenum Press: New York, 1983.

(2) Turro, N. J. *Modern Molecular Photochemistry*; The Benjamin/Cummings Publishing Co. Inc.: Menlo Park, California, 1978.

(3) Gordon, M.; Ware, W. R. *The Exciplex*; Academic Press: New York, 1975.

(4) Itoh, M.; Takita, N. *Chem. Phys. Lett.* **1979**, *62*, 279.

(5) Miwa, T.; Koizumi, M. *Bull. Chem. Soc. Jpn.* **1963**, *36*, 1619.

(6) Ide, R.; Sakata, Y.; Mizumi, Y. *Chem. Commun.* **1972**, 1009.

(7) Chandross, E. A.; Thomas, H. T. *Chem. Phys. Lett.* **1971**, *9*, 393.

(8) Okada, T.; Fujita, T.; Kubota, M.; Masaki, S.; Mataga, N.; Ide, R.; Sakata, Y.; Misumi, S. *Chem. Phys. Lett.* **1972**, *14*, 563.

(9) Taylor, G. N.; Chandross, E. A.; Schiebel, A. H. *J. Am. Chem. Soc.* **1974**, *96*, 2693.

(10) Watkins, A. R. *Austr. J. Chem.* **1980**, *33*, 177.

(11) Hirsch, T.; Port, H.; Wolf, H. C.; Miehlich, B.; Effenberger, F. *J. Phys. Chem. B.* **1997**, *101*, 4525.

(12) Saeva, F. D. *J. Photochem. Photobiol. A: Chem.* **1994**, *78*, 201.

(13) Haenel, M. W.; Lintner, B.; Benn, R.; Rufinska, A.; Schroth, G.; Krüger, C.; Hírsch, S.; Irngartinger, H.; Schweitzer, D. *Chem. Ber.* **1985**, *118*, 4884.

(14) Birks, J. B. *Photophysics of Aromatic Molecules*; Wiley: New York, 1970.

(15) Stevens, B. *Adv. Photochem.* **1971**, *8*, 161.

(16) Valeur, B.; Leray, I. *Coord. Chem. Rev.* **2000**, *205*, 3.

(17) Hirayama, F. *J. Chem. Phys.* **1965**, *42*, 3163.

(18) Chandross, E. A.; Ferguson, J.; McRae, E. G. *J. Chem. Phys.* **1966**, *45*, 3546.

(19) Chandross, E. A.; Ferguson, J. *J. Chem. Phys.* **1966**, *45*, 3554.

(20) Zachariasse, K. A.; Duveneck, G. *J. Am. Chem. Soc.* **1987**, *109*, 3790.

(21) *Techniques of Chemistry*; Siegerman, H.; Weinberg, N. L., Eds.; John Wiley & Sons: New York, 1975; Vol. V, Part II.

(22) Weller, A. *Pure Appl. Chem.* **1968**, *16*, 115.

(23) Kavarnos, G. J. *Fundamentals of Photoinduced Electron Transfer*; John Wiley & Sons: New York, 1993.

(24) Kavarnos, G. J.; Turro, N. J. *Chem. Rev.* **1986**, *86*, 401.

(25) Berlman, I. B. *Handbook of Fluorescence Spectra of Aromatic Molecules*; Academic Press: New York, 1971.

(26) Snare, M. J.; Thistlewaite, P. J.; Ghiggino, K. P. *J. Am. Chem. Soc.* **1983**, *105*, 3328.

Chapter 4

Cation signaling properties of 1-(1-naphthyl)-2-(4-pyridyl)ethane and 1-(1-pyrenyl)-2-(4-pyridyl)ethane

The fluorescence response of **NPY** and **PPY**, whose photophysical properties have been discussed in the previous chapter, towards various metal ions has been presented in this chapter. It is shown that 'off-on' signaling of the metal ions by these *fluorophore-spacer-receptor* systems results from metal ion-induced *enhanced communication* between the terminal moieties of the molecule, whereas in conventional systems with the same architecture, 'off-on' signaling results from disruption of the communication between the fluorophore and the receptor in the presence of the guest. Moreover, it is shown that the fluorescence response of the systems in the presence of the metal ions depends on the monitoring wavelength. The systems offer a wavelength window where the fluorescence is switched 'on' and the fluorescence is switched 'off' when one looks through a different window.

4.1. Spectral features

4.1.1. Absorption

The absorption spectra of **NPY** and **PPY** with various metal ions have been studied in THF and AN. Addition of the solutions of the metal salts leads to significant changes in the absorption behavior of **NPY**. With increase in the

concentration of the metal ion a new band appears at longer wavelength. The new absorption band (λ_{max} ~370 nm) becomes as intense as the 330 nm band of **NPY**. The new band grows at the expense of the original band at around 330 nm. An isosbestic point could be observed with all the metal ions except in the case of Cu^{2+} and Mn^{2+}. Representative absorption spectra of **NPY** in the presence of some metal ions in THF are shown in figure 4.1. In a more polar medium such as AN, the new band appears almost at the same wavelength as that in THF. The absorption spectral changes of **NPY** in AN with certain metal ions is shown in figure 4.2.

Interestingly, in the case of **PPY**, noticeable change in the absorption spectrum could not be observed in the presence of any of the metal ions.

4.1.2. Emission spectra

It is already stated in the last chapter that the emission spectra of **NPY** and **PPY** consist of two peaks, one structured band in the short wavelength region due to the parent fluorophore and a long wavelength broad band corresponding to a ground state intramolecular complex.

The emission behavior of **NPY** and **PPY** has been studied in the presence of metal ions. To begin with, we have one structured emission at 330 nm and a broad emission at 400 nm in the case of **NPY**. Addition of the metal salts leads to fluorescence quenching at both the wavelength regions. Interestingly, a new emission band appears gradually at around 500 nm with the addition of the metal salts. Representative fluorescence spectra of **NPY** in the presence of various amounts of the metal salts are shown in figure 4.3.

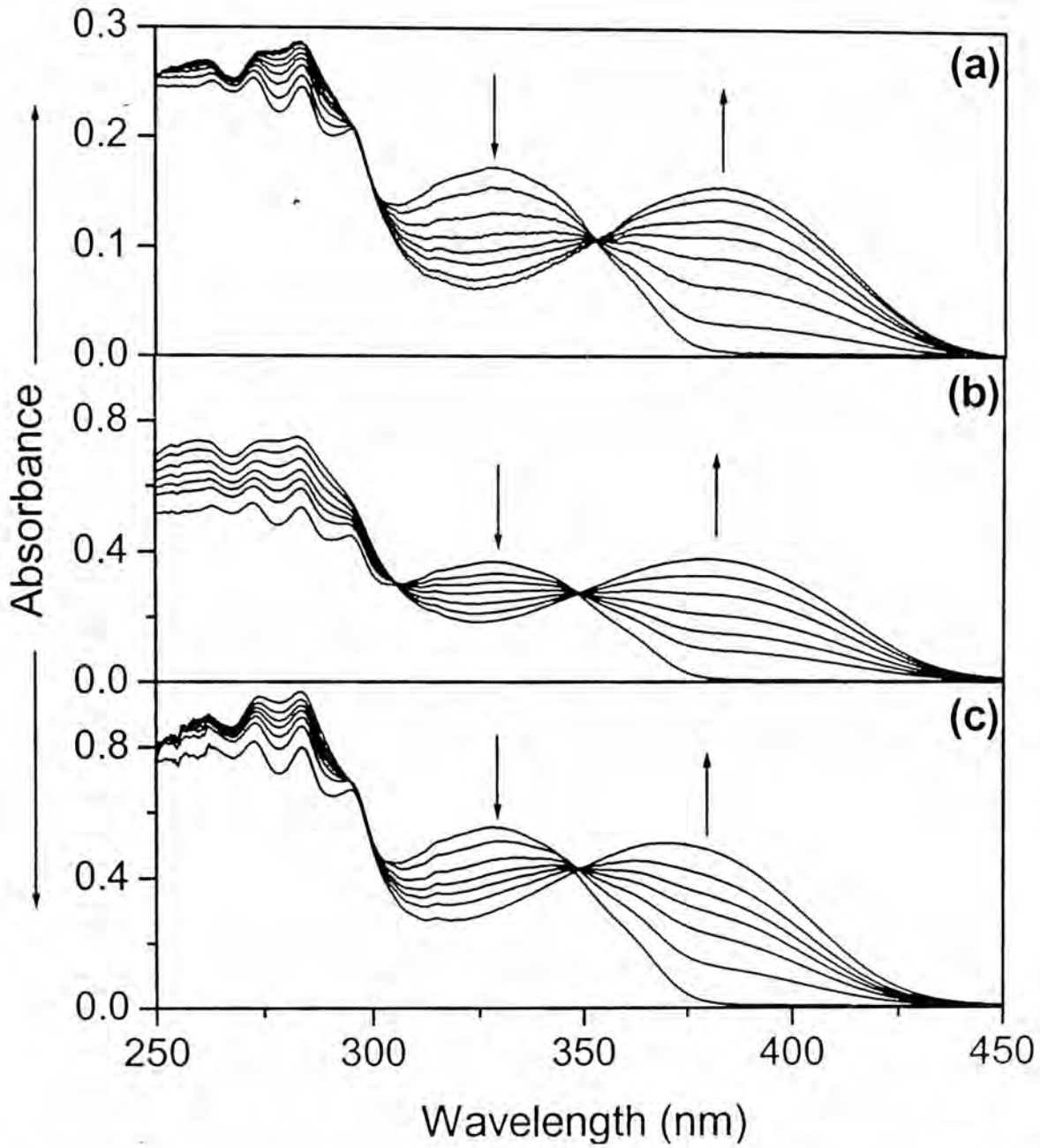

Fig. 4.1. Absorption spectra of **NPY** with (a) Cr^{3+}, (b) Fe^{3+} and (c) H^{+} in THF. The concentrations of the metal ions (in 10^{-4} M) increases from 0 to 2.9 in (a), 3.8 in (b) and 2.0 in (c) in the direction of the arrows.

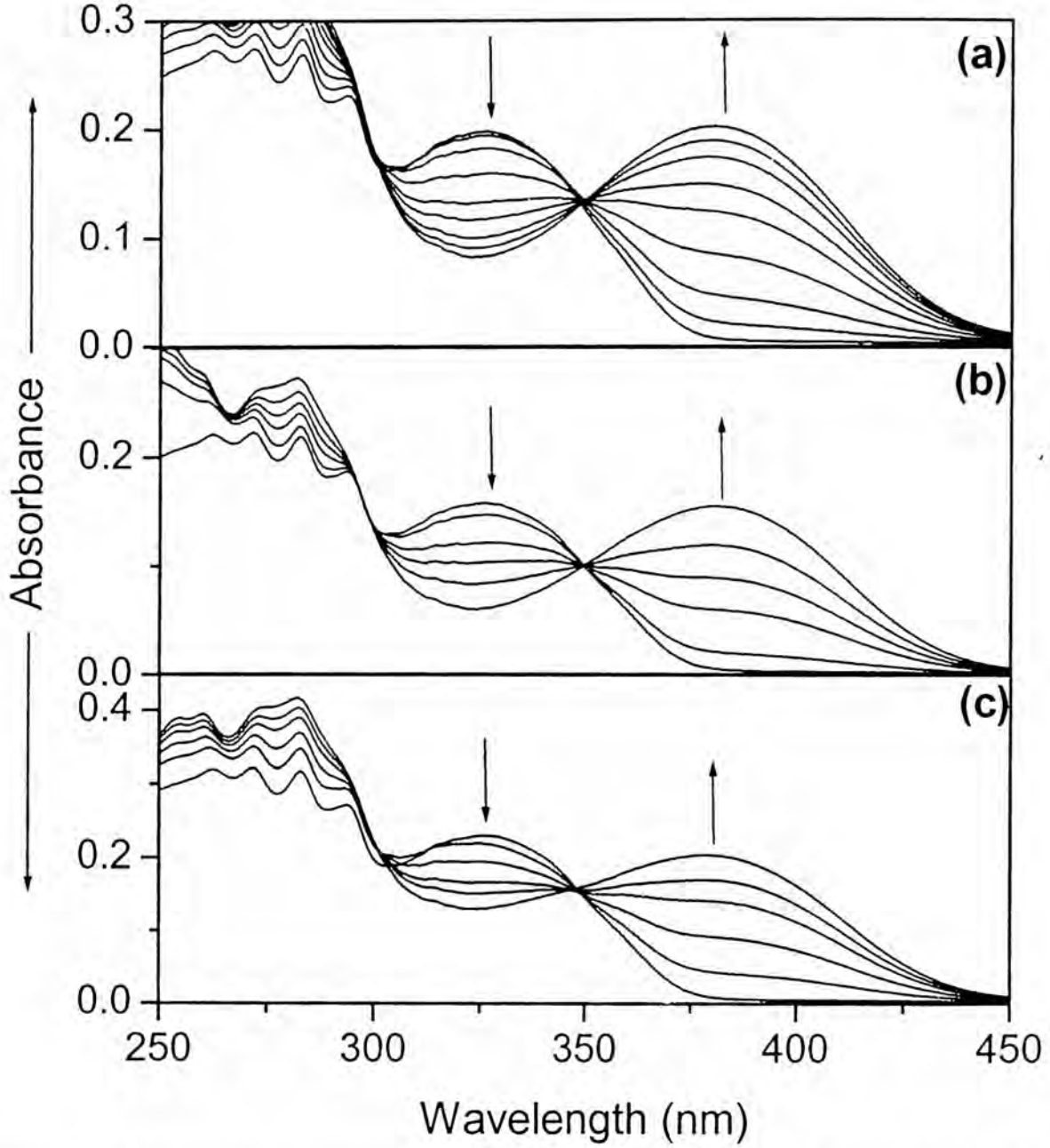

Fig. 4.2. Absorption spectra of **NPY** with (a) Cr^{3+}, (b) Pb^{2+} and (c) Zn^{2+} in AN. The concentrations of the metal ions (in 10^{-4} M) increases from 0 to 0.87 in (a), 4.0 in (b) and 1.4 in (c) in the direction of the arrows.

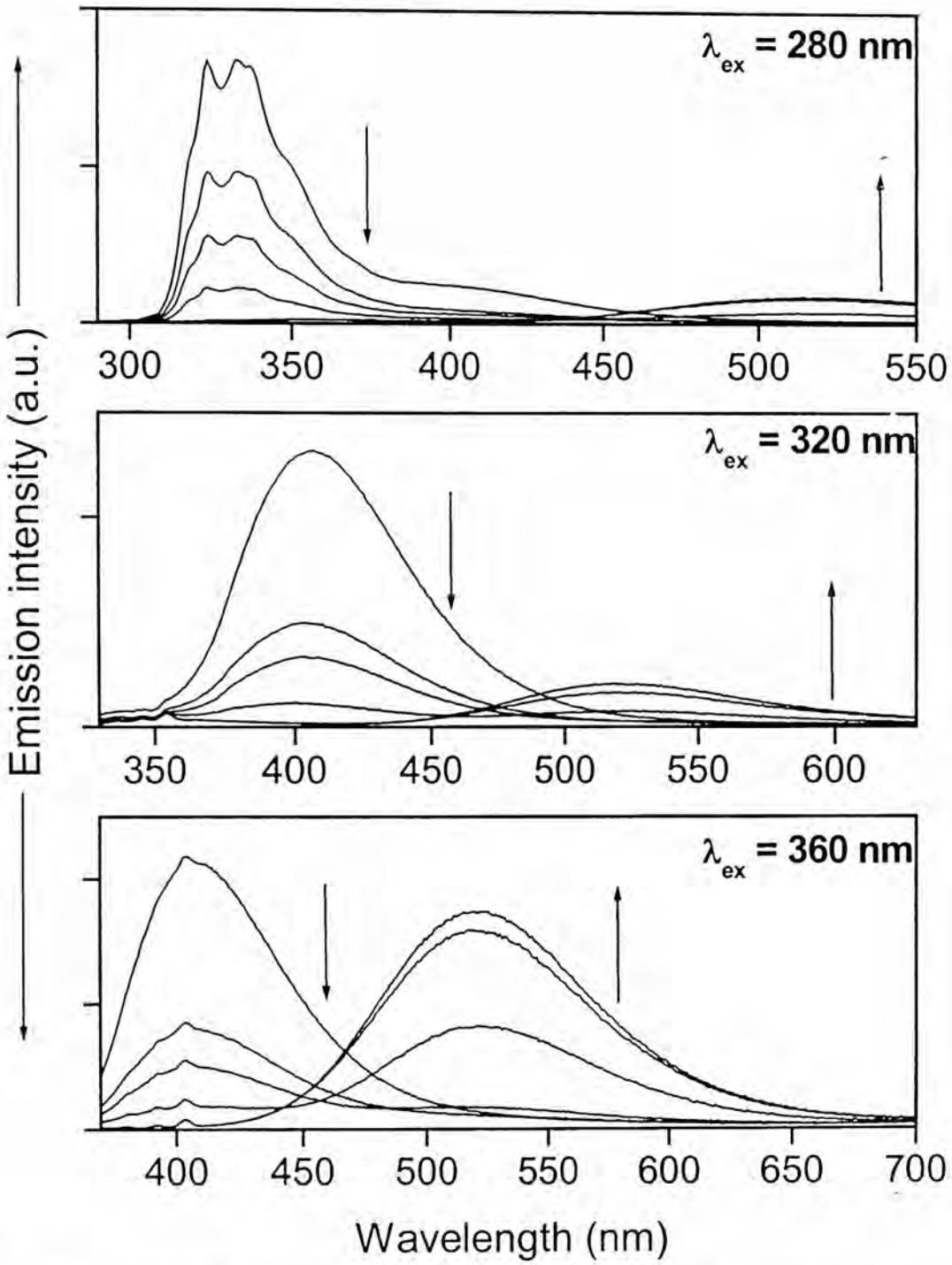

Fig. 4.3. Emission spectra of **NPY** with Co^{2+} in AN for various excitation wavelengths. $[Co^{2+}]$ increases from 0 to 6 x 10^{-4} M in the direction of the arrows.

An excitation wavelength dependent experiment shows that the intensity of the new band is maximum when excitation is made at around 360 nm. This suggests that this new emission band results from excitation of the new absorption band observed in the presence of the metal salts. In AN, the new emission maximum is observed at 525 nm. The new emission could be observed with all the metal ions indicated in Table 4.1. However, in some cases, such as in the case of Mn^{2+}, the emission is not that strong. The situation is shown in figure 4.3.

With **PPY** too, a similar behavior is noticed. The intensity of the structured band at 400 nm (λ_{ex} = 315 nm), and that of the structureless emission at 450 nm (λ_{ex} = 375 nm) go down in the presence of the metal ions. The new band appears at around 585 nm in THF and 610 nm in AN. It is observed that the intensity of this emission increases up to a certain concentration of the metal ion and thereafter, further addition leads to quenching. A representative example of the observed phenomenon is shown in figure 4.4. The emission parameters for **NPY** and **PPY** in THF and AN are collected in Table 4.1.

4.1.3. Excitation spectra

The fluorescence excitation spectra were recorded for the compounds by monitoring the various emission bands in both the solvents studied. For **NPY**, the excitation spectra were monitored at 340, 400 and 500 nms. When monitored at 500 nm, the fluorescence excitation spectrum shows an intense band with maximum at ~370 nm. This band is very similar to the absorption band of the system in the presence of the metal ions. This observation unequivocally establishes that the long wavelength emission is due to the excitation of the new

species that is formed with the metal ions. Some of the representative excitation spectra of **NPY** in the presence of the metal ions monitored at different wavelengths are shown in figure 4.5.

Table 4.1. Wavelength (in nm) corresponding to the fluorescence maximum of **NPY** and **PPY** in THF and AN in the absence and in presence of different metal ions.†

Metal ion	**NPY**		**PPY**	
	THF	AN	THF	AN
None	398	401	450	453
Ag^{+}	489	503	585	607
Cd^{2+}	494	514	583	609
Co^{2+}	494	522	588	610
Cr^{3+}	495	523	585	610
Cu^{2+}	502	522	582	608
Fe^{3+}	498	520	584	608
Hg^{2+}	490	504	583	607
Mn^{2+}	490	518	583	607
Ni^{2+}	500	521	586	610
Pb^{2+}	487	519	585	611
Zn^{2+}	482	520	583	607
H^{+}	479	515	565	607

†Metal ion concentrations were in the range $10^{-5} - 10^{-3}$ M.

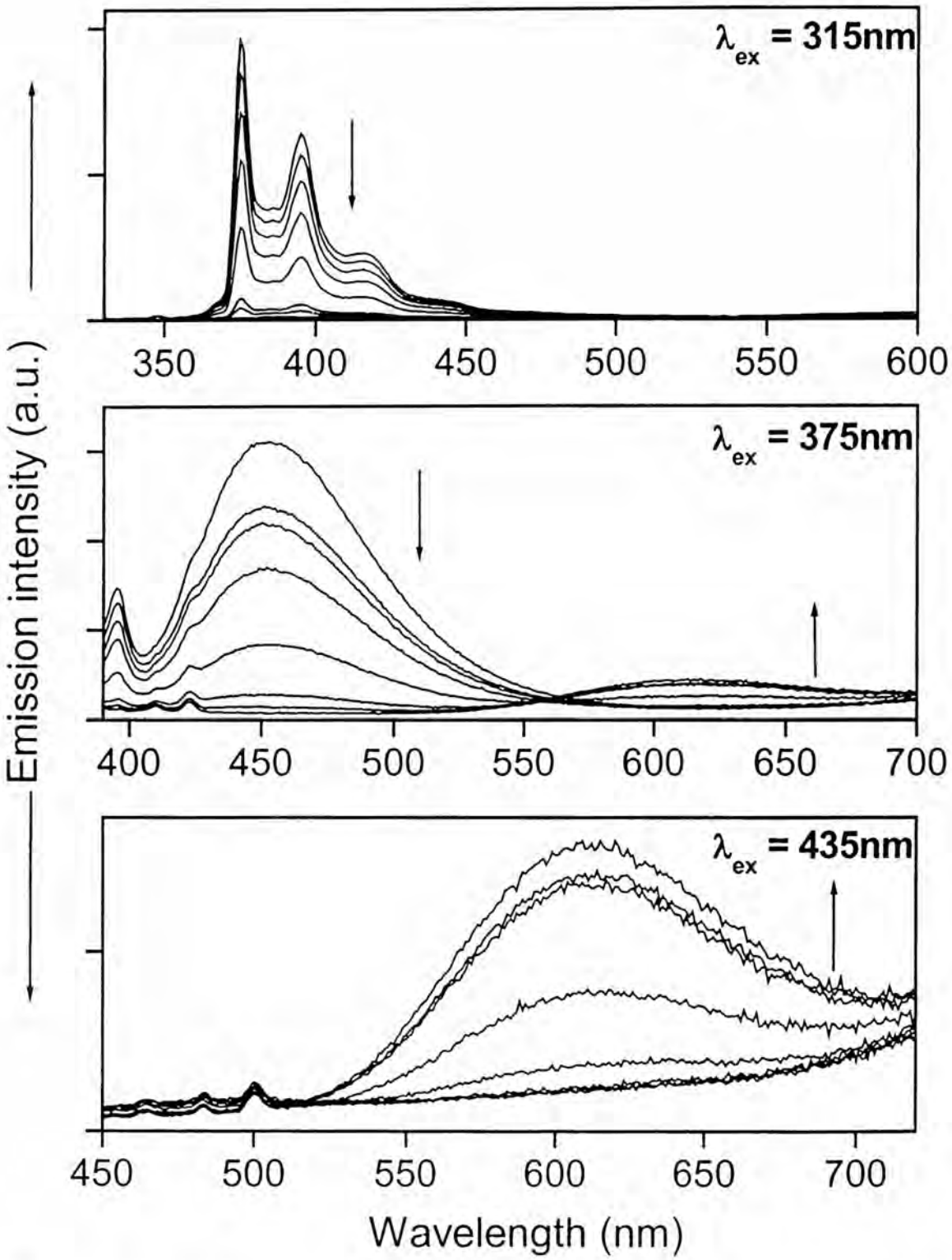

Fig. 4.4. Emission spectra of **PPY** with Ni^{2+} in AN at various excitation wavelengths. [Ni^{2+}] increases from 0 to 3.1.x 10^{-3} M in the direction of the arrows.

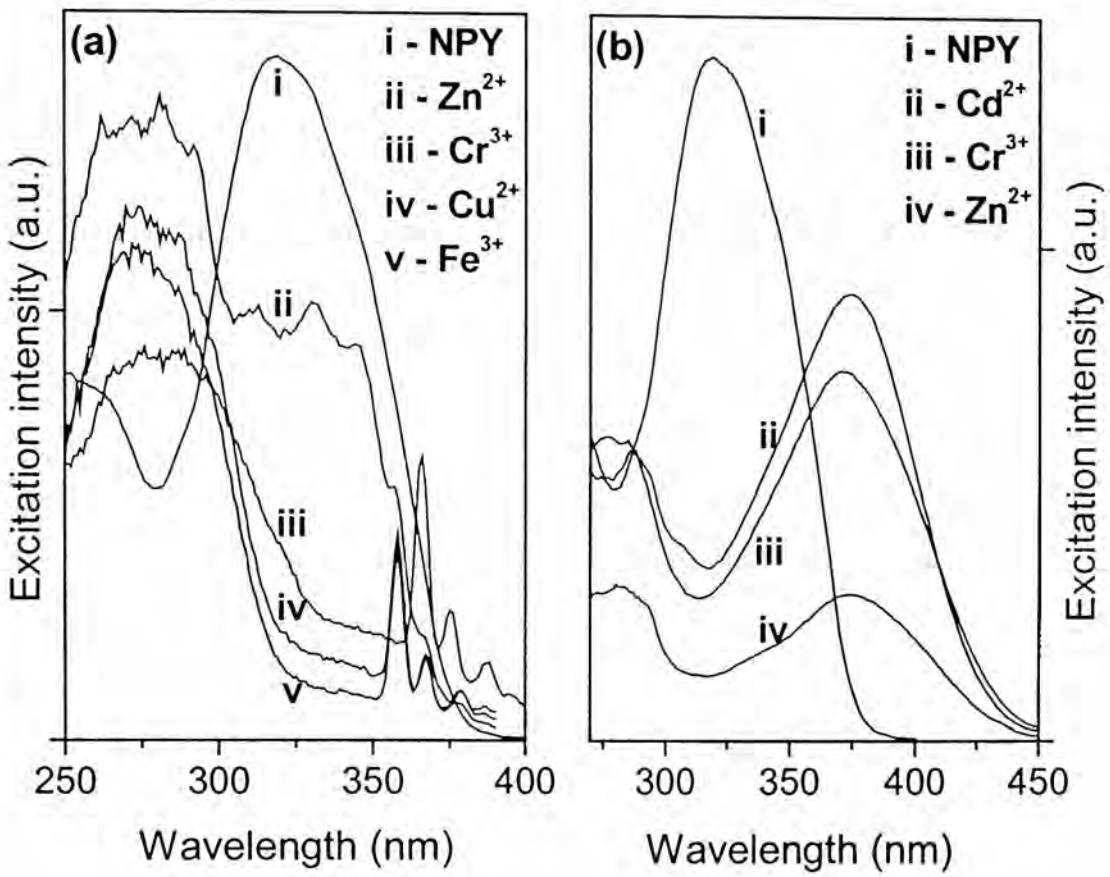

Fig. 4.5. Excitation spectra of **NPY** in AN in the absence and presence of various metal ions. The spectra shown in (a) and (b) are obtained by monitoring the fluorescence at 410 nm and 525 nm respectively. $[M^{n+}]$ corresponds to the concentration of the metal ion for which FE was maximum.

With **PPY** also, similar experiments were conducted. The excitation spectra were measured monitoring the original emission bands at 400 and 450 nm, and the new band at 610 nm. The band that comes up when the excitation spectrum was monitored at 610 nm shows a maximum at 435 nm. This

observation suggests that 610 nm emission arises due to the excitation of a ground state species that absorbs at around 435 nm. Interestingly, at this wavelength, **PPY** virtually shows no absorption. The difference in the absorption and fluorescence excitation behavior of **PPY** can only be rationalized by assuming that the extent of formation of the complex formed between the pyrenyl and pyridyl moieties is too small or the extinction coefficient of the absorption due to the metal – sensor complex is too low at around 435 nm. Since the complex is highly fluorescent it is easier to detect this species through fluorescence compared to absorption. Some representative excitation spectra of **PPY** obtained on monitoring the fluorescence at 610 nm are shown in figure 4.6.

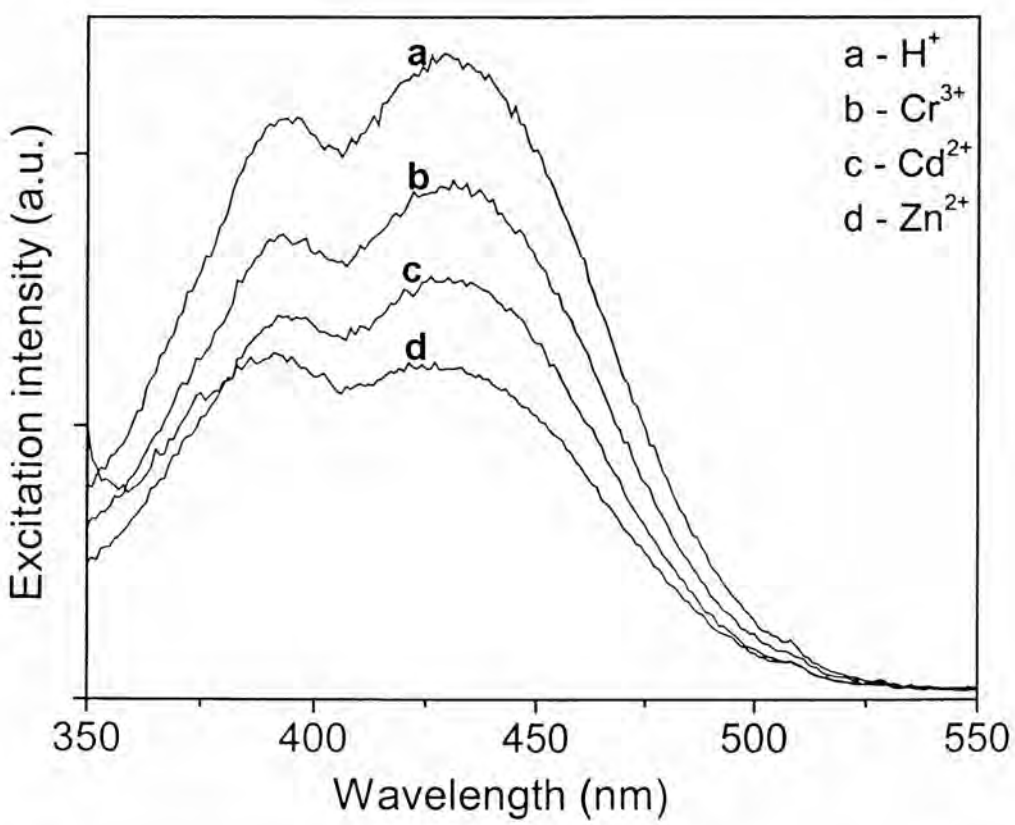

Fig. 4.6. Excitation spectra of **PPY** with various metal ions in AN (λ_{em} = 610 nm). [M^{n+}] corresponds to the concentration of the metal ion for which maximum FE was observed.

4.1.4. Fluorescence lifetime

Fluorescence lifetimes of **NPY** and **PPY** have been measured monitoring the various emission bands of the systems. In the case of **NPY**, the experiments could be performed monitoring all the three emission wavelengths. With **PPY**, only the first band (emission at 400 nm) could be monitored. Fluorescence lifetimes could not be measured monitoring the 450 nm and ~585 nm (in THF) or ~610 nm (in AN) bands due to poor emission intensity at these wavelengths.

The fluorescence decay parameters of the systems for various excitation and emission wavelengths in two solvents are tabulated in the appendix 1. The measured decay parameters for **NPY** show that the fluorescence lifetime of the complex formed between the metal ions and the sensor systems is in the sub-nanosecond range.

4.2. NPY and PPY as metal ion sensors

The usefulness of simple three-component systems, **NPY** and **PPY**, in sensing the transition metal ions, which themselves are quenchers of the fluorescence,[1,2] is described in this section. We have observed that the fluorescence intensity of **NPY** and **PPY** at various emission wavelengths gets altered in the presence of the metal ions. Concentrating on the bands at 330 and 400 nm in the case of **NPY**, we have seen that the addition of metal ions quenches the fluorescence at these wavelengths. This represents a typical 'on-off' action of fluorescence. At the longer wavelength, (500 nm in THF and 525 nm in AN), where the new emission is observed, the emission behavior represents an 'off-on'

fluorescence signaling of the metal ions. The intensity of this emission varies with different metal ions studied.

Table 4.2. Fluorescence output of **NPY** in THF and AN with the addition of metal ions at various wavelengths.

Metal ion	THF			AN		
	335 nm[a]	400 nm[b]	500 nm[b]	335 nm[a]	400 nm[b]	525 nm[b]
None	1	1	1	1	1	1
Ag^{+}	0.017	0.015	11.9	0.39	0.286	1.1
Cd^{2+}	0.02	0.03	7.3	0.01	0.05	13.5
Co^{2+}	0.018	0.027	8.4	0.01	0.016	13.6
Cr^{3+}	0.015	0.01	6.9	0.01	0.02	16
Cu^{2+}	0.37	0.02	2.6	0.008	0.01	10.3
Fe^{3+}	0.018	0.02	4.9	0.003	0.01	10.8
Hg^{2+}	0.33	0.27	1.8	0.117	0.11	1.93
Mn^{2+}	0.26	0.03	1.2	0.27	0.06	8.6
Ni^{2+}	0.011	0.017	6.6	0.01	0.018	17.9
Pb^{2+}	0.137	0.074	7.6	0.012	0.025	13.2
Zn^{2+}	0.31	0.17	1.8	0.03	0.06	11.3
H^{+}	0.19	0.08	2.4	0.011	0.02	15.7

[a]λ_{ex} = 280 nm, [b]λ_{ex} = 360 nm

With **PPY** too, a similar behavior is observed. The first band, the structured emission at 400 nm vanishes on addition of the metal ions. The band at 450 nm too disappears with added metal ion. A new band is generated at 585 nm

in THF and at 610 nm in AN. Hence, we have fluorescence 'on-off' signaling at 400 and 450 nm and 'off-on' response at the longer wavelength. The intensity of the new emission varies with various metal ions studied. The fluorescence output at various emission wavelengths in the presence of different metal ions are given in Table 4.2 for **NPY** and in Table 4.3 for **PPY**.

Table 4.3. Fluorescence output of **PPY** in THF and AN with the addition of metal ions at various wavelengths.

Metal ion	THF			AN		
	395 nm[a]	450 nm[b]	585 nm[c]	395 nm[a]	450 nm[b]	610 nm[c]
None	1	1	1	1	1	1
Ag^{+}	0.008	0.02	8.2	0.31	0.33	1.9
Cd^{2+}	0.016	0.03	19.9	0.017	0.01	25
Co^{2+}	0.044	0.02	11.3	0.015	0.025	8.6
Cr^{3+}	0.016	0.01	22.6	0.023	0.01	25.4
Cu^{2+}	0.023	0.03	11.9	0.014	0.01	13.5
Fe^{3+}	0.013	0.01	19.5	0.015	0.01	35.6
Hg^{2+}	0.45	0.50	1.6	0.18	0.21	2.2
Mn^{2+}	0.382	0.14	14.9	0.20	0.07	16.9
Ni^{2+}	0.01	0.012	12.4	0.013	0.024	6.5
Pb^{2+}	0.08	0.06	7.6	0.025	0.028	12.5
Zn^{2+}	0.222	0.05	15.7	0.201	0.03	16.7
H^{+}	0.560	0.28	7.4	0.017	0.01	35

[a]λ_{ex} = 315 nm, [b]λ_{ex} = 375 nm, [c]λ_{ex} = 435 nm

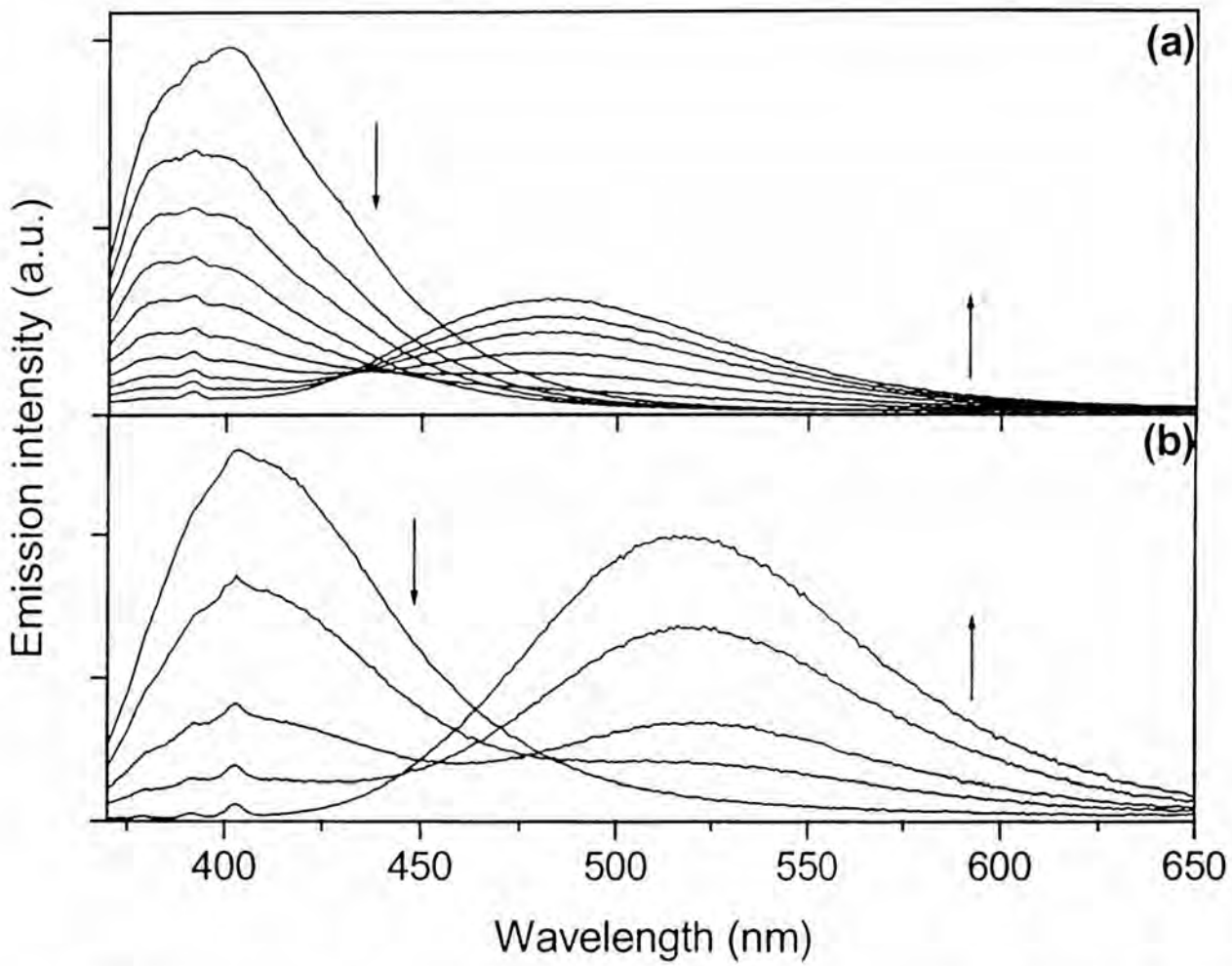

Fig. 4.7. Emission spectra of **NPY** in the presence of Cr^{3+} in THF (a) and AN (b). $[Cr^{3+}]$ (in 10^{-4} M) increases from 0 to 2.9 in (a) and 0.87 in (b) in the direction of the arrows. λ_{ex} = 360 nm.

The new emission is a broad and featureless one and unlike the original emission, is rather sensitive to the solvent polarity. An increase in the polarity of the medium induces Stokes shift of the fluorescence maximum. In the case of **NPY**, as the solvent is changed from THF to AN, the emission maximum shifts from 500 to ~525 nm. With **PPY**, the maximum is shifted from 585 to ~610 nm

when the solvent is changed from THF to AN. The location of the emission maximum for different metal ions is not very different. Representative spectra showing the solvent polarity dependence of the new emission band of **NPY** are shown in figure 4.7.

4.3. Wavelength window based signaling

When we consider the signaling behavior of **NPY** and **PPY**, we can say that the signaling could be achieved by monitoring various emission maxima. To begin with, we have an excitation wavelength dependent emission behavior for these systems and there are two emission maxima to monitor; at 330 and 400 nm for **NPY** and at 400 and 450 nm for **PPY**. We see that the emission at these wavelengths gets quenched in the presence of the metal ions. Hence the systems behave as fluorescence 'on-off' signaling systems at these wavelengths.

Signaling efficiency of the systems can also be assessed concentrating our attention on the new band generated in the presence of the metal ions. As is seen above, this band maximum appears at ~500 nm for **NPY** and at ~600 nm for **PPY** in THF and it shifts by ~25 nm towards the red in AN. Since this band appears only in the presence of the metal ions, the sensing of the metal ions can be termed as 'off-on' fluorescence signaling at these wavelengths.

We now have two systems that display fluorescence signaling of the metal ions, the exact nature of which depends on the monitoring wavelength of emission and also, to some extent on the excitation wavelength. We can say, in short, that we have a multiple excitation and emission wavelength window based fluorescence sensors of the transition metal ions. The excitation/emission

wavelength combinations are 280/330 nm, 320/400 nm and 360/500 nm for the fluorescence 'on-off', 'on-off' and 'off-on' actions for **NPY** and 315/400 nm, 375/450 nm and 435/600 nm for the respective actions for **PPY** on metal ion binding. The situation is represented in figure 4.8. for **NPY** and in figure 4.9. for **PPY**.

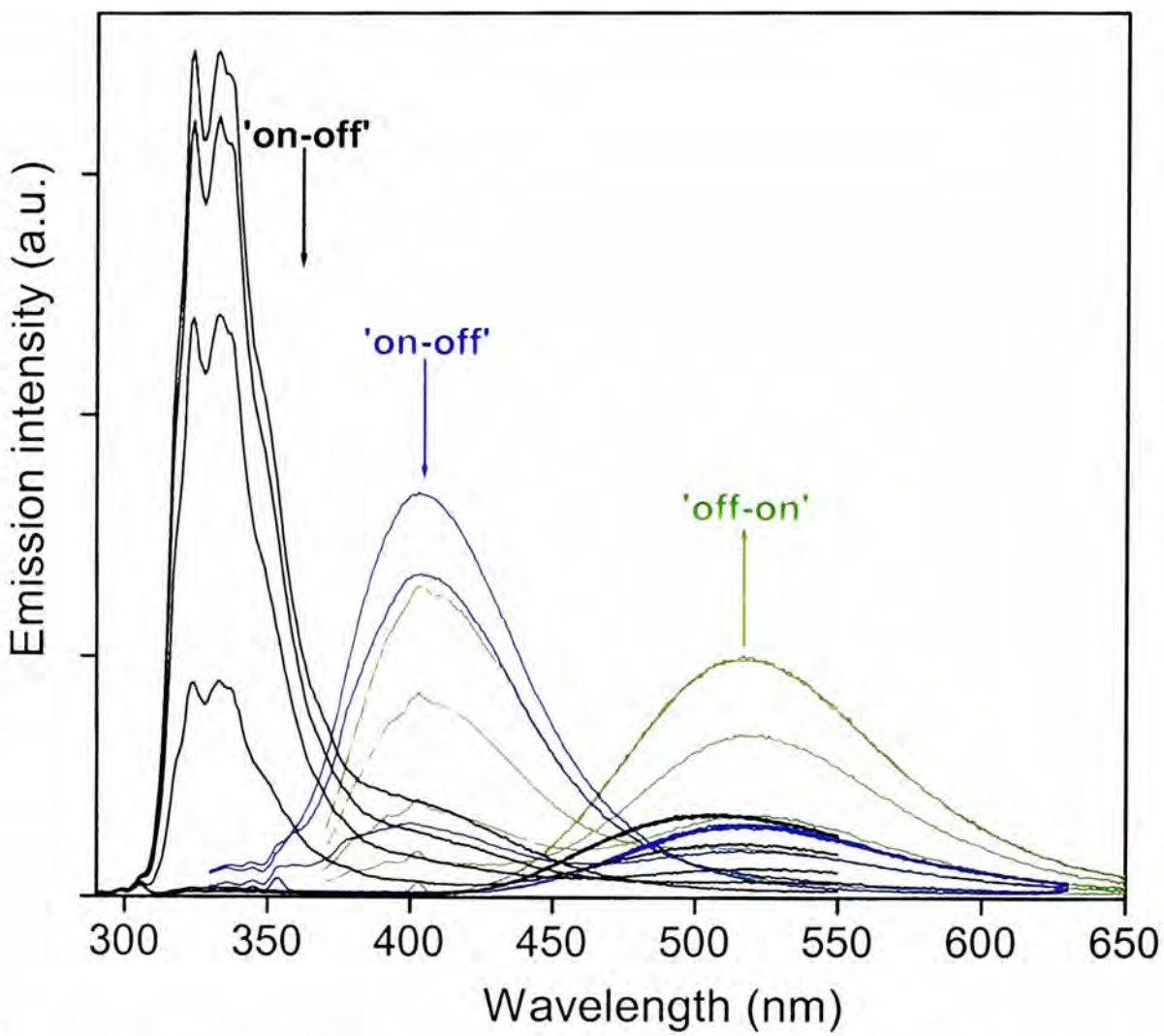

Fig. 4.8. Representative emission spectra of **NPY** showing the wavelength window based fluorescence signaling. The emission behavior of **NPY** in AN with Cr^{3+} is taken as an example. [Cr^{3+}] increases in the direction of the arrows from 0 to 6.5 x 10^{-5} M.

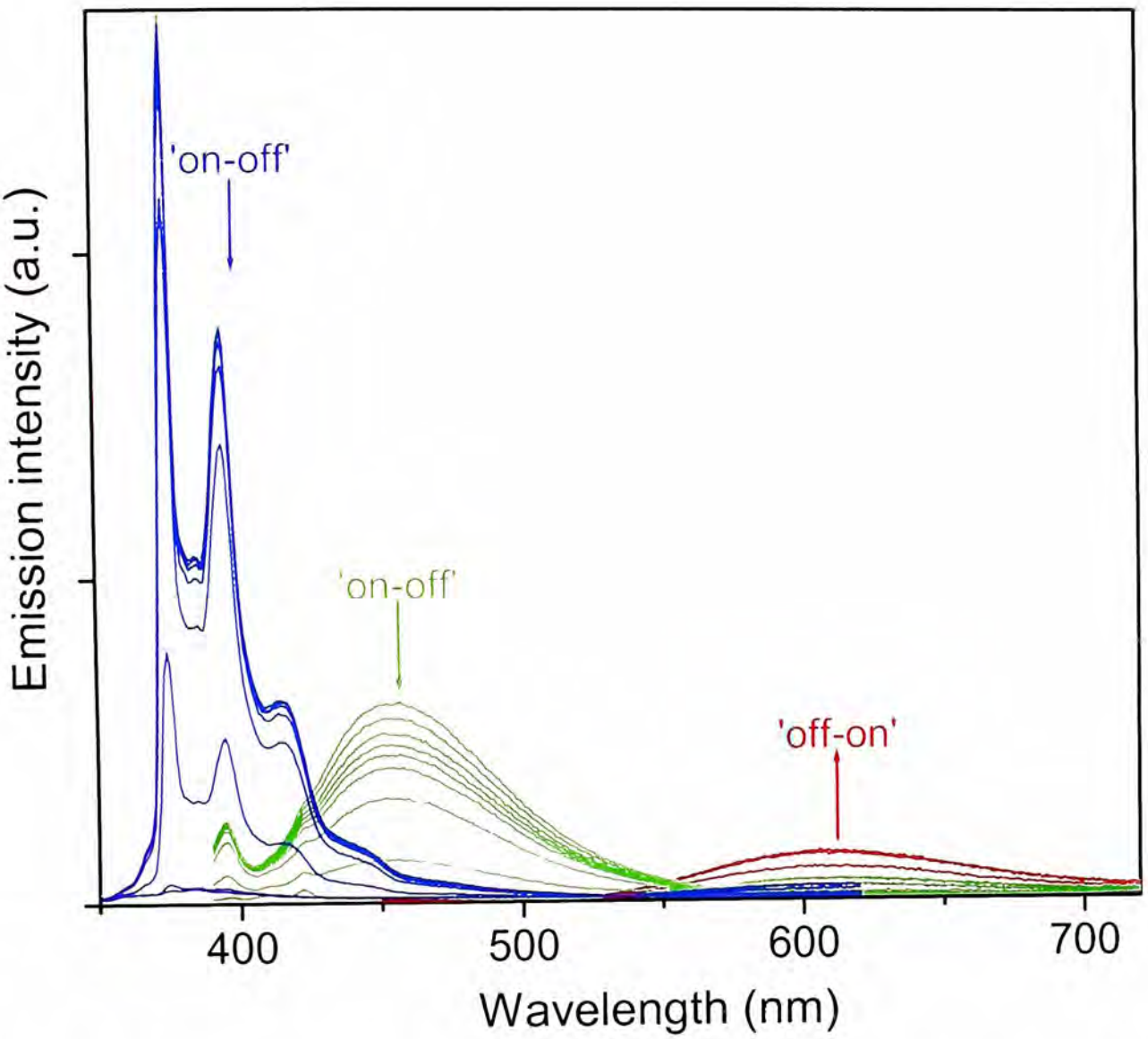

Fig. 4.9. Representative emission spectra of **PPY** showing the multiple wavelength window based fluorescence signaling. Spectral changes produced on the addition of Cr^{3+} to **PPY** in AN is taken as the example. $[Cr^{3+}]$ increases in the direction of the arrows from 0 to 1.6×10^{-4} M.

4.4. Are residual protons the culprits?

It is evident from the data presented in Table 4.2 and Table 4.3 that all metal ions switch 'on' the fluorescence at the longer wavelength for both **NPY** and **PPY**, though some of the metal ions do not show it as prominently as others. With Mn^{2+}, the emission is less intense and with Ag^{+} and Hg^{2+} ions, the emission is meager. Proton gives an intense band. Because of the fact that we are using hydrated perchlorate salts of the metal ions, which are likely to contain protons as impurity, it may be possible that the 'off-on' signaling is due to the protons rather than due to the metal ions. However, this possibility has been ruled out with the help of the following experiments. Addition of sodium perchlorate monohydrate to a solution of **NPY** does not generate any new emission in the long wavelength region. Had the new emission been due to the protons from the hydrated metal salts, we should have observed the new emission in the presence of hydrated sodium perchlorate solution too. This point is further supported by another experiment in which the emission behavior of **NPY** with hydrated zinc perchlorate solution was studied in the presence of 3 - 4 mM of sodium carbonate. The fact that the long wavelength emission could be observed even in the presence of sodium carbonate clearly establishes that the new emission is the result of complexation of the metal ions with the systems studied and not just because of protonation of the sensor systems by the residual protons present in the hydrated salts. The effect of sodium perchlorate on the fluorescence spectra of **NPY** is illustrated in figure 4.10.

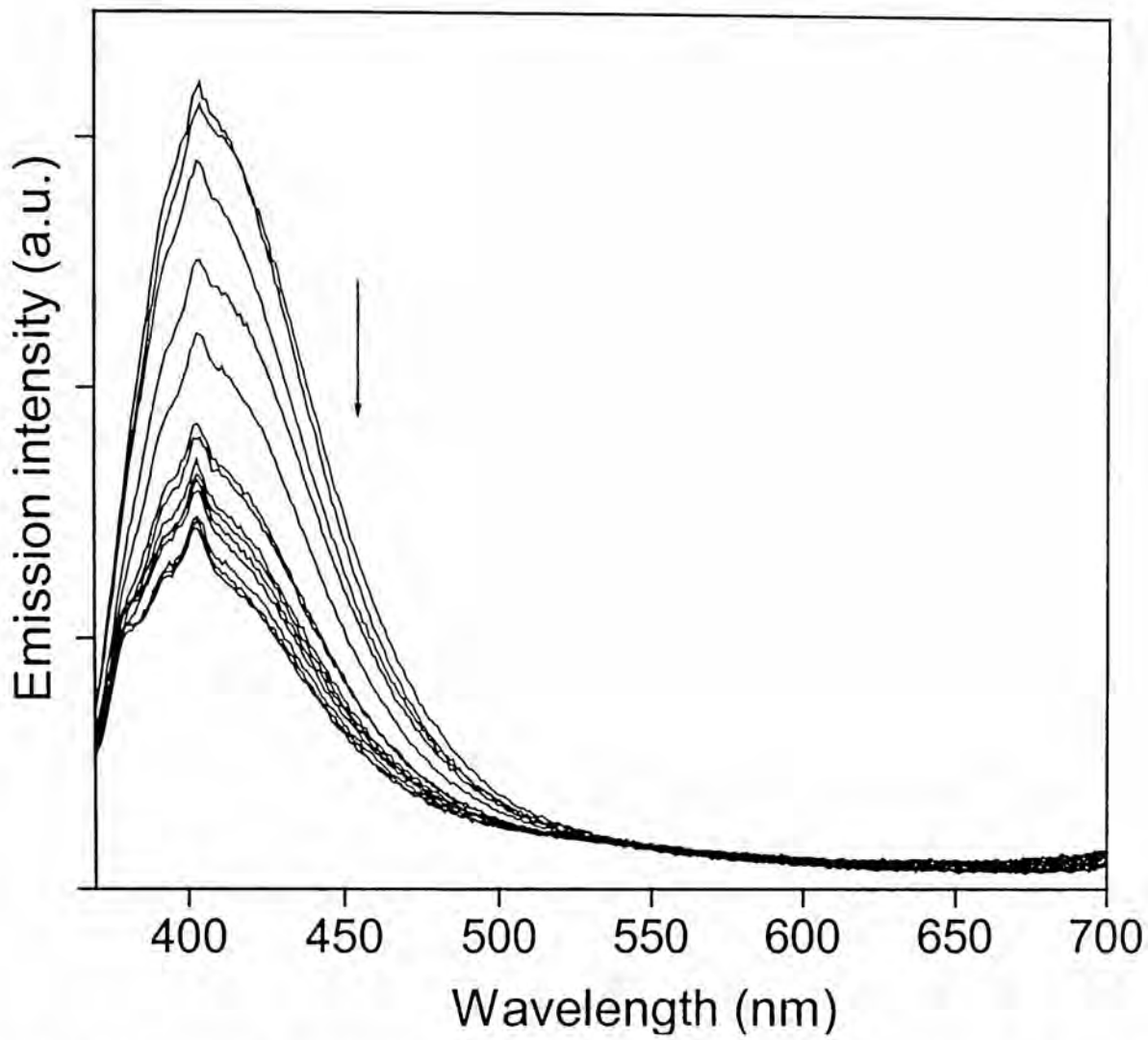

Fig. 4.10. Emission spectra of **NPY** in AN with the addition of sodium perchlorate (hydrated). $[Na^+]$ is varied from 0 to 3 x 10^{-2} M in the direction of the arrow. λ_{ex} = 360 nm.

4.5. Mechanism of 'off-on' fluorescence signaling of the guests

We have stated in the previous chapter that an intramolecular complex is formed as a result of through-space interaction of the π-clouds of the pyridyl and naphthyl/pyrenyl moieties. The present systems contain a pyridyl moiety which

forms complexes with the metal ions under similar experimental conditions.[3] A recent paper shows that bivalent transition metal ions form $[ML]^{2+}$, $[ML_2]^{2+}$, $[ML_3]^{2+}$ and $[ML_4]^{2+}$ complexes with 4-methylpyridine in acetonitrile and that the stability complexes for the mono complexes follow the order $Mn^{2+} > Zn^{2+} > Cu^{2+}$.[3] Quite obviously, the metal ions are likely to attack this pyridyl moiety, making it an electronically deficient moiety analogous to the pyridinium ion. This event is not only expected to enhance its communication with the electron- rich fluorophore, but also expected to introduce significant charge transfer (CT) character to it. The dipolar nature of the complex, as is evident from the fluorescence spectral data in THF and AN, is fully consistent with this interpretation. Moreover, this mechanism is also in agreement with the literature reports on the formation of CT complexes between pyridinium ion and various hydrocarbon moieties.[4-7]

The N-substituted pyridinium derivatives, considered as electron acceptors in intermolecular CT interactions,[5,6,8-11] are found to generate new CT absorption bands when they form electron donor-acceptor complexes with aromatic hydrocarbons such as methylated benzenes, naphthalenes and anthracenes.[4] Based on the literature, the expected absorption maximum for the CT band of the electron donor-acceptor complex of the pyridinium ion with 1-methylnaphthalene and pyrene is ~365 nm and ~404 nm respectively.[4] These estimates are based on a linear correlation between $h\nu_{CT}$ (intermolecular CT excitation energy) and ionization potentials (E_i) of the various hydrocarbons used.[4] E_i values are respectively 7.96 and 7.58 eV for 1-methylnaphthalene and pyrene.[12]

Interestingly, the new absorption maxima observed in our systems after coordination of the metal ions are not very different from the literature values.

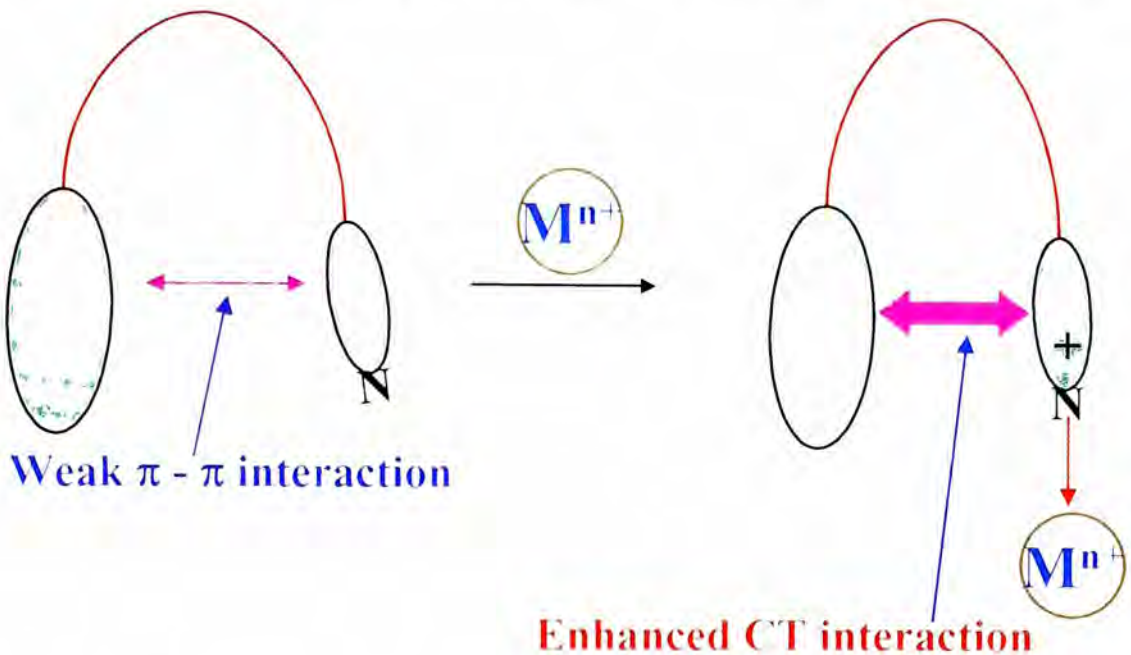

Fig. 4.11. A pictorial representation of intramolecular interaction in **NPY** and **PPY** in the absence and in the presence of metal ions.

The conventional signaling mechanism in *fluorophore-spacer-receptor* systems requires a disruption of the strong communication between the terminal moieties, the fluorophore and receptor, in the presence of a guest. [13-16] However, we would like to stress here that the fluorescence enhancement ('off-on' signaling) of the present systems is the result of an *enhanced* interaction between the receptor and the fluorophore. In this respect the signaling by the present systems can be termed as novel and different from the conventional PET signaling mechanism. The signaling behavior of the present systems is pictorially represented in figure 4.11.

Table 4.4. Molar concentration of the metal ions at the maximum FE of the long wavelength emission for **NPY** and **PPY** in THF and AN.

Metal ion	Concentration of the metal ion			
	NPY		**PPY**	
	THF	AN	THF	AN
Ag^{+}	1.8×10^{-4}	7.3×10^{-3}	7.3×10^{-4}	1×10^{-3}
Cd^{2+}	8.6×10^{-4}	1.2×10^{-4}	4.2×10^{-4}	6.3×10^{-4}
Co^{2+}	7.5×10^{-4}	6×10^{-4}	1×10^{-3}	3.8×10^{-3}
Cr^{3+}	2.9×10^{-4}	8.7×10^{-5}	2.4×10^{-4}	1.6×10^{-4}
Cu^{2+}	6.8×10^{-4}	2.3×10^{-4}	4.5×10^{-4}	2.3×10^{-4}
Fe^{3+}	3.8×10^{-4}	3.9×10^{-4}	7.1×10^{-4}	4.8×10^{-4}
Hg^{2+}	9×10^{-3}	7×10^{-3}	8.5×10^{-3}	9×10^{-3}
Mn^{2+}	9.5×10^{-3}	9.3×10^{-3}	6.5×10^{-3}	7.5×10^{-3}
Ni^{2+}	2.4×10^{-3}	1.8×10^{-3}	5×10^{-3}	3.1×10^{-3}
Pb^{2+}	5.5×10^{-3}	4×10^{-3}	2.4×10^{-3}	3×10^{-3}
Zn^{2+}	4.5×10^{-3}	1.4×10^{-3}	1.1×10^{-3}	9.1×10^{-4}
H^{+}	2×10^{-4}	7.5×10^{-4}	1.4×10^{-4}	5×10^{-4}

Other than the unconventional mechanism of metal ion signaling, a few other points make these sensor systems more interesting. In literature, a few systems are available that offer multiple signaling windows towards proton and alkali metal ions,[17,18] but not for the transition metal ions. As far as the signaling efficiency of the systems are concerned (Table 4.2 and Table 4.3), when monitored at 400 nm, the fluorescence output of **NPY** decreases by a factor of 17 – 110 and increases by a factor of 9 – 16 at 525 nm in AN. When monitored at

335 nm, the decrease in fluorescence occurs by a factor of 2.6 – 333. For **PPY**, the fluorescence quenching factors are 3 – 77 at 395 nm and 14 – 100 at 450 nm, whereas fluorescence enhances by 13 – 36 at 610 nm. In THF, the decrease in fluorescence for **NPY** is by a factor of 3 - 91 at 335 nm and 4 – 100 at 400 nm and enhancement is 1.2 – 12 times at 500 nm. For **PPY**, the decrease in fluorescence in THF occurs by a factor of 1.8 – 125 at 395 nm and by 2 – 100 at 450 nm, the increase in fluorescence at 585 nm being 1.6 – 22.6. The efficiency of the sensor molecules to sense very low concentration of the metal ions is also noteworthy. The concentrations of the metal ions required for the maximum fluorescence enhancement are given in the Table 4.4. The concentrations of **NPY** and **PPY** used in the studies are ~10^{-5} – 10^{-3} M in THF and AN. It is clear from Table 4 that the sensor systems can sense very low concentration of the metal ions giving maximum fluorescence enhancement. The above points make **NPY** and **PPY** really novel and attractive sensors for the transition metal ions.

4.6. Conclusions

To summarize, we have developed a pair of systems that show excitation wavelength window based emission and can be used as fluorosensors for the transition metal ions. The systems offer multiple wavelength windows for monitoring the modulation of the fluorescence intensity in the presence of the metal ions. The excitation/emission wavelength windows are respectively 280/330 nm, 320/400 nm and 360/500 nm for **NPY** and 315/400 nm, 375/450 nm and 435/600 nm for **PPY**. Even though the architecture of the present systems is similar to that of the conventional PET systems, the signaling mechanism,

however, differs significantly. We have shown that an enhanced communication between the fluorophore and the receptor in the presence of the guest is responsible for the 'off-on' signaling response of the systems.

4.7. References

(1) Kemlo, J. A.; Shepherd, T. M. *Chem. Phys. Lett.* **1977**, *47*, 158.

(2) Varnes, A. W.; Dodson, R. B.; Wehry, E. L. *J. Am. Chem. Soc.* **1972**, *94*, 946.

(3) Kurihara, M.; Kawashima, K.; Ozutsumi, K. *Z. Naturforsch., B: Chem. Sci.* **2000**, *55*, 277.

(4) Lee, K. Y.; Kochi, J. K. *J. Chem. Soc. Perkin Trans. 2* **1992**, 1011.

(5) Saeva, F. D. *J. Photochem. Photobiol. A: Chem.* **1994**, *78*, 201.

(6) Hirsch, T.; Port, H.; Wolf, H. C.; Miehlich, B.; Effenberger, F. *J. Phys. Chem. B.* **1997**, *101*, 4525.

(7) Verhoeven, J. W.; Dirkx, I. P.; de Boer, T. J. *Tetrahedron* **1969**, *25*, 4037.

(8) LeGoff, E.; LaCount, R. B. *J. Am. Chem. Soc.* **1963**, *85*, 1354.

(9) Beaumont, T. G.; Davis, K. M. C. *J. Chem. Soc. B* **1968**, 1010.

(10) Beaumont, T. G.; Davis, K. M. C. *Nature* **1970**, *225*, 632.

(11) Kosower, E. M.; Skorcz, J. A. *J. Am. Chem. Soc.* **1960**, *82*, 2195.

(12) Nagy, O. B.; Dupire, S.; Nagy, J. B. *Tetrahedron* **1975**, *31*, 2453.

(13) de Silva, A. P.; Gunaratne, H. Q. N.; Gunnlaugsson, T.; Huxley, A. J. M.; McCoy, C. P.; Rademacher, J. T.; Rice, T. E. *Chem. Rev.* **1997**, *97*, 1515.

(14) Bissel, R. A.; de Silva, A. P.; Gunaratne, H. Q. N.; Lynch, P. L. M.; Maguire, G. E. M.; McCoy, C. P.; Sandanayake, K. R. A. S. *Top. Curr. Chem.* **1993**, *168*, 223.

(15) Bissel, R. A.; de Silva, A. P.; Gunaratne, H. Q. N.; Lynch, P. L. M.; Maguire, G. E. M.; Sandanayake, K. R. A. S. *Chem. Soc. Rev.* **1992**, *21*, 187.

(16) Fabbrizzi, L.; Poggi, A. *Chem. Soc. Rev.* **1995**, *24*, 197.

(17) Ballardini, R.; Balzani, V.; Credi, A.; Gandolfi, M. T.; Hibert, F. K.; Lehn, J. M.; Prodi, L. *J. Am. Chem. Soc.* **1994**, *116*, 5741.

(18) Collado, D.; Perez-Inestrosa, E.; Suau, R.; Desvergne, J.-P.; Bouas-Laurent, H. *Org. Lett.* **2002**, *4*, 855.

Chapter 5

Photophysical and cation signaling properties of some crown derivatives of 4-aminophthalimide

This chapter deals with photophysical and cation signaling properties of some *fluorophore-spacer-receptor* systems involving various crown moieties as the receptors. All these systems have been developed with 4-aminophthalimide as the fluorophore component and a dimethylene moiety as the spacer.

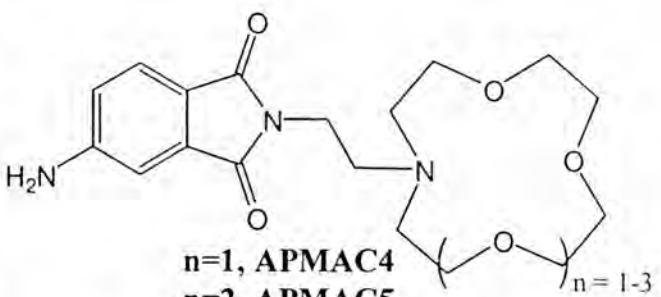

n=1, APMAC4
n=2, APMAC5
n=3, APMAC6

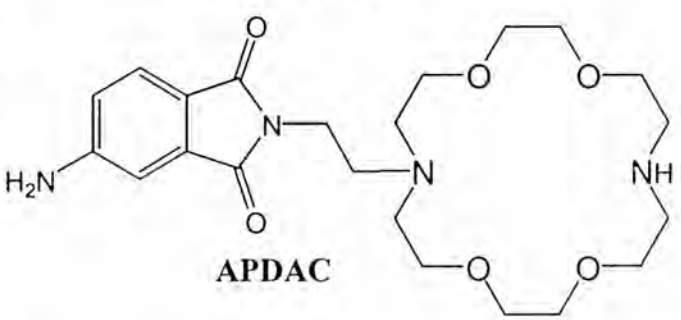

APDAC

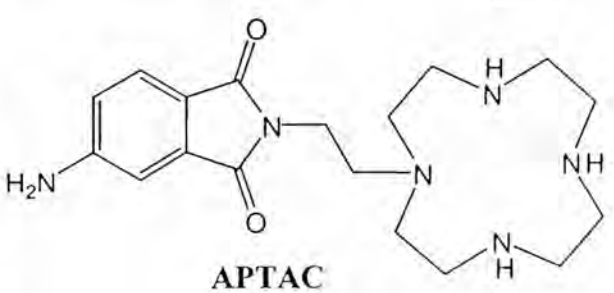

APTAC

Chart 5.1.

As stated earlier, there has been considerable interest in developing efficient fluorescence sensors for the transition metal ions, particularly for the divalent ions of zinc, cadmium, mercury and lead, owing to their importance in biology and environment. The crown ethers are known to complex strongly with s-block

metal ions and have very weak coordinating properties towards the transition metal ions. Thus, a clear distinction between the s- and d-block metal ion coordination can be made by the crown ether compounds.[1] The aza crowns, on the other hand, are expected to complex strongly with the transition and post transition metal ions. The cavity size of the crowns is believed to be an important factor that directs the binding of the metal ions to various crowns.[2] Selectivity in binding can hence be achieved by appropriate selection of the aza crown system. Taking these two aspects into consideration, we designed and developed a few sensor systems wherein various aza crown moieties of different ring sizes containing different number of nitrogen and oxygen atoms have been used as the receptor moieties and studied their fluorescence response in the absence and in presence of various metal ions. The structures of the sensor molecules studied in this chapter are given in Chart 5.1.

5.1. Spectral features

5.1.1. Absorption spectra

The absorption behavior of the systems has been studied in THF and AN. All the compounds show absorption spectra resembling that of the parent fluorophore, 4-aminophthalimide (AP). The longest wavelength absorption maximum of the compounds appears between 365 and 370 nm in the solvents studied. This broad absorption band is typical of the intramolecular charge transfer transition (ICT) within the 4-aminophthalimide moiety.[3-5] In any given solvent, a red-shift of the spectral maxima is observed as one moves from free AP to its crown derivative. This behavior suggests that charge separation in the

fluorophore unit is enhanced on linking the spacer and the receptor moiety to AP. Representative absorption spectra of the crown compounds in AN are shown in figure 5.1. The spectral parameters of the derivatives along with those of the parent fluorophore are tabulated in Table 5.1.

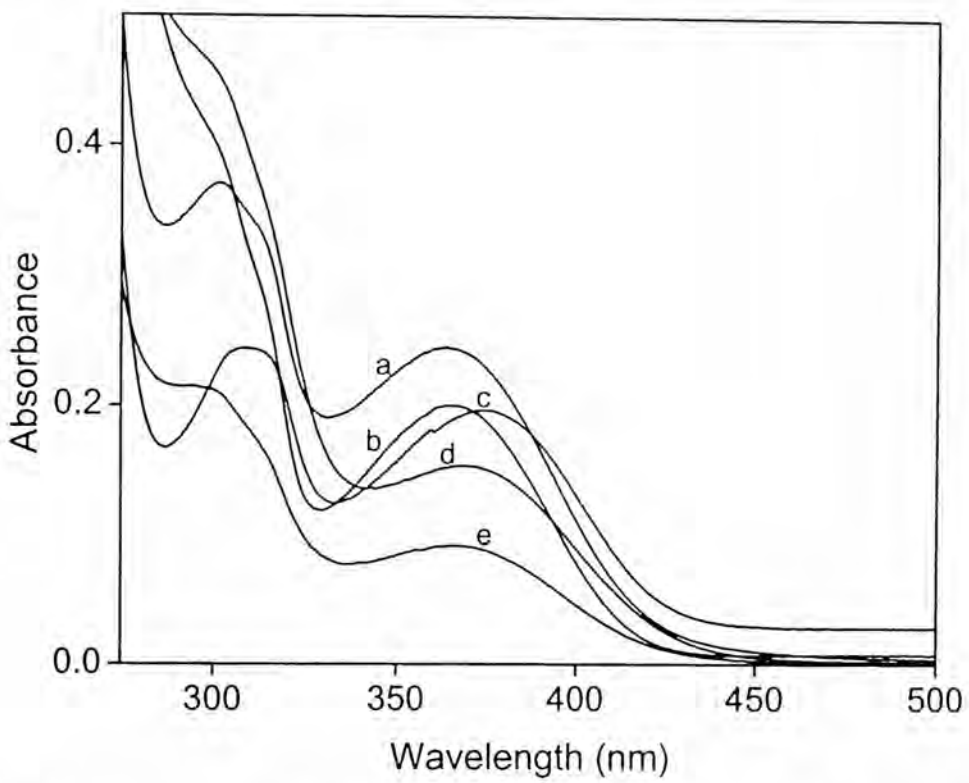

Fig. 5.1. Absorption spectra of the crown compounds in AN. The representative curves are for (a) **APMAC5**, (b) **APTAC**, (c) **APDAC**, (d) **APMAC6** and (e) **APMAC4**.

5.1.2. Fluorescence spectra

The emission behavior of the crown compounds were also studied in THF and AN. The compounds gave a broad structureless emission band in both the solvents, when excited at their absorption maxima. The broad and structureless emission is characteristic of ICT emission of AP. The fluorescence maximum of

the compounds shifts to longer wavelengths as the polarity of the medium is increased. This is obviously due to the dipolar character of the excited state. It may be noted here that while the spectral behavior of the crown systems is very similar to that of AP, the fluorescence quantum yield of the crown derivatives is significantly lower compared to AP (vide Section 5.1.3). Representative fluorescence spectra of various compounds in AN are shown in figure 5.2. The fluorescence parameters of the compounds are tabulated in Table 5.1.

The fluorescence excitation spectra of various compounds (figure 5.2.(b)) show no special characteristics and resemble the absorption spectra (particularly the long-wavelength region) of the systems very closely.

Table 5.1. Wavelength (nm) corresponding to the absorption and emission maxima of the systems in THF and AN.

Compound	THF		AN	
	λ_{abs}	λ_{em}	λ_{abs}	λ_{em}
AP	358	452	359	462
APMAC4	369	466	369	478
APMAC5	366	464	366	478
APMAC6	369	468	370	480
APDAC	367	483	370	484
APTAC	368	460	365	480

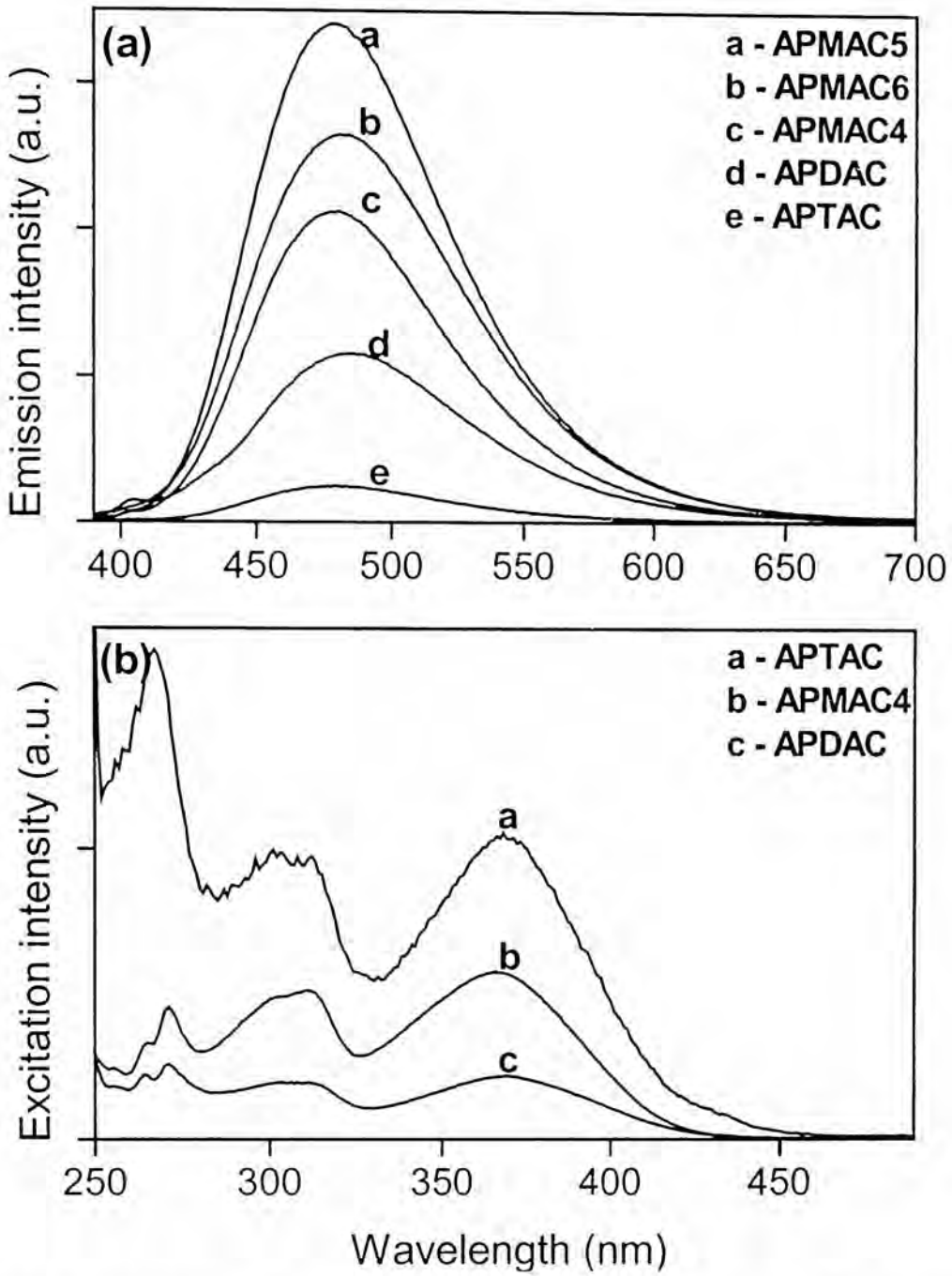

Fig. 5.2. Emission (a) and excitation (b) spectra of the crown compounds in AN. The excitation and emission wavelengths are 360 and 480 nm respectively. The y-axis is not to scale in (a).

5.1.3. Fluorescence quantum yield and lifetime

As stated in the previous section, the fluorescence quantum yields (ϕ_f) of the crown derivatives of AP are significantly less than that of the parent fluorophore (vide Table 5.2). A lower fluorescence quantum yield of the crown derivatives is in accordance with the intramolecular PET interaction between the fluorophore and the receptor. The fluorescence quantum yield is found to be the lowest in the case of **APTAC** indicating that PET is most efficient in this system. The quantum yield of this system is lower than that of AP by a factor of 25 in THF and 50 in AN. Since the magnitude of reduction of the fluorescence quantum yield of a given *fluorophore-spacer-receptor* system compared to the parent fluorophore is an indication of the maximum fluorescence enhancement one can expect in the presence of a guest, **APTAC** is expected to show an excellent signaling efficiency. As far as the other derivatives are concerned, the quantum yields of **APMAC4** and **APMAC5** are almost the same, whereas **APMAC6** has a higher quantum yield in both THF and AN. The fluorescence quantum yield of the diaza crown derivative, **APDAC** is intermediate between that of the monoaza crown and the tetraaza crown derivatives.

The fluorescence decay behavior of different derivatives has also been studied in THF and AN. The measured fluorescence decay parameters are presented in Table 5.2. As can be seen from the table, while AP exhibits a single exponential decay with a long lifetime of 12.4 – 14.0 ns, the crown derivatives show a bi- or tri-exponential decay pattern with the major component having a lifetime significantly shorter than that of AP. One of the minor components has a long lifetime comparable to that of AP. A shorter lifetime of the different

derivatives (as evident from the τ values) is understandable when taken into consideration PET in these systems. The short-lived major component clearly represents the PET quenched fluorophore whereas the long-lived minor component must be arising from those molecules in which the relative orientation of the electron donor and acceptor groups is such that through-space interaction of the receptor and the fluorophore is minimal. The average lifetime, as seen from Table 5.2, is higher in THF compared to that in AN. The fluorescence lifetimes of the systems are in line with the quantum yield values, both being higher in THF compared to that in AN. The short-lived component is the major one except for **APMAC5** and **APMAC6** in THF.

5.2. Effect of metal ions

5.2.1. Absorption

The effect of the transition metal ions on the absorption behavior of the individual compounds, studied in THF and AN, shows that neither the extinction coefficient nor the wavelength of absorption changes drastically. Representative cases are illustrated in figure 5.3. A small shift of the spectral maximum has been observed in most cases following the addition of the metal salts. In most of the cases no isosbestic point in the absorption spectrum could be observed. However, in certain cases such as in the case of **APTAC**, we did observe an isosbestic point over a certain concentration of the metal ions with metal ions such as Zn^{2+} and Pb^{2+}. The spectral data of various systems in the presence of different metal ions have been collected in Tables 5.3 and 5.4.

Table 5.2. Fluorescence quantum yield (ϕ_f) and decay parameters (τ (in ns)) for the various systems in THF and AN. The relative weightage of each decay component (in %) is given in bracket.

Solvent		**AP**	**APMAC4**	**APMAC5**	**APMAC6**	**APDAC**	**APTAC**
THF	ϕ_f	0.70	0.12	0.09	0.25	0.04	0.03
	τ_1	14.0	8.7 (6.4)	9.0 (11.8)	9.3 (16.4)	-	2.3 (4.4)
	τ_2	-	19.8 (5.6)	18.1 (65.2)	17.3 (48.6)	-	13.7 (3.2)
	τ_3	-	0.4 (88)	1.6 (23)	1.9 (35)	-	0.7 (92.4)
	χ^2	-	1.23	1.22	1.19	-	1.16
	τ_{av}	-	2.0	13.3	10.6	-	1.2
AN	ϕ_f	0.63	0.08	0.07	0.24	0.03	0.01
	τ_1	12.4	3.2 (5.1)	2.6 (0.5)	3.8 (8.9)	1.7 (8.7)	3.7 (2.3)
	τ_2	-	18.5 (6.5)	18.6 (1.1)	18.7 (13.1)	16.3 (1.6)	11.6 (2.9)
	τ_3	-	0.2 (88.4)	0.1 (98.4)	0.2 (78)	0.3 (89.7)	0.3 (94.8)
	χ^2	-	1.31	1.42	1.54	1.22	1.07
	τ_{av}	-	1.5	0.3	2.9	0.6	0.7

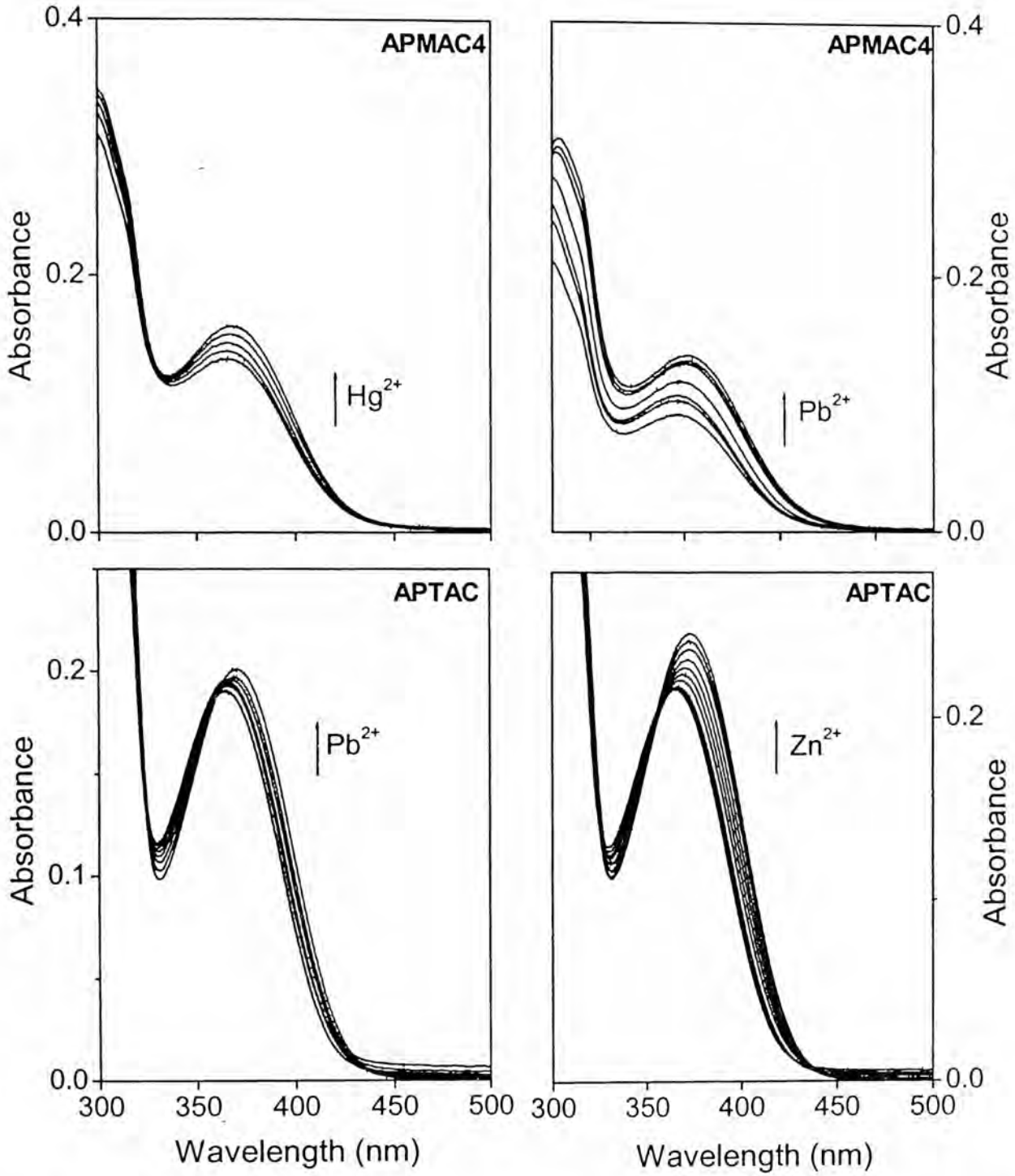

Fig. 5.3. Effect of metal ions on the absorption spectra of **APMAC4** and **APTAC** in AN. The concentration of the metal ions was varied from 10^{-4} to 10^{-3} M.

5.2.2. Fluorescence

The effect of the metal ions on the fluorescence behavior of the systems is found to be much more pronounced than that observed in the case of absorption. Addition of the metal salts leads to a far larger Stokes shift of the fluorescence maximum than that observed in the case of the absorption spectra. This behavior is not surprising when taken into consideration the literature, according to which the fluorescence state of AP is much more sensitive to its surrounding media (compared to absorption) because of a larger dipole moment of the excited state.[3,4] The large Stokes shift in the presence of the metal salts clearly suggests that charge separation in the fluorescent state of the fluorophore is enhanced significantly in the presence of the metal ions. The fluorescence parameters of the systems in the presence of metal ions are given in Table 5.3 and Table 5.4.

The large Stokes shift of the fluorescence maximum of the systems is associated with an enhancement of the fluorescence intensity in the presence of the metal ions. The magnitude of FE differs from system to system. Different metal ions induce FE to a different extent. The monoaza crown compounds receptors have been found to exhibit the minimum FE in the presence of the metal ions. On the other hand, **APTAC** containing cyclen as the receptor gives the maximum FE in most cases studied. This behavior is in line with our expectation based on the fluorescence quantum yield and lifetime of the individual compounds (Table 5.2). Since the quantum yield of **APTAC** is the minimum of all the compounds studied by us, it is expected to give maximum enhancement of fluorescence in the presence of metal ions. The interesting observation is that **APTAC** gives FE only with certain metal ions and not with all the metal ions

studied. Clearly, it discriminates the metal ions while forming the complex. The details of the FE of systems observed on metal ion addition are given in Table 5.5. Typical emission spectra of some of the compounds illustrating the effect of the metal ion are shown in figure 5.4. and figure 5.5. The fluorescence excitation spectra recorded in the presence of metal ions show features similar to the absorption spectra obtained in the presence of metal ions.

Table 5.3. Absorption and fluorescence maxima (in nm) of various systems in THF on metal ion addition.

Metal ion	APMAC4		APMAC5		APMAC6		APDAC		APTAC	
	λ_{abs}^{max}	λ_{flu}^{max}	λ_{abs}^{max}	λ_{flu}^{max}	λ_{abs}^{max}	λ_{flu}^{max}	λ_{abs}^{max}	λ_{flu}^{max}	λ_{abs}^{max}	λ_{flu}^{max}
None	369	466	366	464	369	468	367	483	368	460
Ag^{+}	372	494	373	500	372	493	372	484	369	490
Cd^{2+}	375	501	371	483	373	492	370	494	370	508
Co^{2+}	370	498	371	500	372	492	372	497	370	483
Cr^{3+}	373	503	369	500	372	495	379	498	370	493
Cu^{2+}	369	497	372	493	371	495	372	490	370	473
Fe^{3+}	369	502	366	498	371	494	370	497	382	482
Hg^{2+}	369	479	366	478	371	481	369	490	373	478
Mn^{2+}	370	503	371	493	372	491	374	500	371	492
Ni^{2+}	370	502	372	498	372	491	375	498	369	477
Pb^{2+}	371	497	372	493	373	490	373	488	371	482
Zn^{2+}	372	501	372	488	372	491	374	498	371	492
H^{+}	374	513	375	518	375	516	370	494	371	511

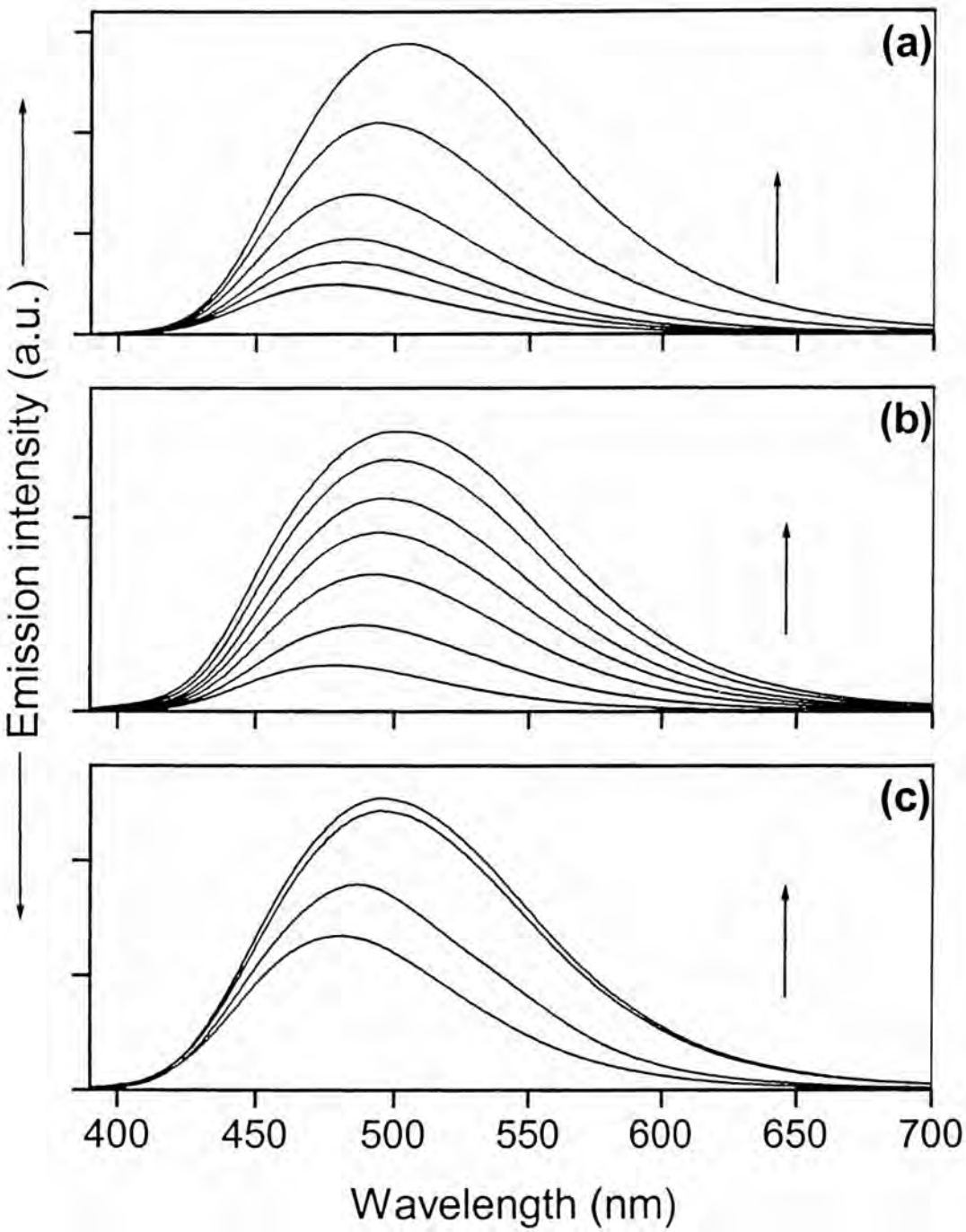

Fig. 5.4. Fluorescence spectra of (a) **APMAC4**, (b) **APMAC5** and (c) **APMAC6** with the addition of Cr^{3+} in AN (λ_{ex} = 360 nm). [Cr^{3+}] was varied from 10^{-4} to 10^{-3} M.

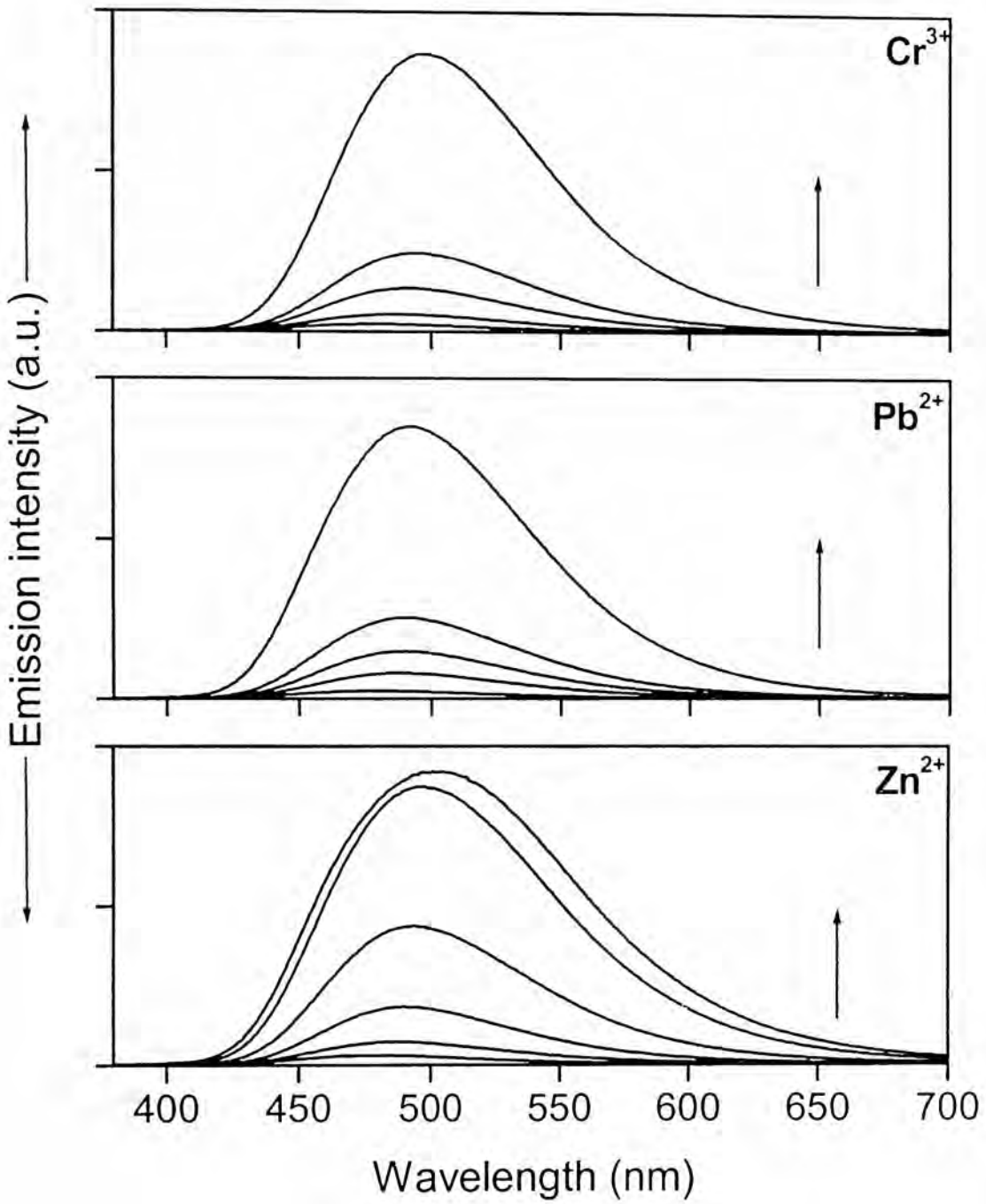

Fig. 5.5. Emission spectra of **APTAC** in AN with (a) Cr^{3+}, (b) Pb^{2+} and (c) Zn^{2+} excited at 360 nm. The metal ion concentrations are in the range 10^{-4} to 10^{-3} M.

5.2.3. Fluorescence lifetime

The fluorescence decay behavior of the various derivatives in the presence of the metal ions have been studied in AN as fluorescence enhancement in this medium is larger than that in THF. The fluorescence lifetime of the compounds in the presence of the metal ions is much higher than that in the absence of metal ions indicating a metal ion induced disruption in the communication between the fluorophore and the receptor. The fluorescence decay curves could be fitted to a biexponential decay function. A representative decay profile of **APTAC** in the absence and in the presence of Zn^{2+} is shown in figure 5.6. The decay parameters are collected in appendix 2.

5.3. Crown derivatives as transition metal ion sensors

As stated above, there is an efficient quenching of the fluorescence of the crown compounds due to PET in the systems. The quenching is most efficient in **APTAC** compared to other crown compounds. This leads us to expect that **APTAC** will show best 'off-on' fluorescence signaling of the metal ions. This is indeed found to be the case. Among the monoaza crown derivatives, the one with the largest ring size, **APMAC6**, is by far the poorest sensor system. The signaling efficiency of the diaza crown derivative, **APDAC**, is intermediate between that of the monoaza crown derivatives and the tetraaza crown derivative. Interestingly, **APTAC** is the only system that exhibits a clear discrimination in its metal ion binding behavior giving high FE with certain metal ions and virtually no FE with certain other metal ions. From Table 5.5, it can be seen that maximum FE is obtained with Zn^{2+}, Cd^{2+}, Pb^{2+}, Cr^{3+} and Hg^{2+}. FE value is considerable in the

case of Mn^{2+} too. The other ions produce only meager enhancements in the fluorescence of this compound.

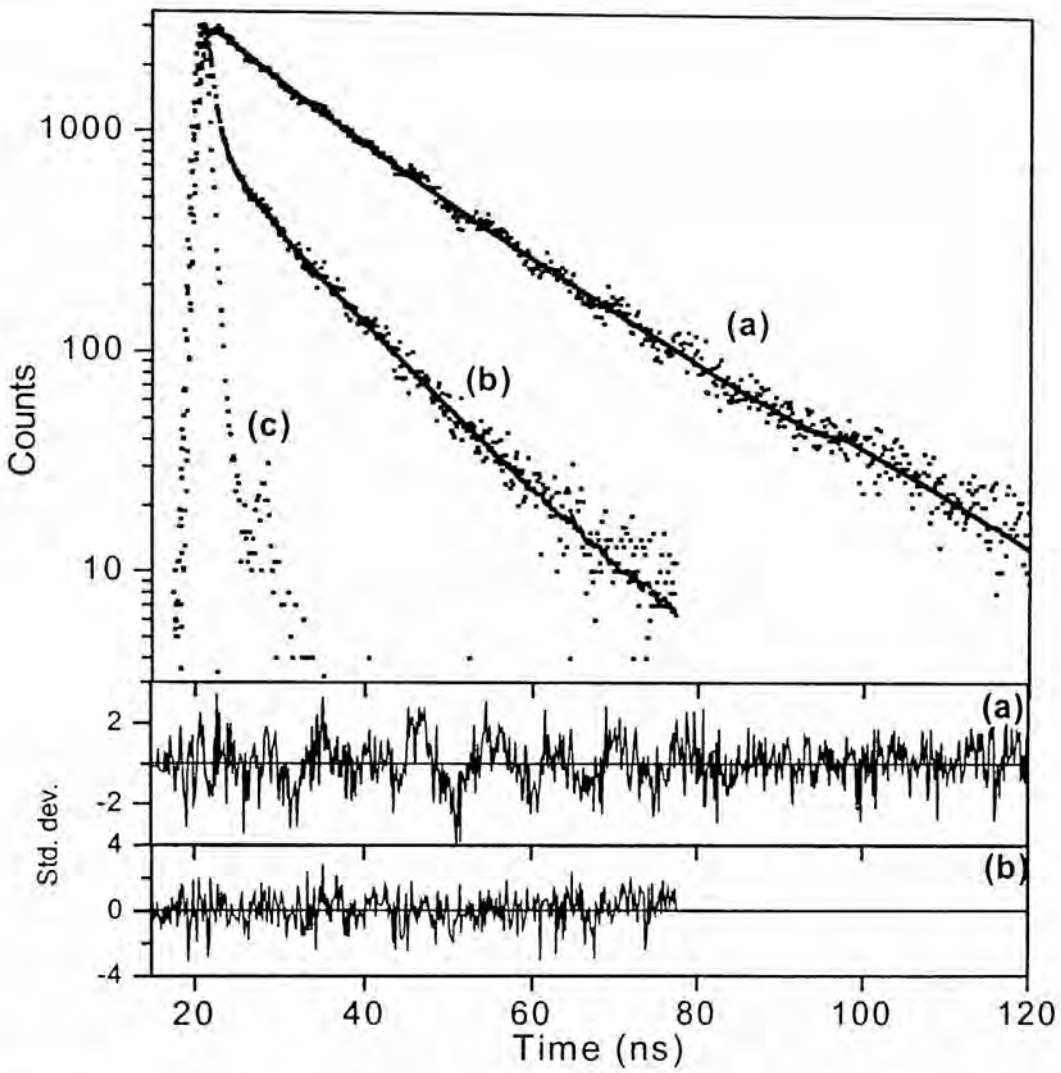

Fig. 5.6. Fluorescence decay curve of **APTAC** in the absence (a) and in the presence (b) of Zn^{2+}. The lamp profile (c) and the weighted residuals are also shown.

Table 5.4. Wavelength (in nm) corresponding to the absorption and fluorescence maxima of the crown systems in AN in the presence of various metal ions.

Metal ion	APMAC4		APMAC5		APMAC6		APDAC		APTAC	
	λ_{abs}^{max}	λ_{flu}^{max}	λ_{abs}^{max}	λ_{flu}^{max}	λ_{abs}^{max}	λ_{flu}^{max}	λ_{abs}^{max}	λ_{flu}^{max}	λ_{abs}^{max}	λ_{flu}^{max}
None	369	478	366	478	370	480	370	484	365	480
Ag^{+}	369	488	369	495	370	486	370	496	369	487
Cd^{2+}	374	499	369	499	373	497	375	508	373	516
Co^{2+}	372	504	369	487	372	496	375	507	370	492
Cr^{3+}	381	505	369	502	370	497	375	510	375	500
Cu^{2+}	370	497	368	500	371	491	372	506	366	486
Fe^{3+}	369	503	367	499	371	495	370	504	381	492
Hg^{2+}	370	488	369	492	370	482	374	500	368	481
Mn^{2+}	372	499	370	485	371	492	374	512	371	497
Ni^{2+}	372	503	367	498	370	496	373	506	367	492
Pb^{2+}	373	499	373	498	374	492	374	504	371	492
Zn^{2+}	373	504	370	493	371	495	377	518	373	503
H^{+}	370	511	369	517	371	503	373	523	372	490

5.4. Possible reason for the specificity shown by APTAC

FE values shown in Table 5.5 for the various derivatives are in agreement with the quantum yields of the systems. Therefore, it is not surprising that **APTAC** exhibits the maximum FE and is followed by **APDAC**. The most interesting observation is that **APTAC** produces very high FE with metal ions such as Cd^{2+}, Cr^{3+}, Hg^{2+}, Mn^{2+}, Pb^{2+} and Zn^{2+} and very low enhancement with

Ag^{+}, Co^{2+}, Cu^{2+}, Fe^{3+}, Ni^{2+}, and H^{+}. In order to find a possible explanation of the observed behavior, we looked through the literature.

There has been a large number of studies on cyclen and related molecules and their metal ion binding properties.[6-16] These reports show the importance of the matching of the size of the metal ion and the ring size of the aza crown moiety for a better binding.[10-12] According to Busch and coworkers, the ideal ring size (of an aza crown moiety) for any given metal ion is described in terms of the metal –nitrogen (M-N) distance.[12] For any given aza crown, there is an ideal M-N distance at which the strain energy is minimum and the binding is most efficient. A larger or smaller metal ion would require readjustment of the M-N distance resulting in an increase in the strain energy of the ligand and weaker complexation. The ideal M-N distance calculated for cyclen by Busch and coworkers is 1.83 Å.[12]

Kodama and Kimura, however, found an anomaly in the size selectivity of cyclen towards the metal ions while studying the metal ion complexation of various aza crown moieties.[7] Contrary to their expectation, they observed an unexpectedly high binding of Zn^{2+} towards cyclen, the smallest of the aza crowns studied by them. The observation that Zn^{2+}, which has a best-fit M-N length of 2.1 - 2.2 Å, forms the most stable complex with cyclen (ideal M-N distance 1.83 Å) compared to other larger aza crowns is unexpected.[7] Based on the best fit M-N distance, Zn^{2+} was expected to bind to the larger aza crowns compared to cyclen. What was more surprising was that even larger metal ions (for which M-N distance is obviously larger) such as Pb^{2+} and Hg^{2+} (vide Table 5.6), form equally

strong or a stronger complex.[7-9] Quite obviously, the metal ion binding behavior of cyclen is more complicated than what one can expect based on its ring size.

Table 5.6. Ionic diameters of the metal ions studied in Å[16].

Ag^{+}	Cd^{2+}	Co^{2+}	Cr^{3+}	Cu^{2+}	Fe^{3+}	Hg^{2+}	Mn^{2+}	Ni^{2+}	Pb^{2+}	Zn^{2+}
2.52	1.94	1.48	1.23	1.44	1.28	2.20	1.60	1.38	2.40	1.48

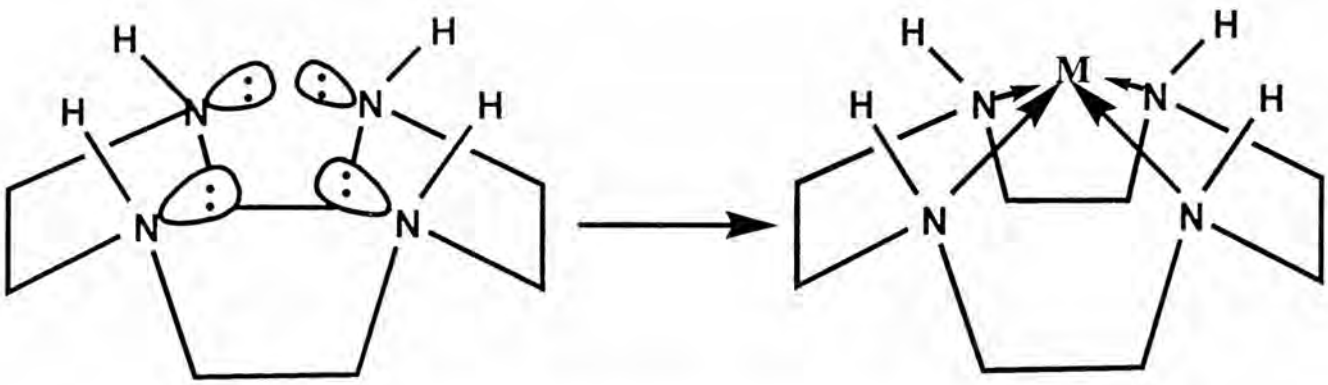

Fig. 5.7. Trans-I isomer of cyclen and its metal complex.

The anomaly in the size selectivity of the cyclen towards the transition metal ions has been later studied theoretically by Hancock and coworkers.[13-15,17] They considered the various conformations that cyclen and related molecules may adopt and found that the lowest strain energy form for cyclen was the trans-I isomer (figure 5.7.), in which all interactions are staggered and the nitrogen atoms lie slightly above the plane.[14] A plot of strain energy vs M-N distance gives a minimum at 2.11 Å for the least energetic trans-I form of cyclen.[17] The shape of this curve for cyclen is rather flat and differs from that for the larger rings. A flat

curve for cyclen clearly shows its tolerance towards accommodating the metal ions of various sizes.

The trans-I form also requires that the metal ion must lie ~0.5 Å above the plane of cyclen.[13] Considerable strain will be induced by smaller metal ions to meet this requirement due to their very strong M-N force constants. Large metal ions such as Pb^{2+} with M-N bond length in the vicinity of 2.5 - 2.7 Å, has a weak M-N force constant and is tolerant to considerable distortion of the M-N bond length. For small metal ions, such as Cu^{2+}, the requirement of lying well above the plane of the nitrogen donors will cause considerable steric strain leading to a destabilization of the complex formed.

In the case of Pb^{2+} a second factor needs to be taken into account. Large Pb^{2+} (electronic configuration: [Xe] $4f^{14}5d^{10}6s^2$) has a lone pair of electrons, which can be stereochemically active.[18,19] When the lone pair of electrons is inactive, Pb^{2+} behaves as a large metal ion with an ionic Pb-L (L = ligand) bonding.[20] However, a shortening of Pb-L bond is reported in complexes where the lone pair of electrons is stereochemically active.[21,22] In view of the fact that when complexed to cyclen, Pb^{2+} generally prefers a stereochemically active form, the anomalous selectivity of Pb^{2+} may hence, be additionally attributed to a stereochemically active 6s lone pair of electrons on the ion, which results in an effective shrinking of the size of the metal ion by 0.3 Å.[20]

The discussions made above help understanding high FE values exhibited by some of the large metal ions. The only exceptions are Cr^{3+}, which in spite of being the smallest metal ion studied, gives a high FE value, and Ag^{+}, which gives a meager enhancement of fluorescence despite being the largest metal ion.

Perhaps these two cases can be explained as follows. With the exception of Cr^{3+}, all the metal ions that show good FE values are large and with a completely-filled or half-filled d-orbital. In the case of Cr^{3+}, which has a preferred octahedral geometry of the complex, the d-orbitals will have three electrons. Hence, the possibility of d orbitals of Cr^{3+} taking part in forming a strong complex with cyclen cannot be ruled out. Further, Cr^{3+}, being hard, may be assisted by the oxygens of the imide ring in forming a strong complex. With Ag^{+}, the largest metal ion that we have studied, lack of any lone electron pair perhaps rules out the possibility of any shrinking of size and the formation of a stable complex.

With Ni^{2+}, which prefers a square planar geometry, the cavity size with a best fit M-N length of 2.11 Å seems to be too big.[17] In the case of Cu^{2+}, which is expected to form strong complexes with cyclen, satisfying the requirement that the metal atom lies above the plane of cyclen by ~0.5 Å will be meted out with considerable difficulty.[17] Further, even though Cu^{2+} is reported to form stable complexes with cyclen and cyclen containing compounds, they are reported to show intracomplex quenching of fluorescence.[23,24]

Thus, it is shown that the magnitude of the FE values of **APTAC** observed with different metal ions can be qualitatively explained taking into account the literature information on the metal ion binding properties of cyclen. A more detailed and concrete interpretation of the individual FE values is possible only when the single crystals of the metal complexes are grown and their structures solved. Attempts in this direction have not been successful so far.

5.5. Conclusions

Some new crown derivatives of 4-aminophthalimide with *fluorophore-spacer-receptor* architecture have been synthesized and 'off-on' fluorescence signaling behavior of these derivatives towards the transition and post transition metal ions has been studied. Specific binding of certain trace metal ions of biological and environmental importance is achieved with the system containing the tetrazacrown receptor moiety. This behavior has been explained taking into consideration the ability of cyclen to bind relatively larger metal ions.

5.6. References

(1) Hancock, R. D. *Pure Appl. Chem.* **1986**, *58*, 1445.

(2) Pedersen, C. J. *J. Am. Chem. Soc.* **1967**, *89*, 7017.

(3) Soujanya, T.; Krishna, T. S. R.; Samanta, A. *J. Photochem. Photobiol. A: Chem.* **1992**, *66*, 185.

(4) Soujanya, T.; Fessenden, R. W.; Samanta, A. *J. Phys. Chem.* **1996**, *100*, 3507.

(5) Ramachandram, B.; Sankaran, N. B.; Samanta, A. *Res. Chem. Interm.* **1999**, *25*, 843.

(6) Hojo, M.; Hisatsune, I.; Tsurui, H.; Minami, S. *Anal. Sci.* **2000**, *16*, 1277.

(7) Kodama, M.; Kimura, E. *J. Chem. Soc. Dalton Tans.* **1977**, 2269.

(8) Kodama, M.; Kimura, E. *J. Chem. Soc. Dalton Trans.* **1978**, 1081.

(9) Kodama, M.; Kimura, E. *J. Chem. Soc. Dalton Trans.* **1980**, 2536.

(10) DeHayes, L. J.; Busch, D. H. *Inorg. Chem.* **1973**, *12*, 1505.

(11) DeHayes, L. J.; Busch, D. H. *Inorg. Chem.* **1973**, *12*, 2010.

(12) Martin, L. Y.; DeHayes, L. J.; Zompa, L. J.; Busch, D. H. *J. Am. Chem. Soc.* **1974**, *96*, 4046.

(13) Thöm, V. J.; Fox, C. C.; Boeyens, J. C. A.; Hancock, R. D. *J. Am. Chem. Soc.* **1984**, *106*, 5947.

(14) Thöm, V. J.; Boeyens, J. C. A.; McDougall, G. J.; Hancock, R. D. *J. Am. Chem. Soc.* **1984**, *106*, 3198.

(15) Thöm, V. J.; Hosken, G. D.; Hancock, R. D. *Inorg. Chem.* **1985**, *24*, 3378.

(16) Hiraoka, M. *Crown Compounds: Their Characteristics and Applications*; Elsevier: Amsterdam, 1982.

(17) Hancock, R. D.; McDougall, G. J. *J. Am. Chem. Soc.* **1980**, *102*, 6551.

(18) Gillespie, R. J.; Nyholm, R. S. *Rev. Chem. Soc.* **1957**, *11*, 339.

(19) Hancock, R. D.; Maumela, H.; de Sousa, A. S. *Coord. Chem. Rev.* **1996**, *148*, 315.

(20) Hancock, R. D.; Shaikjee, M. S.; Dobson, S. M.; Boeyens, J. C. A. *Inorg. Chim. Acta.* **1988**, *154*, 229.

(21) Lawton, S. L.; Kokotailo, G. T. *Inorg. Chem.* **1972**, *11*, 363.

(22) Wieghardt, K.; Kleine-Boymann, M.; Nuber, B.; Weiss, J.; Zsolnai, L. *Inorg. Chem.* **1986**, *25*, 1647.

(23) Akkaya, E. U.; Huston, M. E.; Czarnik, A. W. *J. Am. Chem. Soc.* **1990**, *112*, 3590.

(24) Kimura, E.; Koike, T. *Chem. Soc. Rev.* **1998**, *27*, 179.

Chapter 6

Structure of a self-assembled chain of water in a crystal host

As a part of the characterization of the cyclen molecule, which has been synthesized by us and used as one of the receptor moieties for the development of the fluorescence signaling systems for the transition metal ions, we performed an X-ray crystallographic study of the single crystals of this molecule grown from toluene. During the course of this study, we observed a highly ordered chain of water molecules with a novel hydrogen bonding motif in the single crystals of cyclen. The details of the structure of the water chain are presented in this chapter.

6.1. Introduction

Water is not only the most abundant substance on earth, but more importantly, is the most important chemical substance responsible for the existence of all forms of life and their survival on this planet. Quite obviously, there is a great interest on the water, popularly known as 'nature's solvent'. Interestingly, water exhibits some properties in pure form or in solution that are yet to be understood properly and hence, considered as 'anomalous' even today.[1]

The liquid-phase density maximum is one of the most prominent anomalous behavior of water. When cooled at atmospheric pressure, the density of liquid water increases and reaches a maximum at 277K; thereafter, it falls

rapidly, even in the supercooled region.[2-4] Although water is not the only liquid to exhibit a density maximum, the phenomenon only appears in a few other liquids, such as SiO_2[5] and Ga[6] melts. Another anomaly in the properties of water is its negative volume of melting. The density of most liquids increases as they freeze; however, water expands by about 11%. This is responsible for the top down freezing of lakes and rivers. The strong increase in the specific heat on supercooling is one more anomalous property of water[7,8] because of which it takes more heat to raise the temperature of water than to warm up most other substances by the same amount and hence, is responsible for ocean circulation effects that strongly influence local and global climates. Rapid transport of protons through a network of water molecules is another property of water that is yet to be understood.

The amount of literature that is available on water perhaps replicates its position on this planet. This also highlights that water is one of the most appealing of the open puzzles in science.[1,9-13] The structure adopted by liquid water in close proximity to nonpolar solutes is a fundamental characteristic of modern theories of hydrophobic hydration and hydrophobic effects that are of great relevance to our understanding of many important chemical and biological processes.[14]

6.2. Hydrogen bonding and cooperativity: key to understanding the behavior of water

All the properties of water and aqueous solutions must be explained in terms of the intermolecular forces that are present. The key to understanding

various properties of liquid water and its solutions lies in understanding the exact nature of the hydrogen bonding interaction among the water molecules.[15]

The water molecule, which contains two hydrogen atoms and one oxygen atom, is ideally suited for hydrogen bonding. It can act both as a donor and an acceptor of hydrogens. The water dimer (figure 6.1.) was first observed by Dyke and coworkers.[16,17] A tetrahedral arrangement of water molecules (figure 6.1.) through hydrogen bonding is observed in ice, I_h. The dual ability of water molecule acting as both hydrogen bond donor and acceptor is illustrated clearly by the crystal structure of ordinary hexagonal ice. In ice, each water molecule is hydrogen bonded to four neighboring water molecules. Each molecule acts as hydrogen bond donors to two water molecules and hydrogen bond acceptors to two other molecules (a double donor-double acceptor) in a tetrahedral arrangement in which the bond angles are 104.5^0, slightly less than the ideal tetrahedral angle. The structure of hexagonal ice is depicted in figure 6.2.

The concept of cooperativity of hydrogen bonding in water was originally introduced by Frank and Wen.[18] The diversity of the cooperative association of the water molecules is attested by a large number of polymorphic forms of ice.[19,20] The nature of the hydrogen bonding interactions is still a matter of discussion and the idea oscillates between electrostatic and covalent concepts.[21,22] The key to understanding the behavior of liquid water is precise structural data of various hydrogen-bonded water networks in diverse environments. It is this realization that has prompted extensive investigation on water structures in recent years.[1,23]

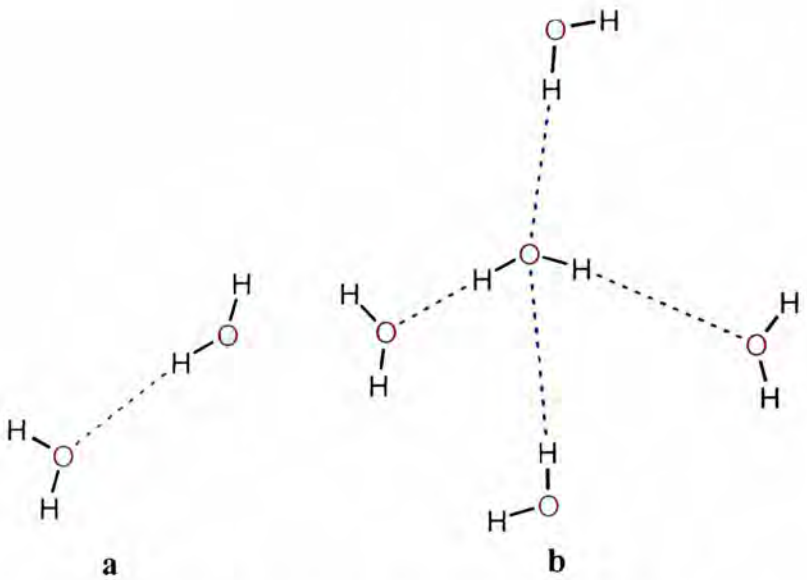

Fig. 6.1. Structure of dimeric (a) and tetrahedral (b) arrangements of water molecules. Hydrogen bonds are shown as blue dotted lines.

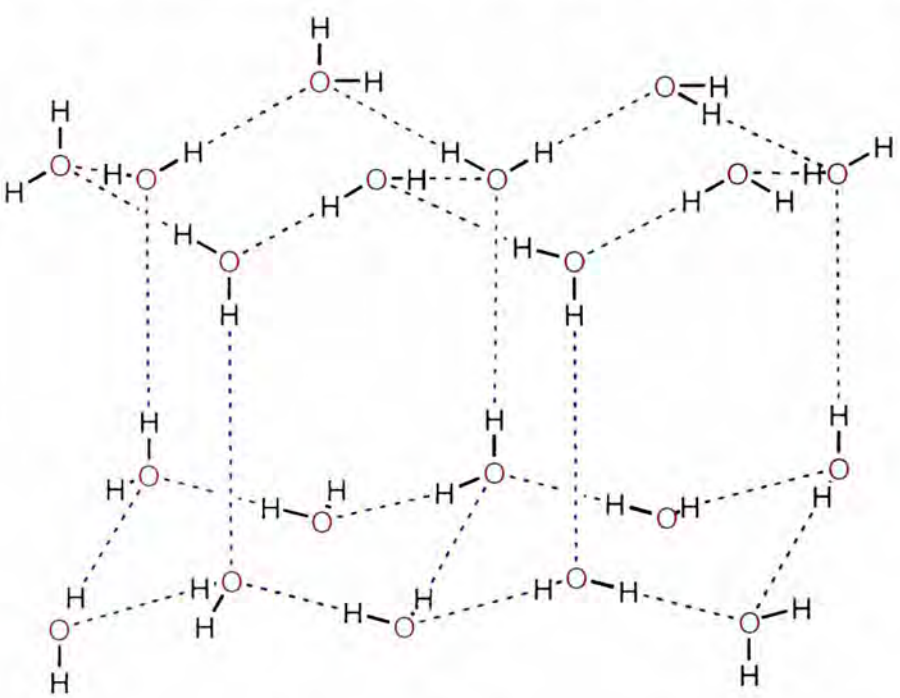

Fig. 6.2. Structure of hexagonal ice. Hydrogen bonds are shown as blue dotted lines.

Since it is possible to obtain precise information on the nature of the cooperative association of a small collection of the water molecules, various water clusters have been studied theoretically and experimentally.[1,22,24,25] These studies have revealed a quasiplanar cyclic structure for the trimer, tetramer and pentamer. Although 3-dimensional structures have been theoretically predicted and experimentally observed for the hexamer and higher water clusters, a quasiplanar hexamer has also been reported.[25] Recent studies have led to the characterization of several water clusters in various crystal hosts at room temperature.[23,26-28] Notable among these are hexamers,[27-29] octamers[23,30] and a decamer.[26] While these studies have significantly advanced our understanding of the structure of several 'discrete' water clusters, very little is known, how these clusters link themselves to form a larger network of water molecules.

6.3. Structure of a tetrameric water chain

As a part of the characterization of cyclen, prepared for the synthesis of signaling systems for the transition metal ions, we decided to undertake a structure determination of the molecule by single crystal X-ray spectroscopic studies. Single crystals of X-ray quality were developed from toluene at room temperature. The structure of cyclen is shown in figure 6.3.

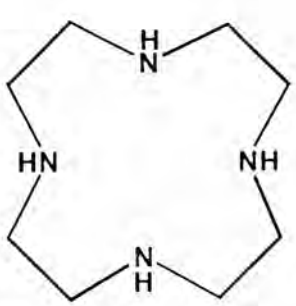

Fig. 6.3. Chemical structure of cyclen.

The X-ray data were collected using an Enraf-Nonius Mach-3 single crystal diffractometer employing graphite monochromated Mo Kα radiation (λ =

0.71073Å) by ω scan method as explained in chapter 2. Unit cell parameters were determined by least squares fit of 25 reflections having 2θ values in the range 18 - 21^0. The crystal dimension was 0.68 x 0.48 x 0.40 mm. The crystal structure details are collected in Table 6.1.

Interestingly, the crystal structure of cyclen has earlier been reported.[31] The compound was reported to crystallize with three molecules of water. Even though the crystallographic details of the molecule are reported, there was no attempt to find out how the water molecules are arranged in the crystal. Since cyclen contains several amino moieties mimicking those present in biological systems, we considered it important to probe the water structure that the cyclen crystals contained.

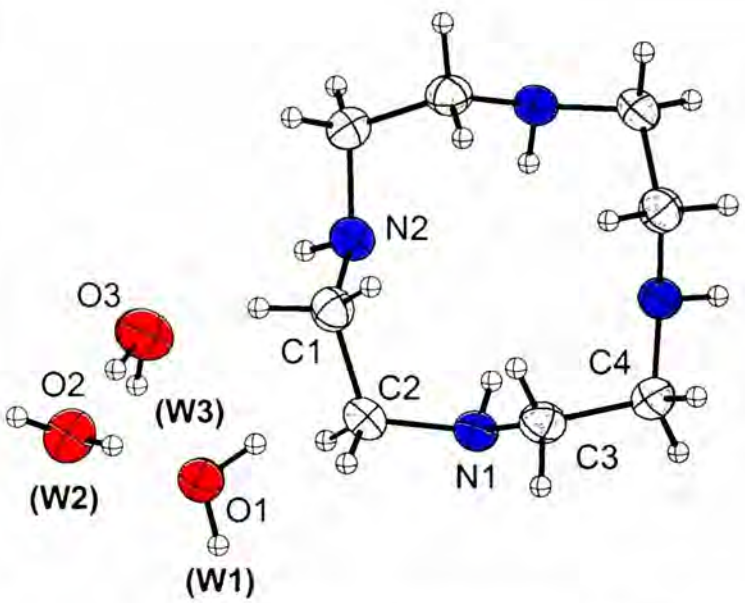

Fig. 6.4. Structure of Cyclen.$3H_2O$. The water molecules are labeled W1, W2 & W3.

The crystal structure of cyclen is shown in figure 6.4. As is seen from the figure, cyclen crystallizes with three molecules of water, denoted in the figure as W1, W2 and W3.

Table 6.1. Crystallographic details for cyclen.

Identification code	Cyclen.$3H_2O$
Empirical formula	$C_8 H_{26} N_4 O_3$
Formula weight	226.33
Temperature	298 K
Wavelength	0.71073 Å
Crystal system, space group	Orthorhombic, C_c_c_a:2
Unit cell dimensions	a = 16.658(2) Å $\alpha = 90^0$ b = 16.908(5) Å $\beta = 90^0$ c = 8.891(4) Å $\gamma = 90^0$
Volume	2504.3 (12) $Å^3$
Z, Calculated density	8, 1.201 mg/m^3
Absorption coefficient	0.091 mm^{-1}
F(000)	1008
Crystal size	0.68 x 0.48 x 0.40 mm
θ range for data collection	2.41 to 27.95^0
Index ranges	$0 \leq h \leq 21, 0 \leq k \leq 22, 0 \leq l \leq 11$
Reflections collected / unique	1713 / 1514 [R(int) = 0.0000]
Completeness to 2θ	27.95 44.5%
Absorption correction	None
Refinement method	Full-matrix least-squares on F^2

Data / restraints / parameters	1514 / 0 / 90
Goodness-of-fit on F^2	1.016
Final R indices [$I>2\sigma$ (I)]	R1 = 0.0404, wR2 = 0.0900
R indices (all data)	R1 = 0.0876, wR2 = 0.1081
Largest diff. peak and hole	0.155 and -0.175 e. $Å^{-3}$

As revealed by the crystallographic packing diagram, shown in figure 6.5., the cyclen molecules are packed one on the top of another and are hydrogen bonded to the water molecules through N-H---O and O-H---N hydrogen bonding interactions. The water molecules, on the other hand, occupy the space between the cyclen moieties and extend along the crystallographic c-axis to form an infinite chain. The hydrogen bonding motif of the water chain is illustrated in figure 6.6. A space-filling model of the chain is shown in figure 6.7. and a skeletal arrangement of the chain is shown in figure 6.8. The infinite chain is made up of cyclic water tetrameric units bridged by two water molecules. The cyclic water tetramers are formed by water molecules of types W1 and W2, the corresponding oxygens of which are represented by O1 and O2 respectively in figure 6.6. The tetrameric clusters are bridged along the c-axis by two water molecules of type W3. While W2 is hydrogen bonded to four other water molecules of types W1 and W3, W1 and W3 are involved in forming two N-H---O and O-H---N hydrogen bonds respectively with the neighboring organic molecule other than forming two hydrogen bonds with W2. All the oxygen atoms involved in the formation of the tetramer lie in a plane. It may appear from figure 6.6. that the

chain is formed by corner sharing tetramers, where the successive tetrameric units lie in perpendicular planes. However, we consider 'bridged tetramers' is a more appropriate description of the chain than the former one. This is because of the following observations: the distance between two O2 atoms forming the tetramer is 3.968(2) Å, while that separating the O2 atoms of the successive tetramers is significantly larger at 4.923(2) Å along the c-axis. The O---O hydrogen bonding distance is measured to be 2.896(2) Å in the tetramer while that involved in the bridging is 3.004(2) Å. The data presented in Table 6.2 also suggest that the hydrogen bonding O1-H---N interaction of W1 with the surrounding amino moieties is significantly stronger than the N-H---O3 interaction of W3. These structural parameters imply that one of the three water molecules, W3, is held less tightly compared to two other water molecules in the lattice.

Table 6.2. Hydrogen bonds for Cyclen.3H_2O [Å and ^{0}].

D-H...A	d(D-H)	d(H...A)	d(D...A)	<(DHA)
O(1)-H(1E)...N(1)#2	0.87(2)	1.97(2)	2.8383(17)	170(2)
O(2)-H(2E)...O(1)#3	0.83(2)	2.07(2)	2.896(2)	172(3)
O(3)-H(3E)...O(2)#2	0.93(2)	2.08(3)	3.004(2)	172(2)
N(1)-H(1D)...N(2)#1	0.846(17)	2.487(16)	2.924(2)	113.1(13)
N(1)-H(1D)...N(2)	0.846(17)	2.588(16)	3.0057(19)	111.7(13)
N(2)-H(2D)...O(3)	0.897(18)	2.401(18)	3.1871(19)	146.4(14)

Symmetry transformations used to generate equivalent atoms: #1 -x+1/2,-y,z #2 -x+1/2,-y+1/2,-z #3 -x+0,-y+1/2,z

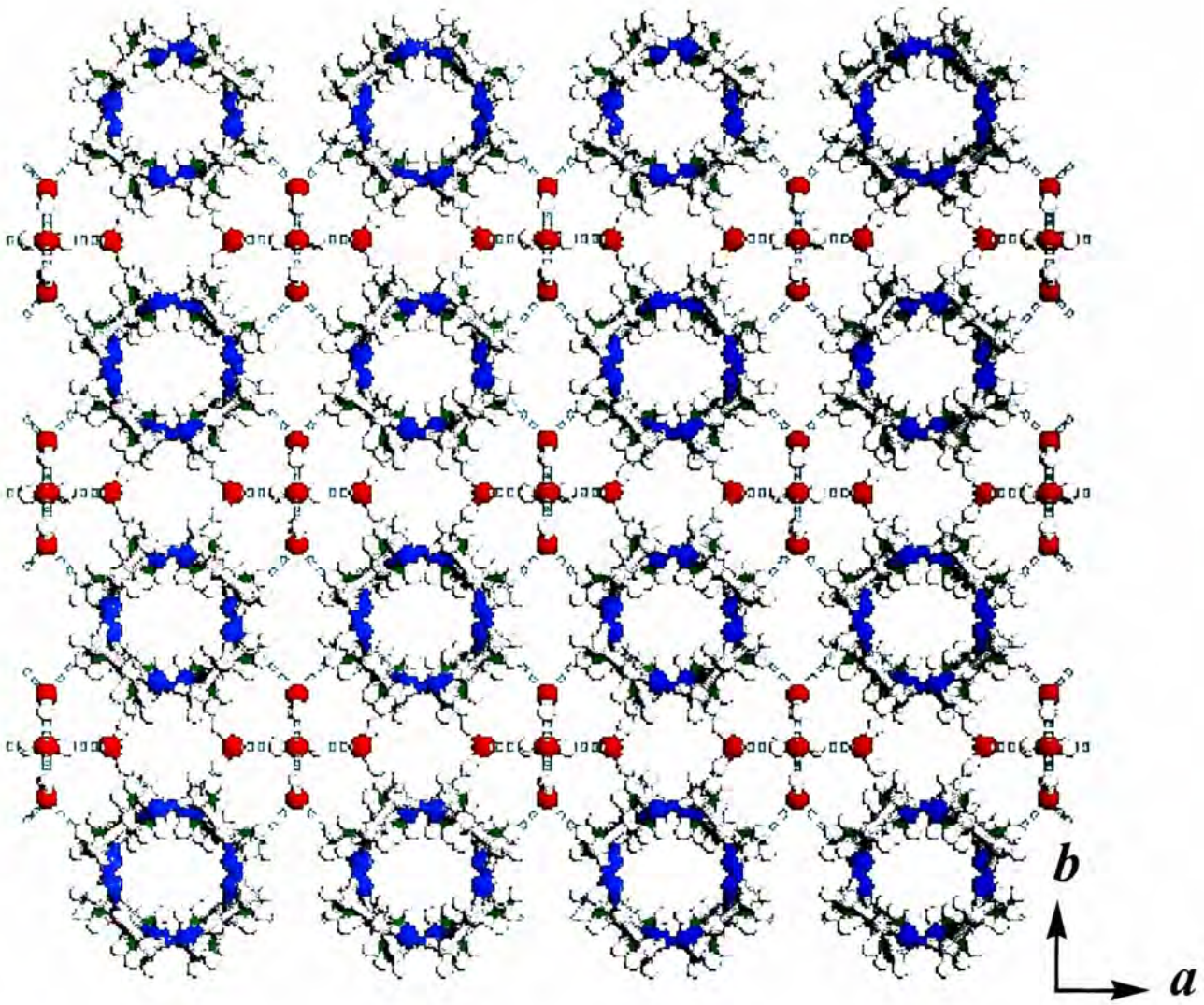

Fig. 6.5. Packing diagram of the molecule viewed along the crystallographic c-axis. The color codes are: red - oxygen, blue – nitrogen, dark gray – carbon and light gray – hydrogen. Hydrogen bonds are shown as dashed lines.

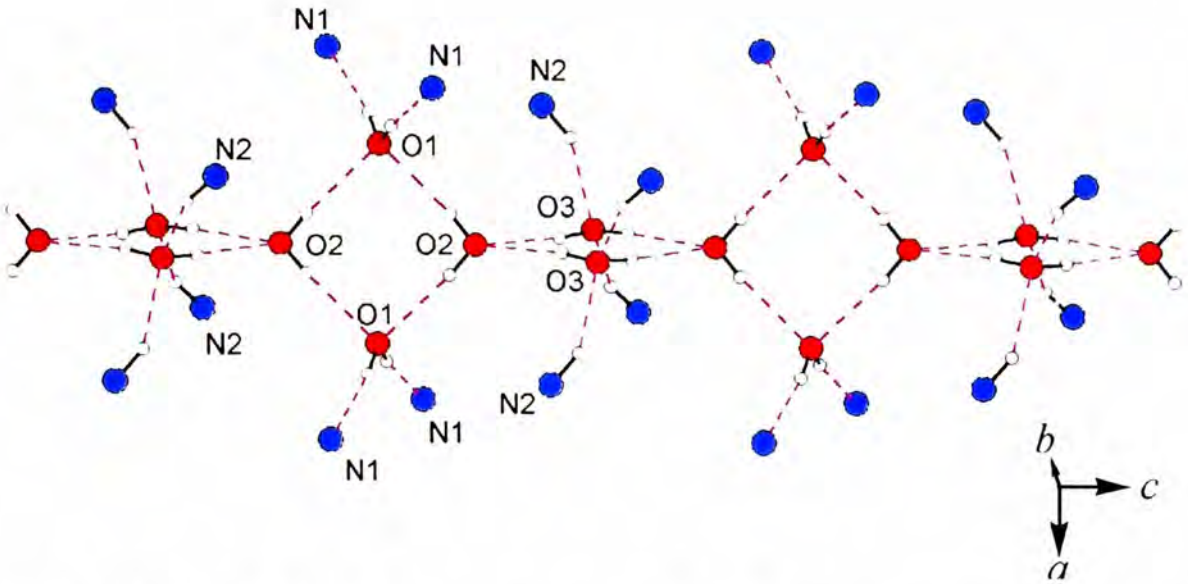

Fig. 6.6. Linear chain of water molecules with tetrameric units linked to form the chain. The color codes are: red – oxygen, blue – nitrogen & white – hydrogen. The pink lines represent hydrogen bonds.

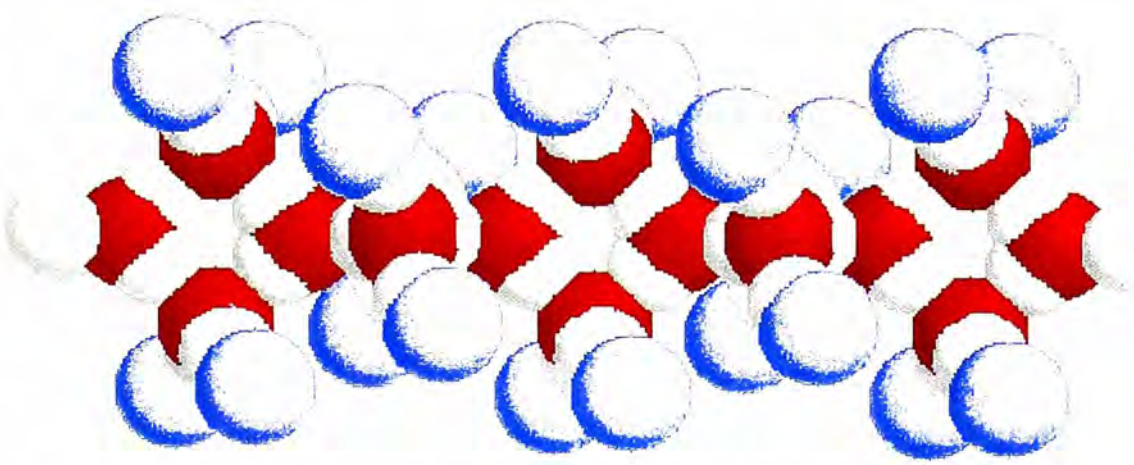

Fig. 6.7. A space filling model of the water chain along with the nitrogen atoms of cyclen. Color codes are the same as in the previous figure.

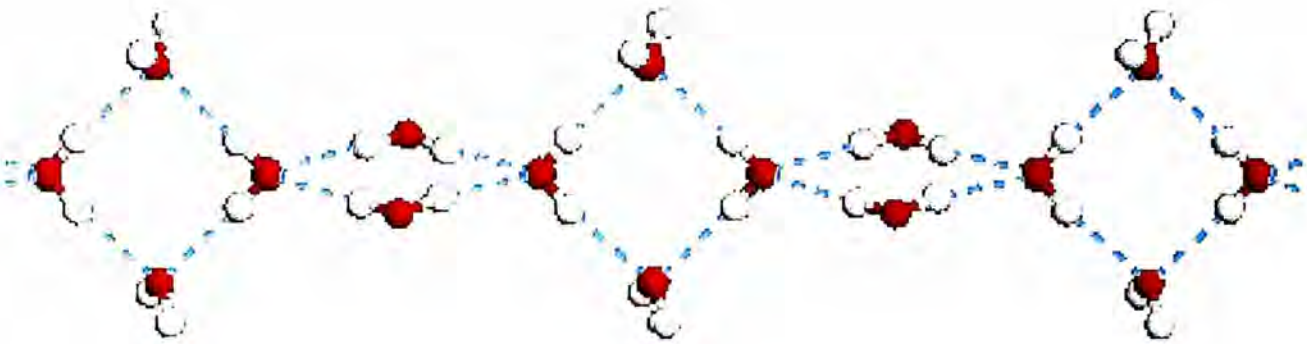

Fig. 6.8. A novel hydrogen bonding motif of the water chain. The color codes are: red – oxygen, gray – hydrogen. Dashed lines represent hydrogen bonds.

Tetrameric clusters of water molecules have been investigated earlier theoretically and experimentally.[32,33] Both theoretical calculations and vibration rotation tunneling spectroscopy of the water tetramer in the gas phase have indicated a quasi-planar cyclic structure in which each water molecule forms two hydrogen bonds, one as a donor and other as an acceptor. The free hydrogen available with each water molecule alternates above and below the plane. Assuming an S_4 symmetry for the tetramer, the average O-H---O bond length in this tetramer was estimated as 2.79 Å.[33] Interestingly, the hydrogen-bonding motif of the water tetramer in our self-assembled system, where each water molecule is involved in the formation of four hydrogen bonds, is very different from that theoretically predicted or experimentally observed in the gas phase. This difference is clearly because of the influence of the surrounding organic moieties and nearby water molecules. What appears even more interesting is the manner in which tetrameric water clusters are self-assembled in the form of an infinite chain.

We believe that this motif of association of the water molecules has not even been speculated earlier.

The water structure as observed here suggests that tetrameric water clusters can be important constituents of a water chain. Since water molecules play crucial role in contributing to the stability and function of the biological assemblies and that the details of the water structures in channels, in energy transducing proteins and in enzymes are largely unknown,[34,35] the present finding may provide insight into the hydrogen-bonding motif of the aqueous environments in living systems and help unraveling the mechanism of the conduction of protons in living systems.

6.4. Conclusions

We have characterized a hitherto unknown water structure in an organic molecular host. Since the surrounding of the water molecules in cyclen bears some resemblance to that in biological environments, we can expect that the present water structure can be considered as an important discovery that may be helpful in throwing light on some of water anomalies.

6.5. References

(1) Ludwig, R. *Angew. Chem., Int. Ed.* **2001**, *40*, 1807.

(2) Kell, G. In *Water: A Comprehensive Treatise*; Franks, F., Ed.; Plenum: New York, 1972; Vol. 1.

(3) Angell, C. A. In *Water: A Comprehensive Treatise*; Franks, F., Ed.; Plenum: New York, 1972; Vol. 7.

(4) Fine, R. A.; Millero, F. J. *J. Chem. Phys.* **1973**, *59*, 5529.

(5) Angell, C. A. *Science* **1976**, *193*, 1121.

(6) Mon, K. K.; Ashcroft, N. W.; Chester, G. V. *Phys. Rev. B* **1979**, *19*, 5103.

(7) Angell, C. A.; Shuppert, J.; Tucker, J. C. *J. Chem. Phys.* **1973**, *77*, 3092.

(8) Angell, C. A.; Oguni, M.; Sichina, W. J. *J. Chem. Phys.* **1982**, *86*, 998.

(9) Dorsey, N. E. "Properties of Ordinary Water Substance," American Chemical Society Monograph, 1968.

(10) *Water: A Comprehensive Treatise*; Franks, F., Ed.; Plenum: New York, 1972; Vol. 1-7.

(11) Debenedetti, P. G. *Metastable Liquids*; Princeton University Press: Princeton, 1996.

(12) Ball, P. *H_2O: A Biography of Water*; Weidenfeld & Nicolson: London, 1999.

(13) Stillinger, F. H. *Science* **1980**, *209*, 451.

(14) Blokzij, W.; Engberts, J. B. E. N. *Angew. Chem., Int. Ed.* **1993**, *32*, 1545.

(15) Latimer, W. M.; Rodebush, W. H. *J. Am. Chem. Soc.* **1920**, *42*, 1419.

(16) Dyke, T. R.; Mack, K. M.; Muenter, J. S. *J. Chem. Phys.* **1977**, *66*.

(17) Odutola, J. A.; Dyke, T. R. *J. Chem. Phys.* **1980**, *72*, 5062.

(18) Frank, H. S.; Wen, W. Y. *Discuss. Faraday Soc.* **1957**, *24*, 133.

(19) Koza, M.; Schober, H.; Tölle, A.; Fujara, J.; Hansen, T. *Nature* **1999**, *397*, 660.

(20) Lobban, C.; Finney, J. L.; Kuhs, W. F. *Nature* **1998**, *391*, 268.

(21) Dannenberg, J. J.; Haskamp, L.; Masunov, A. *J. Phys. Chem. A* **1999**, *103*, 7083.

(22) Ugalde, J. M.; Alkorta, I.; Elguero, J. *Angew. Chem., Int. Ed.* **2000**, *39*, 717.

(23) Atwood, J. L.; Barbour, L. J.; Ness, T. J.; Raston, C. L.; Raston, P. L. *J. Am. Chem. Soc.* **2001**, *123*, 7192.

(24) Liu, K.; Cruzan, J. D.; Saykally, R. J. *Science* **1996**, *271*, 929.

(25) Nauta, K.; Miller, R. E. *Science* **2000**, *287*, 29.

(26) Barbour, L. J.; Orr, G. W.; Atwood, J. L. *Nature* **1998**, *393*, 671.

(27) Custelcean, R.; Afloroaei, C.; Vlassa, M.; Polverejan, M. *Angew. Chem., Int. Ed.* **2000**, *39*, 3094.

(28) Park, K.-M.; Kuroda, R.; Iwamoto, T. *Angew. Chem., Int. Ed.* **1993**, *32*, 884.

(29) Narasimha Moorthy, J.; Natarajan, R.; Venugopalan, P. *Angew. Chem., Int. Ed.* **2002**, *41*, 3417.

(30) Blanton, W. B.; Gordon-Wylie, S. W.; Clark, G. R.; Jordan, K. D.; Wood, J. T.; Geiser, U.; Collins, T. J. *J. Am. Chem. Soc.* **1999**, *121*, 3551.

(31) Reibenspies, J. H. *Acta Cryst.* **1992**, *C48*, 1717.

(32) Xantheas, S. S.; Dunning Jr, T. H. *J. Chem. Phys.* **1993**, *99*, 8774.

(33) Cruzan, J. D.; Braly, L. B.; Liu, K.; Brown, M. G.; Loeser, J. G.; Saykally, R. J. *Science* **1996**, *271*, 59.

(34) Okamura, M. Y.; Paddock, M. L.; Graige, M. S.; Feher, G. *Biochem. Biophys. Acta* **2000**, *1458*, 148.

(35) Zaslavsky, D.; Gennis, R. B. *Biochem. Biophys. Acta* **2000**, *1458*, 164.

Chapter 7

Concluding remarks

This chapter presents an overall summary of the results of the current investigation. Also described in this chapter is the scope of further work that can be initiated based on the findings of the present study.

7.1. Summary of the present work

That the development of various molecular devices has become a fascinating area of contemporary research is evident from the discussions made in the first chapter of the thesis. Nanoscale devices, which mimic the macroscale operations of electronic components such as diodes, transistors, etc. hold high promise in the field of molecular electronics and photonics. Molecular systems, which are capable of performing light induced logic operations, are of considerable importance not only from the point of view of the development of molecular electronics, but also from the view point of signaling of species of biological and environmental importance utilizing the principles of molecular recognition.

As is clear from the opening chapter of the thesis, fluorescence is a powerful technique for the signaling of chemical species and quite understandably, the literature on fluorescence signaling systems for the metal ions is enormous. Various mechanisms have been exploited for fluorescence signaling of different analytes. One of the most commonly utilized mechanisms for this

purpose is the photoinduced electron transfer (PET) mechanism. PET signaling is based on the switching 'off/on' of the fluorescence of the sensor systems in the absence/presence of the various guest molecules. A large number of PET sensor molecules developed have been illustrated in brief in the introduction of the thesis.

We have developed and studied the photophysical and transition metal ion signaling behavior of a few new systems with a *fluorophore-spacer-receptor* architecture. During the course of this investigation we have interesting photophysics of simple multi-component systems, identified a novel mechanism of fluorescence signaling of the metal ions. We have also been successful in developing molecular systems which show a large degree of specificity while binding the metal ions. Another important finding of the present study is a water structure with a novel hydrogen bonding motif in an organic crystal.

Keeping in mind the fact that pyridine is an excellent coordinating ligand for the transition metal ions, we designed and developed two simple systems comprising a naphthyl/pyrenyl moiety as the fluorophore, a dimethylene chain as the spacer and a pyridyl moiety as the receptor. In order to develop sensor molecules that are specific to a or few metal ions, we have synthesized *fluorophore-spacer-receptor* systems wherein various azacrown moieties of different ring sizes have been used as the receptor moieties.

The synthetic details of the systems constitute a small but important part of the thesis. The details of the synthetic procedures adopted in the present investigation are given in chapter 2 along with a brief description of the instrumentation and various other methodologies.

The photophysical and fluorescence signaling properties of the systems synthesized constitute the major part of the thesis. The salient findings of the investigation are summarized below.

Photophysical behavior of simple molecules (described in chapter 3), **NPY** and **PPY**, turned out to be more interesting than what we expected initially. These systems were found to show excitation wavelength dependent emission characteristics. In addition to the structured emission of the naphthyl or pyrenyl moiety, both the systems were found to exhibit a long-wavelength broad band. Absorption and emission behavior of these systems reveal the formation of an intramolecular complex resulting from the interaction of the π-clouds of the terminal chromophore moieties in the ground state. Interestingly, it was found that intermolecular interaction between the constituting chromophores does not lead to the formation of any complex. The lack of an intermolecular complexation between the interacting partners has been ascribed to a smaller change in entropy associated with the complexation process.

The fluorescence signaling ability of **NPY** and **PPY** towards the transition metal ions, which has been described in chapter 4, revealed that these systems represent a new class of compounds whose fluorescence signaling of the transition metal ions is due to a mechanism that is different from the conventional PET mechanism. As against in conventional PET sensors, where the fluorescence signaling is due to a guest induced *cut-off* in the communication between the fluorophore and the receptor, the signaling mechanism in the present systems involves a guest induced *enhancement* in the communication between the fluorophore and the receptor. We encounter here a multiple wavelength window

dependent signaling of the metal ions. It is observed that different wavelength windows exist for the systems where the emission either switches 'off' or switches 'on' on addition of the guest metal ions.

The study of the photophysical and metal ion signaling properties of the crown containing compounds, described in chapter 5, bring into a light a molecular system, abbreviated as **APTAC**, which shows discrimination in its metal ion binding properties. Some of the metal ions for which this system display excellent fluorescence signaling are Cd^{2+}, Zn^{2+}, Cr^{3+}, Pb^{2+} and Hg^{2+}, most of which are of biological and environmental significance. The anomalous binding ability of the cyclen receptor thus turns out quite useful in fluorescence signaling of these metal ions.

One of the side products of this investigation is proved to be quite an important one. While examining the crystal structure of cyclen, which we have used as a receptor moiety, we noted the crystals to contain some water. We probed the structure of the water molecules in the crystal in detail taking into consideration the diversity of the cooperative hydrogen bonding interaction between the water molecules and its importance in understanding the behavior of water in pure state or in biological assemblies. We found that the water molecules form an infinite chain consisting of bridged tetrameric clusters (chapter 6). This hydrogen bonding motif of the water molecules in the organic host is found to be a novel one that has not been observed previously. Perhaps, our finding will be helpful in understanding the anomalous properties of the water in pure state or in biological assemblies.

7.2. Scope of further work

Our results on **NPY** and **PPY** have revealed the interaction of the π-clouds of the naphthyl/pyrenyl and pyridyl moieties giving rise to new absorption and emission features. Since it is known that it is possible to attain a perfect sandwich geometry of the overlapping moieties when the two moieties are separated by $(CH_2)_3$ spacer, it is worthwhile to synthesise systems where the naphthyl/pyrenyl and pyridyl moieties are separated by $-CH_2CH_2CH_2-$ unit and examine their photophysical and fluorescence signaling behavior. It will be of interest to examine the effect of systematic variation of the spacer length from single CH_2 to $(CH_2)_4$ on the photophysical properties of the systems. One needs to establish the structure of the complex in the absence and in the presence of metal ions by growing single crystals and determining the structure through X-ray single crystal diffraction studies. Studies in this direction were unsuccessful so far, but have to be taken up as a future challenge.

With the crown systems, a lot remains to be done. First, a detailed study on higher members of the nitrogen crown series and mixed N and S crowns needs to be undertaken in order to attain the goal of specificity in fluorescence signaling of the metal ions. Since we have observed that cavity size of the crown is not really the determining factor in metal ion binding, one approach could be to increase the number of binding sites in the crown moiety.

Even though we have established based on the available literature that the sensor molecule containing cyclen as receptor prefers larger metal ions, it still remains a point to be established with additional evidence. Developing single crystals of our systems was unsuccessful so far and studies have to be taken up in

this direction. Crystallographic structures will be the most direct and convincing experimental evidence in this regard.

Another aspect of current interest is to develop sensor molecules exhibiting efficient signaling in aqueous medium. Our systems are not very efficient in aqueous solution. Attempts have to be directed in developing molecules capable of signaling metal ions in aqueous medium.

Our discovery of a novel hydrogen bonded arrangement of water molecules in cyclen raises interesting possibilities. Apart from attesting the diversity of the nature of the cooperative association of the water molecules, the finding clearly suggest that the structure of even simple amino system could be quite instructive in unraveling the structural motif of hydrogen bonded network of water molecules. One therefore needs to reexamine the packing diagrams of the crystals containing water molecules to know more about the water structure in biological assemblies.

Appendix-1

Table A1.1. Fluorescence lifetimes (in ns) of **NPY** in THF with the addition of metal salts λ_{ex} = 370 nm; λ_{em} = 510 nm. The relative weightage of individual components (%) are given in the bracket.

Metal ion	τ_1 (%)	τ_2 (%)	τ_3 (%)	χ^2
Ag^+	2.3 (1.5)	11.9 (0.9)	0.1 (97.6)	1.2
Cd^{2+}	2.6 (0.8)	12.3 (0.3)	0.1 (98.9)	1.2
Co^{2+}	0.1 (1.1)	11.6 (0.4)	2.4 (98.5)	1.1
Cr^{3+}	2.8 (8.5)	12.3 (1.6)	0.2 (89.9)	1.1
Cu^{2+}	2.1	9.7	0.04 (>99.9)	1.3
Fe^{3+}	2.6 (5.1)	11.8 (0.7)	0.2 (94.2)	1.1
Hg^{2+}	2.0	6.3	0.01 (>99.9%)	1.2
Mn^{2+}	2.7 (0.9)	11.3 (0.2)	0.1 (98.9)	1.2
Ni^{2+}	3.3 (13.8)	13.1 (9.3)	0.3 (76.9)	1.3
Pb^{2+}	2.8 (1.7)	13.1 (1.5)	0.2 (96.8)	1.2
Zn^{2+}	2.8 (2.4)	11.6 (0.4)	0.2 (97.2)	1.2
H^+	2.4 (0.9)	11.1 (0.2)	0.1 (98.9)	1.2

Table A1.2. Fluorescence decay parameters (in ns) of **NPY** in AN with the addition of metal salts. λ_{ex} = 370 nm; λ_{em} = 525 nm. The relative weightage of individual components (%) are given in the bracket.

Metal ion	τ_1 (%)	τ_2 (%)	τ_3 (%)	χ^2
Ag^+	2.9 (0.18)	10.5 (0.02)	0.07 (99.8)	1.2
Cd^{2+}	6.7 (9.2)	18.3 (2.7)	1.8 (88.1)	1.2
Co^{2+}	1.8	14.7	0.01 (>99.9%)	1.2
Cr^{3+}	2.1 (10.1)	12.9 (0.9)	0.4 (89)	1.1
Cu^{2+}	5.9 (1.4)	19.5 (3.2)	0.1 (95.4)	1.3
Fe^{3+}	1.5	13.9	0.01 (>99.9)	1.2
Hg^{2+}	3.3	5.4	0.4 (>99.9)	1.0
Mn^{2+}	1.7	7.5	0.02 (>99.9)	1.3
Ni^{2+}	1.3 (0.8)	12.8 (0.1)	0.08 (99.1)	1.3
Pb^{2+}	1.5	12.1	0.01 (>99.9)	1.1
Zn^{2+}	2.5 (2.5)	13.0 (0.2)	0.2 (97.3)	1.1
H^+	2.2 (2.75)	14.0 (0.25)	0.2 (97)	0.98

Appendix-2

Table A2.1. Fluorescence decay parameters (in ns) for **APMAC4** and **APMAC5** in AN in the presence of metal ions. The relative weightage of individual components (%) are given in bracket.

Metal ion	APMAC4			APMAC5		
	τ_1	τ_2	χ^2	τ_1	τ_2	χ^2
Ag^+	3.7 (40.2)	16.9 (59.8)	1.2	2.7 (29.3)	17.0 (16.98)	1.2
Cd^{2+}	4.7 (29.7)	18.4 (70.3)	1.2	4.1 (18.7)	17.4 (81.3)	1.3
Co^{2+}	3.9 (32.1)	16.2 (67.9)	1.2	0.6 (72)	18.79 (28)	1.3
Cr^{3+}	3.9 (34.3)	17.9(65.7)	1.2	4.3 (20.5)	19.4 (79.5)	1.2
Cu^{2+}	6.1 (25.2)	18 (74.8)	1.1	3.4 (18.3)	19.4 (81.7)	1.1
Fe^{3+}	4.1 (30.2)	17.7 (69.8)	1.2	4.8 (19.5)	19.5 (80.5)	1.1
Hg^{2+}	3.7 (56)	13.9 (44)	1.2	3.6 (22.8)	16.6 (7.72)	1.2
Mn^{2+}	3.1 (50.6)	15.6 (49.4)	1.2	2.2 (85.8)	14.2 (14.2)	1.2
Ni^{2+}	4.1 (35.9)	17.1 (64.1)	1.3	4.4 (17.5)	19.3 (82.5)	1.1
Pb^{2+}	4.8 (37.4)	16.6 (62.6)	1.3	8.7 (63.2)	18.0 (36.8)	1.2
Zn^{2+}	3.9 (34.6)	17.8 (85.4)	1.3	9.0 (14.1)	20.0 (85.9)	1.3
H^+	4.6 (47.8)	15.4 (52.2)	1.2	1.8 (19.3)	13.7 (80.7)	1.0

Table A2.2. Fluorescence decay parameters (in ns) for **APMAC6** and **APDAC** in AN in the presence of metal ions. The relative weightage of individual components (%) are given in the bracket.

Metal ion	APMAC6			APDAC		
	τ_1	τ_2	χ^2	τ_1	τ_2	χ^2
Ag^+	3.7 (40.9)	18.1 (59.1)	1.2	3.4 (25)	16.8 (75)	1.3
Cd^{2+}	4.2 (33.8)	17.5 (66.2)	1.3	4.9 (15.6)	15.8 (84.4)	1.2
Co^{2+}	3.9 (34.4)	14.9 (65.6)	1.3	2.9 (21)	16.1 (79)	1.3
Cr^{3+}	3.6 (21.8)	18.9 (78.2)	1.2	3.2 (19)	16.0 (81)	1.2
Cu^{2+}	13.1 (71.6)	23.4 (28.4)	1.5	3.7 (20.8)	15.6 (79.2)	1.3
Fe^{3+}	4.7 (21.5)	17.6 (78.5)	1.3	2.4 (18.9)	16.5 (81.1)	1.3
Hg^{2+}	3.8 (53.3)	14.8 (46.7)	1.23	4.0 (25.9)	14.2 (74.1)	1.1
Mn^{2+}	3.9 (43)	17.6 (57)	1.3	2.4 (33.5)	13.4 (66.5)	1.4
Ni^{2+}	4.2 (31.8)	17.0 (68.2)	1.2	2.6 (20.5)	16.4 (79.5)	1.5
Pb^{2+}	4.3 (36.1)	14.1 (63.9)	1.1	6.2 (53)	14.9 (47)	1.1
Zn^{2+}	3.9 (25.7)	17.9 (74.3)	1.3	4.1 (17.5)	15.9 (82.5)	1.3
H^+	4.5 (37.6)	16.9 (62.4)	1.3	2.9 (24.3)	11.4 (75.7)	1.3

Table A2.3. Fluorescence decay parameters (in ns) for **APTAC** in AN in the presence of metal ions. The relative weightage of individual components are given in bracket.

Metal ion	APTAC			
	τ_1	τ_2	τ_3	χ^2
Ag^{+}	6.3 (3.5)	16.7 (91.5)	0.8 (5)	1.2
Cd^{2+}	26.8 (22)	15.3 (78)	-	1.4
Co^{2+}	3.9 (21)	0.5 (74.3)	12.2 (4.7)	1.1
Cr^{3+}	17.4 (74.5)	28.1 (25.5)	-	1.3
Cu^{2+}	9.1 (80.6)	18.7 (19.4)	-	1.4
Fe^{3+}	3.3 (93.3)	13.3 (6.7)	-	1.4
Hg^{2+}	14.9 (87.2)	23.1 (12.8)	-	1.1
Mn^{2+}	1.3 (75.4)	20.1 (24.6)	-	1.4
Ni^{2+}	2.2 (25.6)	19.9 (74.4)	-	1.7
Pb^{2+}	-	-	-	-
Zn^{2+}	8.0 (35.7)	18.1 (64.1)	-	1.5
H^{+}	2.1 (86.6)	13.3 (13.4)	-	1.3

Appendix-3

Table A3.1. Atomic coordinates ($x10^4$) and equivalent isotropic displacement parameters ($A^2 x1\ 0^3$) for Cyclen.$3H_2O$. U(eq) is defined as one third of the trace of the orthogonalized Uij tensor.

	x	y	z	U(eq)
O(1)	1267(1)	2500	-2500	39(1)
O(2)	0	2500	-268.2	48(1)
O(3)	0	1481(1)	2500	54(1)
N(1)	2783(1)	1241(1)	1364(2)	32(1)
N(2)	1298(1)	232(1)	1362(2)	33(1)
C(1)	1467(1)	827(1)	212(2)	36(1)
C(2)	1985(1)	1491(1)	833(2)	36(1)
C(3)	3335(1)	1026(1)	150(2)	35(1)
C(4)	4010(1)	517(1)	752(2)	37(1)

Table A3.2. Bond lengths [Å] and angles [^{0}] for Cyclen.$3H_2O$.

N(1)-C(3)	1.464(2)
N(1)-C(2)	1.473(2)
N(2)-C(1)	1.461(2)
N(2)-C(4)#1	1.469(2)
C(1)-C(2)	1.520(2)
C(3)-C(4)	1.513(2)
C(4)-N(2)#1	1.469(2)
C(3)-N(1)-C(2)	113.72(13)
C(1)-N(2)-C(4)#1	113.67(13)
N(2)-C(1)-C(2)	111.32(13)
N(1)-C(2)-C(1)	114.61(12)
N(1)-C(3)-C(4)	110.33(13)
N(2)#1-C(4)-C(3)	111.20(13)

Symmetry transformations used to generate equivalent atoms: #1 -x+1/2,-y,z

Table A3.3. Anisotropic displacement parameters ($A^2 \times 10^3$) for Cyclen.$3H_2O$. The anisotropic displacement factor exponent takes the form: $-2\pi^2 [h^2a^{*2} U11 + ... + 2 h k a^* b^* U12]$

	U11	U22	U33	U23	U13	U12
O(1)	37(1)	35(1)	44(1)	-5(1)	0	0
O(2)	45(1)	56(1)	43(1)	0	0	-2(1)
O(3)	62(1)	43(1)	57(1)	0	10(1)	0
N(1)	36(1)	28(1)	32(1)	1(1)	0(1)	-1(1)
N(2)	36(1)	32(1)	32(1)	1(1)	5(1)	1(1)
C(1)	35(1)	35(1)	37(1)	5(1)	-3(1)	2(1)
C(2)	37(1)	28(1)	42(1)	2(1)	-1(1)	4(1)
C(3)	38(1)	31(1)	35(1)	2(1)	4(1)	-2(1)
C(4)	32(1)	35(1)	43(1)	-2(1)	1(1)	-3(1)

Table A3.4. Hydrogen coordinates ($x10^4$) and isotropic displacement parameters ($A^2 \times 10^3$) for Cyclen.$3H_2O$.

	x	y	z	U(eq)
H(1E)	1568(13)	2905(13)	-2260(3)	74(7)
H(2E)	-387(13)	2538(17)	-860(3)	82(8)
H(3E)	32(18)	1835(14)	3310(3)	99(9)
H(1D)	2703(9)	827(10)	1876(19)	33(5)
H(2D)	940(11)	437(10)	2010(2)	38(5)
H(1A)	966	1044	-158	43
H(1B)	1742	578	-627	43
H(2A)	2054	1888	56	43
H(2B)	1702	1739	1663	43
H(3A)	3556	1501	-299	42
H(3B)	3046	738	-623	42
H(4A)	4388	406	-50	44
H(4B)	4292	802	1537	44

Table A3.5. Torsion angles [^{0}] for Cyclen.3H_2O.

C(4)#1-N(2)-C(1)-C(2)	-164.61(13)
C(3)-N(1)-C(2)-C(1)	71.55(18)
N(2)-C(1)-C(2)-N(1)	61.95(19)
C(2)-N(1)-C(3)-C(4)	-160.10(13)
N(1)-C(3)-C(4)-N(2)#1	62.62(17)

Symmetry transformations used to generate equivalent atoms: #1 -x+1/2,-y,z